Guidance on sampling effort to monitor mesozooplankton communities at Canadian bivalve aquaculture sites using an optical imaging system

Stephen Finnis, Thomas Guyondet, Christopher W. McKindsey, Julie Arseneau, Jeffrey Barrell, Johannie Duhaime, Ramón Filgueira, Daria Gallardi, David Gaspard, Olivia Gibb, Claire Goodwin, Khang Hua, Tara Macdonald, Rebecca Milne, Anaïs Lacoursière-Roussel*

St. Andrews Biological Station
Fisheries and Oceans Canada
125 Marine Science Drive
St. Andrews, New Brunswick
E5B 0E4

2023

Canadian Technical Report of
Fisheries and Aquatic Sciences 3581

Fisheries and Oceans Canada | Pêches et Océans Canada

Canada

Canadian Technical Report of Fisheries and Aquatic Sciences

Technical reports contain scientific and technical information that contributes to existing knowledge but which is not normally appropriate for primary literature. Technical reports are directed primarily toward a worldwide audience and have an international distribution. No restriction is placed on subject matter and the series reflects the broad interests and policies of Fisheries and Oceans Canada, namely, fisheries and aquatic sciences.

Technical reports may be cited as full publications. The correct citation appears above the abstract of each report. Each report is abstracted in the data base *Aquatic Sciences and Fisheries Abstracts*.

Technical reports are produced regionally but are numbered nationally. Requests for individual reports will be filled by the issuing establishment listed on the front cover and title page.

Numbers 1-456 in this series were issued as Technical Reports of the Fisheries Research Board of Canada. Numbers 457-714 were issued as Department of the Environment, Fisheries and Marine Service, Research and Development Directorate Technical Reports. Numbers 715-924 were issued as Department of Fisheries and Environment, Fisheries and Marine Service Technical Reports. The current series name was changed with report number 925.

Rapport technique canadien des sciences halieutiques et aquatiques

Les rapports techniques contiennent des renseignements scientifiques et techniques qui constituent une contribution aux connaissances actuelles, mais qui ne sont pas normalement appropriés pour la publication dans un journal scientifique. Les rapports techniques sont destinés essentiellement à un public international et ils sont distribués à cet échelon. II n'y a aucune restriction quant au sujet; de fait, la série reflète la vaste gamme des intérêts et des politiques de Pêches et Océans Canada, c'est-à-dire les sciences halieutiques et aquatiques.

Les rapports techniques peuvent être cités comme des publications à part entière. Le titre exact figure au-dessus du résumé de chaque rapport. Les rapports techniques sont résumés dans la base de données *Résumés des sciences aquatiques et halieutiques.*

Les rapports techniques sont produits à l'échelon régional, mais numérotés à l'échelon national. Les demandes de rapports seront satisfaites par l'établissement auteur dont le nom figure sur la couverture et la page du titre.

Les numéros 1 à 456 de cette série ont été publiés à titre de Rapports techniques de l'Office des recherches sur les pêcheries du Canada. Les numéros 457 à 714 sont parus à titre de Rapports techniques de la Direction générale de la recherche et du développement, Service des pêches et de la mer, ministère de l'Environnement. Les numéros 715 à 924 ont été publiés à titre de Rapports techniques du Service des pêches et de la mer, ministère des Pêches et de l'Environnement. Le nom actuel de la série a été établi lors de la parution du numéro 925.

Canadian Technical Report of
Fisheries and Aquatic
Sciences 3581

2023

GUIDANCE ON SAMPLING EFFORT TO MONITOR MESOZOOPLANKTON COMMUNITIES AT CANADIAN BIVALVE AQUACULTURE SITES USING AN OPTICAL IMAGING SYSTEM

by

Stephen Finnis[1], Thomas Guyondet[2], Christopher W. McKindsey[3], Julie Arseneau[1], Jeffrey Barrell[2], Johannie Duhaime[4], Ramón Filgueira[5], Daria Gallardi[6], David Gaspard[7], Olivia Gibb[6], Claire Goodwin[8], Khang Hua[4], Tara Macdonald[9], Rebecca Milne[11], Anaïs Lacoursière-Roussel[1*]

[1*]St. Andrews Biological Station
125 Marine Science Drive, St. Andrews
New Brunswick E5B 0E4
[2]Gulf Fisheries Center
343 Université Ave, Moncton
New Brunswick E1C 5K4
[3]Maurice Lamontagne Institute
850 Rte de la Mer, Mont-Joli
Quebec G5H 3Z4
[4]200 Kent Street, Ottawa
Ontario K1A 0E6
[5]Marine Affairs Program, Dalhousie University
1459 Oxford Street PO Box 15000, Halifax
Nova Scotia B3H 4R2
[6]Northwest Atlantic Fisheries Center
80 E White Hills Road, St. John's
Newfoundland A1A 5J7
[7]Pacific Science Enterprise Center
4160 Marine Drive, West Vancouver
British Columbia V7V 1H2
[8]Huntsman Science Center
1 Lower Campus Road, St. Andrews
New Brunswick E5B 2L7
[9]Biologica Environmental Services Ltd.
488F Bay Street, Victoria
British Columbia V8T 5H2
[11]Bedford Institute of Oceanography
1 Challenger Drive PO Box 1006 Dartmouth
Nova Scotia B2Y 4A2

*Corresponding author. Email: Anais.Lacoursiere@dfo-mpo.gc.ca

Cat. No. Fs97-6/3581E-PDF ISBN 978-0-660-68776-6 ISSN 1488-5379

Correct citation for this publication:

Finnis, S., Guyondet, T., McKindsey, C.W., Arseneau, J., Barrell, J., Duhaime, J., Filgueira, R., Gallardi, D., Gaspard, D., Gibb, O., Goodwin, C., Hua, K., Macdonald, T., Milne, R., Lacoursière-Roussel, A. 2023. Guidance on sampling effort to monitor mesozooplankton communities at Canadian bivalve aquaculture sites using an optical imaging system. Can. Tech. Rep. Fish. Aquat. Sci. 3581: vii + 101 p.

CONTENTS

ABSTRACT

Finnis, S., Guyondet, T., McKindsey, C.W., Arseneau, J., Barrell, J., Duhaime, J., Filgueira, R., Gallardi, D., Gaspard, D., Gibb, O., Goodwin, C., Hua, K., Macdonald, T., Milne, R., Lacoursière-Roussel, A. 2023. Guidance on sampling effort to monitor mesozooplankton communities at Canadian bivalve aquaculture sites using an optical imaging system. Can. Tech. Rep. Fish. Aquat. Sci. 3581: vii + 101 p.

Despite the critical roles zooplankton play in marine food webs, the alterations to their communities by bivalve aquaculture have never been investigated empirically in Canadian waters. Collecting zooplankton data in bivalve aquaculture sites in a way that is interoperable over space and time is the first critical step to building consistent time series to detect changes over time and accurately inform management decisions. As part of the development of a nationally-consistent sampling design within the Aquaculture Monitoring Program, this report evaluates mesozooplankton assemblages observed at nine coastal aquaculture sites, located across four DFO regions, with sampling across months, tide phases, and sampling locations. In most sites, strong spatial effects were observed, while tide effects were generally less important for structuring the mesozooplankton communities. Seasonality was identified as an important monitoring requirement to increase diversity coverage and conduct interannual data comparisons. Conclusions provide direct advice on the minimal sampling effort required to monitor mesozooplankton community changes over time in Canadian bivalve aquaculture embayments. This report represents the first large-scale Canadian coastal study using imaging technology for plankton taxonomic identification; a method with the potential to enable more efficient, cost-effective monitoring and refine our understanding of the state of the Canadian oceans.

RÉSUMÉ

Finnis, S., Guyondet, T., McKindsey, C.W., Arseneau, J., Barrell, J., Duhaime, J., Filgueira, R., Gallardi, D., Gaspard, D., Gibb, O., Goodwin, C., Hua, K., Macdonald, T., Milne, R., Lacoursière-Roussel, A. 2023. Guidance on sampling effort to monitor mesozooplankton communities at Canadian bivalve aquaculture sites using an optical imaging system. Can. Tech. Rep. Fish. Aquat. Sci. 3581: vii + 101 p.

Malgré le rôle fondamental du zooplancton dans les réseaux trophiques marins, les changements de ces communautés liés à la conchyliculture n'ont jamais été étudiés empiriquement dans les eaux canadiennes. Assurer la collecte des données de zooplancton dans les sites conchylicoles de façon interopérable dans l'espace et dans le temps est la première étape critique pour établir des séries chronologiques cohérentes et informer la gestion avec précision. Afin d'élaborer un plan d'échantillonnage consistent à l'échelle nationale au sein du Programme de la surveillance en aquaculture, ce rapport évalue l'assemblage du mésozooplancton observé à neuf sites conchylicoles, situés dans quatre régions du MPO, échantillonnés à différents mois, marées et emplacements. Dans la plupart des sites, l'effet spatial était hautement significatif et l'effet de la marée était moins important. La saisonnalité a également été identifiée comme un facteur important pour augmenter la détection de la diversité et effectuer des comparaisons de données interannuelles. Les conclusions fournissent des conseils sur l'effort d'échantillonnage minimal requis pour surveiller les changements de communautés de mésozooplancton au fil du temps. Ce rapport représente la première étude à grande échelle en zones côtières canadiennes mettant en œuvre une technique d'imagerie pour identifier le plancton; une méthode susceptible de permettre une surveillance plus efficace et rentable et d'affiner notre compréhension de l'état des océans canadiens.

PREFACE

To date, bivalve aquaculture research has predominantly focused on near-field benthic effects, while limited research has documented far-field (i.e., bay-scale) effects on lower trophic levels (nutrients, phytoplankton, and zooplankton) (Weitzman et al. 2019). Previous Fisheries and Oceans Canada Program for Aquaculture Regulatory Research (DFO-PARR) projects highlighted that pelagic ecosystem perturbations at low trophic levels may cause fundamental shifts to food web dynamics, especially with reduced predator-prey size ratios resulting in longer, less efficient food chains (Gianasi et al. 2023). However, earlier research on carrying capacity assessments and models could only consider zooplankton as a bulk secondary producer component, as opposed to a main trophic link between primary producers and fisheries productivity due to limited knowledge on the structure and dynamics of zooplankton communities in Canadian bivalve aquaculture sites. In 2018, the Aquaculture Monitoring Program Working Group (AMP-WG) was thus mandated to develop a nationally-consistent program to monitor ecosystem impacts from bivalve aquaculture at the bay-scale. It was decided that the use of zooplankton to monitor potential ecosystem interactions of bivalve aquaculture would be evaluated. The long-term AMP data will allow for the development of new and updated models to explore how bivalve aquaculture potentially impacts fisheries resources, which may vary between aquaculture sites and in future climate scenarios. This improved scientific understanding will support the Department through an increased capacity to develop evidence-based advice and mitigation strategies. Collectively, this research will help inform aquaculture policy and regulatory decision-making to enhance the sustainability of the aquaculture in Canada.

1 INTRODUCTION

The bivalve aquaculture industry offers many potential benefits to communities, including food security, economic opportunities, and ecosystem services (Flaherty et al. 2019; Wijsman et al. 2019; Azra et al. 2021). However, concerns and uncertainties related to the ecosystem effects of intensive bivalve farming still remain (Filgueira et al. 2016; Grant and Pastres 2019; Holden et al. 2019; Hulot et al. 2020). In particular, the potential effects of bivalve aquaculture on zooplankton communities are largely unknown, and this may have important repercussions as zooplankton represent a key link for energy and mass transfer between trophic levels (Lindeman 1942; Kiørboe 2009; Hulot et al. 2014). The alterations to zooplankton communities have mostly been studied through laboratory research or field studies of invasive bivalves (Davenport et al. 2000; Zeldis et al. 2004; Lehane and Davenport 2006; Pace et al. 2010). Overall, there are few examples of these effects in the field (Hulot et al. 2020), although Maar et al. (2008) observed zooplankton depletion in a mussel aquaculture site. Generally, the effects of bivalves on zooplankton communities are thought to be both indirect (i.e., through food limitation and increased competition as a result of the filtration of phytoplankton) and direct (i.e., filtration and ingestion) (Lehane and Davenport 2006). Thus, research of these understudied interactions between bivalves and zooplankton communities are critical for the sustainable development of the bivalve aquaculture industry.

In 2018, Fisheries and Oceans Canada (DFO) launched the Aquaculture Monitoring Program (AMP) to increase departmental availability of scientific data to support aquaculture policy and decision-making for enhanced aquaculture sustainability. The national program is currently in development, and aims to implement long-term monitoring of the spatiotemporal variations of potential far-field environmental effects of aquaculture (i.e., hundreds of meters beyond the lease boundaries; Weitzman et al. 2019) using nationally-consistent sampling approaches. One component of AMP is focused on improving scientific understanding of zooplankton-bivalve dynamics at aquaculture sites, and characterizing long-term natural variability in zooplankton communities to determine whether natural variations can be disentangled from aquaculture-induced effects. Ultimately, analyzing zooplankton size and community structure could potentially be used to describe and monitor how bivalve aquaculture might impact energy flows to higher trophic levels within pelagic food webs. More specifically, monitoring zooplankton communities in bivalve aquaculture sites over time will allow researchers to: (i) evaluate if bivalve farms directly or indirectly impact zooplankton size and community structure, (ii) better understand ecosystem-level changes to zooplankton communities during variations of the production levels (i.e., increasing or decreasing bivalve production) or transitions between bivalve culture types, (iii) elucidate complex trophic interactions, including benthic-pelagic food-web coupling, (iv) monitor potential trophic cascades, including impacts on zooplankton abundance, biomass and productivity, and (v) provide historical databases to address potential issues related to aquaculture (e.g., monitoring the larval stages of lobsters, crabs, or tunicates) or future climate change scenarios.

Effective zooplankton monitoring requires reliable estimates of the biodiversity within an area, yet monitoring programs routinely face challenges of determining when a location has been adequately sampled (Angermeier and Smogor 1995; Olsen et al. 1999; Yoccoz et al. 2003). Measurable components of biodiversity, such as richness (the total number of species within an area), are often highly dependent on the level of sampling effort, since more species will be detected by increasing the number of samples collected (Colwell et al. 2012; Chao et al. 2014, 2020). Rare taxa are often of interest in aquatic bioassessments as they may play critical roles in ecosystems and can be useful indicators of human-induced changes (Cao et al. 1998), although they can require substantially more sampling effort to detect (Colwell et al. 2012). Defining the “appropriate” level of sampling effort is essential, since too few samples may lead to incorrect conclusions about an ecosystem, whereas too

many samples may result in redundant or minimal new information being collected, thereby resulting in an overallocation of resources (Angermeier and Smogor 1995; Danielsen et al. 2000). Various statistical approaches exist to identify the number of samples at which little new information (e.g., few new species) are added (Colwell et al. 2012). Monitoring programs, especially those in their infancy, may benefit substantially from applying these approaches by using data-driven estimates to indicate the most effective allocation of resources or funding (Danielsen et al. 2000; Hoffman et al. 2011).

Identifying the appropriate spatial and temporal scales for sampling is a key feature in designing environmental monitoring programs since selecting the incorrect scales may result in the wrong processes being measured (Birk et al. 2020; Ma et al. 2022). For example, in coastal environments, zooplankton distributions are patchy at a range of spatial and temporal scales, resulting from a combination of both large scale physical (i.e., passive displacement with the water) and biological (i.e., active movement for predation, mating, food searching, etc.) processes (Folt and Burns 1999; O'Brien and Oakes 2020). In bivalve aquaculture sites (i.e., bays), little is known about how depletion from direct bivalve grazing may alter these spatiotemporal zooplankton variations. Spatially, coupled biological-hydrodynamic models and remote sensing have shown that seston depletion from bivalve aquaculture can occur at the bay scale (Grant et al. 2007, 2008; Filgueira et al. 2014, 2015; Taylor et al. 2021). Complex aquaculture and ecosystem interactions might also occur at various temporal scales, such as tidal exchange, water residence time, and daily variation due to environmental stochasticity (i.e., daily to weekly). Furthermore, the interaction between bivalve aquaculture and zooplankton might vary seasonally due to changes related to (i) bivalve feeding rates, (ii) plankton production rates, (iii) water-column stability and (iv) circulation patterns (Grant et al. 2008; Steeves 2018). Basic understanding of these short-term spatiotemporal variations is thus crucial to interpret factors altering long-term zooplankton shifts, distinguish between natural and potential bivalve aquaculture-related effects, and define an optimal sampling effort. Further examination of zooplankton distributions, both spatially and temporally, is therefore an important first step to provide a more detailed understanding of these processes.

Historically, biodiversity assessments have relied on microscopy for the identification and enumeration of zooplankton specimens (Le Bourg et al. 2015; Detmer et al. 2019). However, in the last decade, the use of innovative imaging instruments and machine learning algorithms has grown to automatically identify and classify plankton images, which can help quantify plankton diversity and functional traits (Luo et al. 2018; Ramkissoon 2021; Orenstein et al. 2022). These offer many benefits when compared to traditional microscopy, including more rapid identification of taxa at lower cost (Álvarez et al. 2014; Le Bourg et al. 2015; Detmer et al. 2019). To improve our ability to better understand impacts of human stressors on coastal food webs, a collaborative international effort is currently underway to improve the reference libraries of zooplankton images (e.g., Ibarbalz et al. 2019; Kerr et al. 2020). For example, flow cytometer and microscope (FlowCam) methodologies are being developed to explore zooplankton size and abundance as part of the Continuous Plankton Recorder Survey, an extensive global marine monitoring program (Batten et al. 2019). In this context, AMP is the first DFO initiative to capitalize on these new monitoring approaches to detect changes in zooplankton communities.

This report examines spatiotemporal variations of mesozooplankton (i.e., 0.25 mm - 5 mm) collected in four coastal DFO regions (Pacific, Maritimes, Gulf, and Newfoundland and Labrador; herein referred to solely as "Newfoundland"), and analyzed using an optical imaging system. Specifically, we provide science-based recommendations on optimal sampling effort to monitor mesozooplankton in Canadian bivalve aquaculture sites by accomplishing the following objectives:

1. Evaluate the optimal sampling effort by examining how taxa diversity changes with increasing sample size.

2. Examine differences in mesozooplankton community structure among regions, sites, and/or months.
3. Characterize variations in mesozooplankton community structure within sites, including how assemblages vary by tides and stations (i.e., locations within each bay).

2 METHODS

2.1 Sample collection

Mesozooplankton counts have been compiled from various sampling sites across Canada, in different seasons, tide phases and sampling stations. For clarity, we use the following terminology for the various spatial scales: *region* refers to DFO regions (i.e., Pacific, Maritimes, Gulf, and Newfoundland); *site* refers to an individual bay, inlet, lagoon or harbour; *station* represents the different locations sampled within a given site (e.g., Inner, Mid, or Outer); and *sample* refers to the individual collected measurements from a zooplankton net tow. Data were collected from nine sites across Canada within four DFO regions and across varying collection months (February to December) (Fig. 1; Table 1). Sites were selected to span a range of oceanographic conditions and bivalve aquaculture intensity levels, with varying pre-existing knowledge of the hydrodynamics and bivalve aquaculture-environment interactions in each of them. Within each site, the number of bivalves per lease is often not known as this information is generally proprietary. However, bivalves were present within all sampling sites, except for Argyle and Country Harbour, in which all leases were empty during the time of sampling (Fig. 1). Within each site, samples were collected at three stations to gain a general understanding of spatial dynamics in zooplankton community structure. In general, for sites with a single point of exchange with the open ocean that follow a linear path, stations were labeled as “Inner”, “Mid”, and “Outer”. For instances where this labeling scheme would not be applicable (e.g., in bays with more complex coastlines and >1 location of exchange with the ocean), stations were generally instead labeled according to cardinal directions (e.g., “North,” “South,” and “Central”) (Fig. 1). For these sites without linear morphology, the location of the three sampling stations were selected according to a variety of factors including logistics (e.g., suitable depth, having enough space to avoid the nets getting tangled in leases) or knowledge of the circulation patterns (e.g., selecting a station close to a point of exchange with the open ocean). In addition, station locations were chosen to sample areas both near and far from the leases, while keeping an approximately even spacing of stations throughout the site.

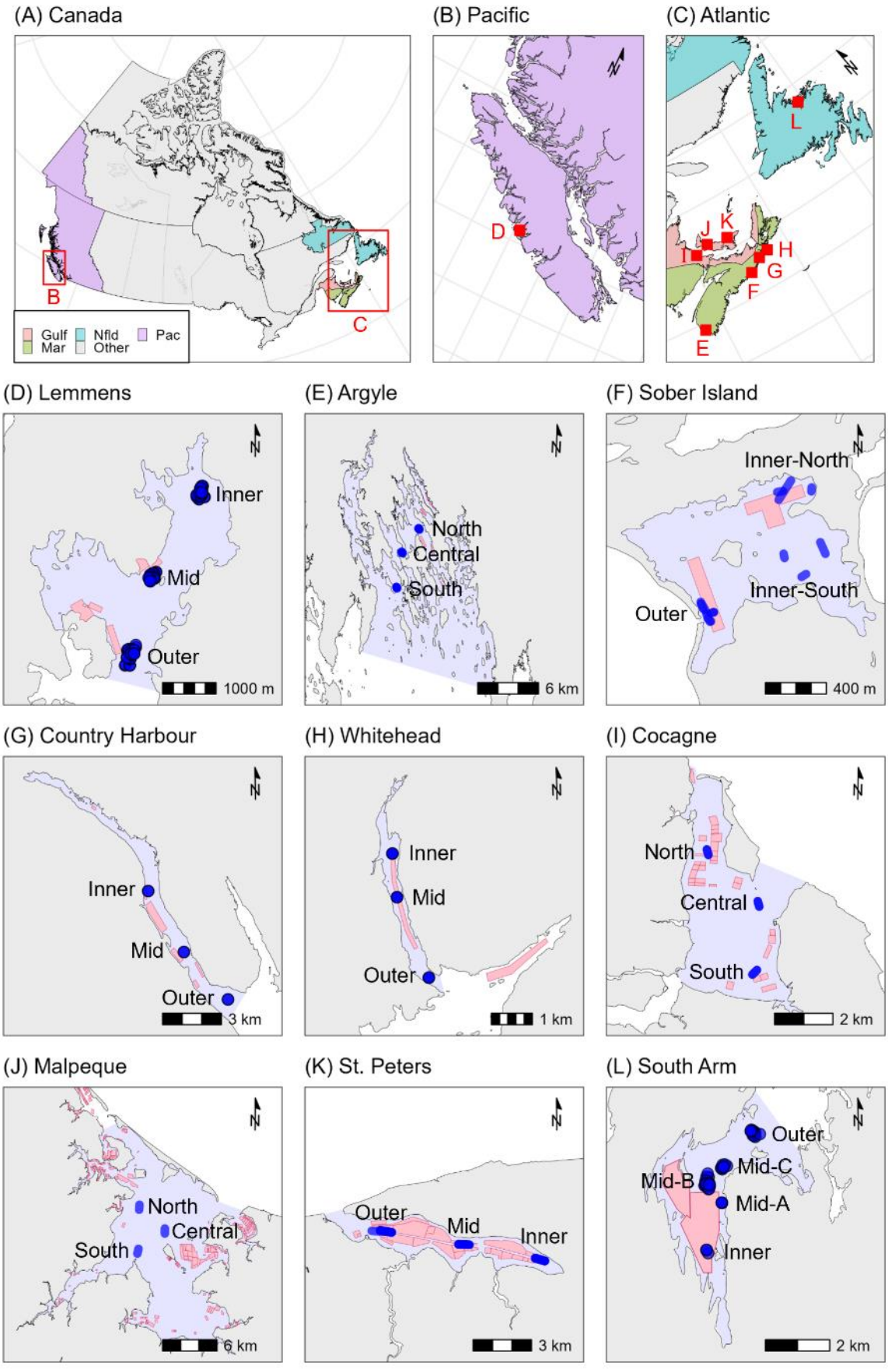
(A) Canada
(B) Pacific
(C) Atlantic
B
C
D
L
J
K
I
H
G
F
E
Gulf
Mar
Nfld
Other
Pac
(D) Lemmens
Inner
Mid
Outer
1000 m
(E) Argyle
North
Central
South
6 km
(F) Sober Island
Inner-North
Inner-South
Outer
400 m
(G) Country Harbour
Inner
Mid
Outer
3 km
(H) Whitehead
Inner
Mid
Outer
1 km
(I) Cocagne
North
Central
South
2 km
(J) Malpeque
North
Central
South
6 km
(K) St. Peters
Outer
Mid
Inner
3 km
(L) South Arm
Outer
Mid-C
Mid-B
Mid-A
Inner
2 km

Figure 1. Study area maps showing sampling locations for mesozooplankton (0.25 mm - 5.00 mm) as part of the Aquaculture Monitoring Program. Insets show data sampled from within the Pacific (Pac; D), Maritimes (Mar; E-H), Gulf (I-K) and Newfoundland regions (Nfld; L), as labelled in panels B and C. Samples were obtained either as vertical tows (blue circles) or as transects (blue lines), and text labels indicate station names. Pink polygons represent the bivalve aquaculture leases obtained from TANTALIS Crown Features for the Pacific region (D; https://fisheries-map-gallery-crm.hub.arcgis.com/datasets/governmentofbc::tantalis-crown-tenures), the Nova Scotia Department of Fisheries and Aquaculture mapping tool for sites in Nova Scotia (E-H; https://novascotia.ca/fish/aquaculture/site-mapping-tool/), the Marine Aquaculture Site Mapping Program for sites in New Brunswick (I; https://www2.gnb.ca/content/gnb/en/departments/10/aquaculture/content/masmp.html), the Prince Edward Island (PEI) Aquaculture Interactive Leasing Maps for sites in PEI (J, K; https://www.dfo-mpo.gc.ca/aquaculture/management-gestion/pei-lic-ipe-baux-eng.htm), and Crown Title leases from the Newfoundland Land Use Atlas for Newfoundland (L; https://www.gov.nl.ca/landuseatlas/details). Only active leases present at the time of sampling are shown (i.e., “under review” or “proposed” leases are not included). The presence of leases does not necessarily mean leases were stocked with bivalves during sampling, as this information is often proprietary, although it is known that leases in Argyle (E) and Country Harbour (G) were not stocked with bivalves during the time of sampling. The shaded blue polygons in each inset represent the boundaries used for calculations of site area and total lease area shown in Table 1. The exact boundaries of these polygons are subjective, yet were shown for an approximate comparison of relative size among study sites.

Table 1. Data summary table for mesozooplankton (0.25 mm - 5.00 mm) samples obtained within study sites and regions, as part of the Aquaculture Monitoring Program. The site and lease areas were calculated within the shaded blue areas shown in Fig. 1. Coverage (%) represents the ratio of the lease area to site area. The tidal range (m) is presented as the range between the lower low water mean tide to higher high water mean tide, from the nearest Canadian Hydrographic Service tide station to the sampling stations (https://wla.iwls.azure.cloud.dfo-mpo.gc.ca/stationMgmt). Several additional opportunistic surveys from various funding sources resulted in different temporal coverage for some sites. Samples were therefore obtained in more than one month for Cocagne (Gulf), South Arm (Newfoundland), and Lemmens Inlet (Pacific). *n* refers to the number of samples obtained at each site and/or month. Pac: Pacific, Mar: Maritimes, Nfld: Newfoundland.

Region	Site and/or month	Site area (km^2)	Lease area (km^2)	Coverage (%)	Bivalve type	Tide range (m)	Hydro. model	Max depth (m)	Year	Date range	Tow type	*n*
Pac	Lemmens Aug 2020	6.44	0.23	3.6	Pacific oyster	0.74-3.39 (Tofino, 08615)	[1]	27.9	2020	Aug 29-31	Vertical	18
	Lemmens Mar 2021								2021	Mar 3-5	Vertical	2
	Lemmens Jun 2021									Jun 9-11	Vertical	18
	Lemmens Sept 2021									Sep 14-15	Vertical	12
Mar	Argyle	137.00	0.62	0.5	Eastern oyster	0.66-3.71 (Wedgeport, 00374)	N/A	16.5	2021	Aug 30-Sep 1	Oblique	15
	Country Harbour	10.40	0.84	8.1	Eastern oyster	0.53-1.87 (Isaacs Harbour, 00535)	N/A	21.9	2021	Aug 24	Vertical	6

Region	Site and/or month	Site area (km^2)	Lease area (km^2)	Coverage (%)	Bivalve type	Tide range (m)	Hydro. model	Max depth (m)	Year	Date range	Tow type	*n*
	Sober Island	0.90	0.09	9.6	Eastern oyster	No tidal station	[2]	4.0	2021	Aug 27	Horizontal	12
	Whitehead	1.68	0.23	13.9	Eastern oyster	0.45-1.80 (Whitehead, 00545)	[2]	14.3	2021	Aug 25	Vertical	9
Gulf	Cocagne	18.90	1.44	7.6	Eastern oyster	0.32-1.05 Cocagne (01812)	[3]	8.3	2021	Jul 21	Horizontal	3
										Aug 26	Horizontal	3
	Malpeque	207.40	14.76	7.1	Blue mussel, eastern oyster	0.24-0.96 (Malpeque, 01905)	[4, 5, 6]	14.2	2020	Sept 29	Horizontal	3
	St. Peters	15.78	6.37	40.4	Blue mussel, eastern oyster	0.23-0.79 (St. Peters Bay, 01935)	[7]	5.0	2020	Sept 1-4	Horizontal	26
Nfld	South Arm Sep 2020	11.31	2.80	24.8	Blue mussel	0.27-1.18 (Leading Tickle, 01087)	[8]	45.0	2020	Sep 15-16	Vertical	10
	South Arm Oct 2021								2021	Oct 5-7	Vertical	12

Region	Site and/or month	Site area (km^2)	Lease area (km^2)	Coverage (%)	Bivalve type	Tide range (m)	Hydro. model	Max depth (m)	Year	Date range	Tow type	*n*
	South Arm (monthly surveys)								2021-2022	2021: Jun 9, Aug 12, Sept. 8, Nov. 9, Dec. 14 2022: Feb. 8, Mar. 29, Apr. 22, May 17, Jun 7, Jul 6	Vertical	31 (2-3 per month)

[1] Foreman et al. (submitted for publication); [2]: Filgueira et al. (2021); [3] Guyondet et al. (unpublished), [4]: Filgueira et al. (2015); [5]: Bacher et al. (2016); [6]: Lavaud et al. (2020); [7]: Guyondet et al. (2015); [8] Gallardi et al. (in development, 2023).

31

In each region, mesozooplankton samples were collected using plankton nets at three stations per site (i.e. bay) at low and high tide for three consecutive days, although there were deviations to this sampling strategy (see Appendix 1 for a complete overview of sampling effort per tide phase). The net mesh of all tows was 250 µm, except a 236 µm net was used for the August 2020 dataset in Lemmens Inlet (Pacific), and a 150 µm net was used in St Peters (Gulf), due to a lack of available 250 µm nets. These were assumed to produce similar results, since samples were all sieved in the lab for specific fraction sizes, and particles <250 µm were further removed during FlowCam imaging (see below). Sample collection covered both the holoplankton (i.e., planktonic for their entire life cycle) and meroplankton (i.e., planktonic for one portion of their life cycle).

At each station, zooplankton tows were obtained to sample the full water column to overcome the confounding factor of vertical migrations. To target approximately 7000 L filtered water volume, one or two tow(s) were collected and combined within a single jar. Vertical, oblique, or horizontal tows were collected, with the type of tow selected according to depth of the water column (see Table 1 for the type of tow used). The tow aimed to sample as much of the water column as possible, without the net contacting the seabed (1-2 m above the seabed). When possible, vertical tows were used, in which nets were lowered to 1-2 m above the seabed at a rate of approximately 0.5 m per second, and retrieved at approximately 1 m per second. In shallower waters where a vertical tow would result in minimal zooplankton being collected, oblique tows were obtained. For oblique tows, the tow was started at 3 m above the seafloor, and slowly raised through the water column, starting at the deep end and moving towards the shore. Lastly, horizontal tows (i.e., used in the shallowest waters) were obtained at a fixed depth of approximately 1 m below the surface. For horizontal and oblique tows, multiple 3 minute tows were collected, and a tow speed of approximately 2-3 knots was used to limit avoidance of the nets by the zooplankton. Upon retrieval, samples were preserved in a 4% solution of buffered formaldehyde. A calibrated mechanical flowmeter (General Oceanics Inc.; Product code 203001) was mounted through the net opening to calculate the filtered water volume. In instances where the water volumes calculated from the flowmeter appeared unreliable, the water volume filtered was instead calculated using the depth of the water column or length of the tow.

2.2 Sample laboratory processing

Samples were split into four equal subsamples using a Folsom Plankton Splitter and each subsample was used for different measurements including (1) biomass, (2) imaging (i.e. abundance, size spectra, community structure) and (3) traditional taxonomy (image/specimen reference collection, quantitative assessment, diversity). This report presents only results for the community structure obtained from the imaging system, while the other components are being analyzed as part of ongoing departmental work. The terminology “samples” is used below instead of subsample, but in fact they are thus only 0.25 samples. Samples were analyzed using a flow imaging microscopy system, FlowCam Macro (Yokogawa Fluid Imaging Technologies, Inc.) Detailed methods of the FlowCam procedures are in progress as a separate report, which will also include a detailed comparison of counts of mesozooplankton taxa obtained from traditional microscopy to counts obtained by the FlowCam. However, following the recommendations of Owen et al. (2022), key details required for creating reproducible work involving FlowCam technology is included in tabular format in Appendix 2. A brief description of the laboratory procedures is also described below.
Samples were rinsed through a series of stacked sieves; 2 mm mesh sieve stacked on a 125 µm or 212 µm mesh sieve. Taxa collected on the 2 mm mesh that were <5 mm, were processed using a 5 mm flow cell, while the specimens collected on the 125 µm or 212 µm mesh were kept separate and run through the FlowCam using a 2 mm flow cell. Particles >5 mm were uncommon, and too large to fit within the 5 mm flow cell. These were therefore not included in the study due to the size limits of the instrumentation. The specimens from both

size fractions (i.e., <2 mm and 2 mm-5 mm) were then rinsed into a sample beaker containing approximately 400 ml of 0.2% Triton-x. Using a large volume of 0.2% Triton-x and a magnetic stirrer in the sample beaker was shown to be successful in reducing the clumping of plankton. Images were completed for the full samples. Based on variable funding between regions and years and the difference in taxa and debris to classify, the number of images identified varied between sample sets. *VisualSpreadsheet* version 5.6.14 was used to classify images for data collected in 2020 in Newfoundland, while *VisualSpreadsheet* version 4.18.5 used for all other samples (Yokogawa Fluid Imaging Technologies, Inc. 2020, n.d.). First, images of objects <250 µm in length were removed using a pre-set filter. Then, a fraction of the samples were cleaned by removing images of debris, fragments of plankton (i.e. <15% body size), bubbles, cropped images and clumped plankton. Images produced by the FlowCam appear as black and white pictures, and the images of confirmed zooplankton were then classified in the categories as described in Appendix 3. These categories have been defined specifically for this project by experts in zooplankton taxonomy using the shapes of the organisms in the images collected from all regions. For Copepoda, the most abundant zooplankton taxon, there are six copepodite developmental stages (Ci to Cvi). However, for the FlowCam reference collection, Ci-Ciii are classified only at the order level, due to the limitation in image quality of the FlowCam. Copepodite developmental stages Civ-Cvi were identified to the genus level, because that is when the copepod shape becomes discernible from FlowCam images. Although the entire subsample was run through the FlowCam, due to time constraints, generally only a fraction of the specimens with entire sample were identified by the taxonomists. The identification of specimens was manually performed by the taxonomists using the two-dimensional black and white digital images in VisualSpreadsheet. These classifications are also being used to create libraries for the automated identification of mesozooplankton taxa using machine learning algorithms, which is being investigated as part of ongoing departmental work.

2.3 Study area descriptions

2.3.1 Pacific region

Within the Pacific region, samples were obtained solely from Lemmens Inlet on the west coast of Vancouver Island (Fig. 1D). The sampled site covers 6.44 km^2, and has complex bathymetry, where depths increase toward the middle of the inlet, and generally range from 12-17 m (Table 1). A maximum depth of 27.9 m occurs near the Mid station. The tidal cycle is mixed semidiurnal, and the nearest Canadian Hydrographic Service (CHS) tide station (Tofino 08615, 49.154°N, 125.913°W) experiences a tidal range from 0.74 m Lower Low Water Mean Tide (LLWMT) to 3.39 m Higher High Water Mean Tide (HHWMT). Samples were obtained as vertical tows across four time periods including August 2020 (n = 18), March 2021, June 2021 (n = 18), and September 2021 (n = 12). Samples were obtained at high tide and low tide, at three stations, over either 2 or 3 days total (Appendix 1). Due to a handling error, the samples in March 2021 were combined by tide, resulting in a single “High Tide” sample (consisting of data from five combined samples), and a single “Low Tide” sample (consisting of data from six combined samples). Stations were positioned with approximately 1.6 km spacing, for a 3.2 km total distance between the Inner and Outer stations. Within the study area (Fig. 1D), bivalve aquaculture leases cover 0.23 km^2, or 3.6% of the surface area. Pacific oysters (*Crassostrea gigas*) are the main cultured bivalve within Lemmens Inlet.

2.3.2 Maritimes region

The Argyle sampling site is located in southern Nova Scotia and comprises a highly complex coastline with numerous channels and islands (Fig. 1E). The region opens into the Atlantic Ocean, and when using this boundary as an approximate site delineation (Fig. 1E), covers a

surface area of 133.66 km^2 (Table 1). For most of the site, depths are less than 6 m, although certain areas have carved underwater channels with depths ranging from 13.0-16.5 m. The exact tidal range at the study stations is unknown, but tides from the nearest CHS station (Wedgeport 00374, 43.733°N, 65.983°W) range from 0.66 m LLWMT to 3.71 m HHWMT. Samples were collected from August 30 to September 1, 2021 (*n* = 15, oblique transects) at a range of tide phases (Appendix 1). The South and Central stations were spaced by 5.2 km, and the Central and North ones by 3.1 km. Eastern oysters (*Crassostrea virginica*) represent the main cultured bivalve within the site, and leases cover a surface area of 0.62 km^2 (i.e., 0.45% of the total bay area), although leases were empty at the time of sampling.

Sober Island is a small lagoon on the eastern shore of Nova Scotia (Fig. 1F) with an approximate bay area of 0.90 km^2 and average depth of 2.9 m (Filgueira et al. 2021). Sober Island is separated from the ocean by a narrow channel (~20 m wide, ~1 m depth) and receives minimal freshwater input (Filgueira et al. 2021). A hydrodynamic model was constructed for Sober Island by Filguiera et al. (2021), who used a Finite Volume Community Ocean Model (FVCOM) to evaluate the ecological carrying capacity of bivalve aquaculture. Results showed water renewal times of less than three days for most of Sober Island, although some small sections in the northwestern and southwestern portions of the bay had water renewal times exceeding 12 days. Samples were obtained on August 27, 2021 (*n* = 12, horizontal transects) at various tide phases, with stations separated by distances ranging from 0.5 km - 1.0 km (Table 1, Appendix 1). Eastern oysters are the farmed bivalves within Sober Island and leases cover 0.09 km^2, or 9.6%, of the bay.

Country Harbour is situated on the eastern shore of Nova Scotia and covers an approximate surface area of 10.4 km^2 (Fig. 1G). The site is a long channel that opens into the exposed Atlantic Ocean. Depths generally range from 10-17 m, and reach a maximum depth of 21.9 m near the Mid station. Tides are semidiurnal, and the nearest tide station (Isaacs Harbour, 00535, 45.183°N, 61.667°W) has a tidal range from 0.53 m LLWMT to 1.87 m HHWMT (Table 1). Samples were obtained on August 24, 2021 (*n* = 6, vertical tows) from both high and low tide phases (Appendix 1). Sampling stations span the length of the bay and were approximately evenly spaced at distances of 3.1 km, for a total distance of 6.2 km separating the Inner and Outer stations. Eastern oysters are the main cultured bivalve at Country Harbour, with leases covering 0.84 km^2 (8.1% of total bay area), although leases were empty at the time of sampling.

The Whitehead sampling site is located on the northeast coast of Nova Scotia (Fig. 1H). The sampled area consists of a long, narrow channel 1.68 km^2, that opens into Whitehead Harbour (Table 1). Within the channel, depths generally range from 4-7 m but reach a maximum depth of 14.3 m near the Mid station. Tides are semidiurnal and range from approximately 0.45 m LLWMT to 1.80 m HHWMT (Whitehead tide station 00545, 45.233°N, 61.183°W). An FVCOM hydrodynamic model was constructed for Whitehead by Filgueira et al. (2021), which calculated that water renewal time for the channel exceeds 20 days. Sampling occurred on August 25, 2021 (*n* = 9, vertical tows) along a linear path at three tide phases (Appendix 1). The Inner and Mid stations were located 1.1 km apart, and the Mid and Outer stations were spaced 2.1 km apart. Within the site, there is one large lease (0.23 km^2) for eastern oysters, which covers 13.9% of total area.

2.3.3 Gulf region

Cocagne is a large (18.90 km^2) bay on the eastern coast of New Brunswick (Fig. 1I). Cocagne Island separates the bay from the Northumberland Strait at two main openings. Depths are generally shallow (0.3 m-2.1 m) and tides range from approximately 0.32 m LLWMT to 1.05 m HHWMT (Cocagne tide station 01812, 46.333°N, 64.617°W; Table 1). Samples were obtained from horizontal transects at three stations, which had varying

exposure to the Strait (Fig. 1I). The Central station was located approximately 2.4 km from the North and South stations, while North and South separated by 4.4 km. Three samples were collected on July 21, 2021 (one at each station, low tide only), while three additional samples were collected on August 26, 2021 (one at each station, mid-rising tides only) by horizontal transects (Appendix 1). The study area consists of numerous aquaculture leases, mostly eastern oysters, covering a total area of 1.44 km^2, i.e., 7.6% of the bay area.

Malpeque is a large bay composed of multiple sub-basins covering a surface area of 207.40 km^2 (Fig. 1J) on the north shore of Prince Edward Island (PEI). The bay opens into the Gulf of St. Lawrence at three openings and receives freshwater input from 12 rivers and several smaller streams (Lavaud et al. 2020). Depths are generally shallow (<10 m), and reach a maximum depth of 14.2 m between the North and Central stations. Tides range from approximately 0.24 m LLWMT to 0.96 m HHWMT (Malpeque tide station 01905, 46.533°N, 63.700°W; Table 1). The potential expansion of the aquaculture industry in Malpeque Bay drove the development of a series of hydrodynamic models. For example, a two-dimensional spatially explicit hydrodynamic model developed in Filgueira et al. (2015) to evaluate the potential effects of varying levels of mussel aquaculture expansion on the ecological carrying capacity in the bay. This model was expanded in Lavaud et al. (2020) to incorporate sea lettuce, wild and cultured oysters, and clams. Additionally, Bacher et al. (2016) used Markov Chain to evaluate the residence time (21-35 days in the sampling area), and connectivity with respect to aquaculture in the bay. Three samples were obtained on Sept 29, 2020 at three locations (all at low tide, horizontal transects; Appendix 1), termed South, Central, and North. Stations were spaced at distances ranging from 3.6 to 4.5 km apart. The blue mussel (*Mytilus edulis*) is the dominant bivalve in terms of biomass produced (5120-9600 t; Filgueira et al., 2015), although cultures of eastern oysters are also present. The numerous leases cover a surface area of 14.76 km^2, equivalent to 7.1% of the surface area of the bay.

St. Peters Bay is an elongated inlet on the north shore of PEI, covering an area of 15.78 km^2 (Fig. 1K). The bay opens into the Gulf of St. Lawrence, and is mostly shallow, with depths ranging from 3-5 m throughout the length of the bay. Tides range from approximately 0.23 m LLWMT to 0.79 m HHWMT (St. Peters Bay tide station 01935, 46.433°N, 62.733°W; Table 1). Except at the region exposed to the Gulf of St. Lawrence, most of the bay experiences poor flushing and tidal currents are several centimeters per second (Guyondet et al. 2015). A spatially explicit coupled hydrodynamic-biogeochemical model developed by Guyondet et al. (2015) suggests that water renewal time increases along the length of the bay, taking up to ~90 days in the innermost region. Samples were obtained along the length of the bay, separated by 4.1 km (8.1 km total distance between Inner and Outer stations) from September 1-4, 2020, at a range of tide phases (n = 26, horizontal transects) (Appendix 1). Within St. Peters, bivalve aquaculture consists of a combination of blue mussels and eastern oysters, with leases covering 6.37 km^2, or approximately 40.4% of the bay area.

2.3.4 Newfoundland region

South Arm, Newfoundland, is a long channel that opens to the Atlantic Ocean (Fig. 1L). The innermost portion of the channel has a surface area of 11.31 km^2 (Table 1). South Arm is the deepest of all study sites within AMP, with spatially variable depths exceeding 45 m. Tides from the nearest CHS station range from 0.27 m LLWMT to 1.18 m HHWMT (Leading Tickle tide station 01087, 49.502°N, 55.447°W). Samples were collected across a range of months for a full examination of seasonal dynamics within the site. As for other AMP sites, multiple samples were collected in September 2020 (n =10) and October 2021 (n = 12) to examine the effects of station and tide phase on mesozooplankton composition. In addition, either two or three samples were obtained monthly from June 2021 to July 2022 (excluding January 2022) for a more detailed examination of temporal dynamics (Appendix 1). Across all months, samples were obtained from five stations in total, separated at various distances, but the Inner and Outer stations were located ~3.8 km apart. All samples were obtained as

vertical tows. The region includes two large leases for blue mussels (2.80 km^2), which cover 24.8% of the bay area.

2.4 Adjustments to the taxa list

As mentioned, specimens were identified to a predetermined taxonomic level (Appendix 3). Taxa were then corrected for minor discrepancies in names (e.g., fixed typos, removed underscores, adjusted capitalization, etc.). Next, other adjustments were made to the list of taxa for consistency in the dataset. Since this study focused on broad biodiversity patterns, at each taxonomic level specified in Appendix 1, we combined the stages of the various taxa to prevent the over-specification of stages in some taxa compared to others. For example, *Euphausiacea* calyptopsis, furcilia and nauplii were combined as one taxa (*Euphausiacea* larvae), as opposed to treating them as three separate taxa. This also helps overcome discrepancies, where some taxa (e.g., *Cirripedia*) had larval stages separated in some datasets (e.g., *Cirripedia* cypris and *Cirripedia* nauplii) but combined in others (*Cirripedia* cypris/nauplii). Furthermore, invertebrate trochophores and eggs were difficult to decipher and were often combined by the taxonomists. Therefore, Osteichthyes egg and larval stages were also combined as one taxonomic group. A more detailed overview of additional adjustments to the taxa list is provided in Appendix 4.

2.5 Converting counts to abundances in seawater

Raw mesozooplankton counts measured by the FlowCam were converted to abundances in seawater (abund; individuals m^{-3}) for each sample following the equation:

$$\text{Abund.} = counts * \frac{1}{fraction\ analyzed} * \frac{1}{water\ volume} * \frac{4\ subsamples}{1\ tow} \quad (1)$$

Where *counts* represent the number of individuals identified by the taxonomist, *fraction analyzed* represents the portion of the sample analyzed by the taxonomist, and *water volume* is the volume filtered from each tow. Values were multiplied by 4 (the final term of *Equation 1*) since the total obtained was split in 4 using a Folsom splitter and only 1 sample was run through the FlowCam. For data in the Pacific region, zooplankton from two tows were combined to gain a representative sample of the zooplankton community. Therefore, the *count*s in *Equation 1* were summed from two samples, and the *water volume* was the sum of the water volumes from both tows.

All data cleaning and consolidating, and statistical analyses (next section) were conducted using R v. 4.2.2 (R Core Team 2022). The code for all processes is publicly available at https://github.com/AtlanticR/AMP.

2.6 Statistical analysis

2.6.1 Objective 1: Determining the optimal sampling effort per site

Hill numbers

While multiple biodiversity indices exist to characterize community structure, the use of Hill numbers (Hill 1973) is facing a resurgence (Chao et al. 2014; Cox et al. 2017). This family of indices has many advantages over other diversity indices (e.g., see Chao et al. (2014) or Jost (2006) for a more thorough review). Hill Numbers integrate species richness and incidence (i.e., presence) information into a unified class of diversity metrics, and are parameterized by a diversity order *q* where higher values of *q* place an increased emphasis on incidence frequency.

For incidence data, Hill Numbers are interpreted as the effective number of equally frequent species (taxa), and are defined as (Chao et al. 2014):

$$ {}^{q}\Delta = \left(\sum_{i=1}^{S} \left[\frac{\pi_i}{\sum_{j=1}^{S} \pi_j} \right]^{q} \right)^{\frac{1}{1-q}} \quad q \geq 0 \text{ and } q \neq 1 \qquad (2) $$

where *S* represents the number of species (taxa), π denotes the incidence probability of the *i*th taxon, and *q* determines the sensitivity of ${}^{q}\Delta$ to the relative frequencies of each taxon. When *q* = 0, the equation considers taxa equally, regardless of their relative frequencies, and therefore equates to richness (Hill 1973; Chiu and Chao 2014; Hsieh et al. 2016).

Since equation *(2)* is undefined when *q* = 1, the boundary value is used, giving:

$$ {}^{1}\Delta = \lim_{q \to 1} {}^{q}\Delta = exp\left(\sum_{i=1}^{S} \frac{\pi_i}{\sum_{j=1}^{S} \pi_j} log \frac{\pi_i}{\sum_{j=1}^{S} \pi_j} \right) \qquad (3) $$

which equates to Shannon diversity for incidence data. This is equivalent to the exponential of Shannon entropy based on relative incidences in the assemblage, and can be interpreted as the number of frequent taxa in a sample (Chao et al. 2020).

For *q* = 2, equation *(2)* becomes:

$$ {}^{2}\Delta = 1/\sum_{i=1}^{S} \left(\frac{\pi_i}{\sum_{j=1}^{S} \pi_j} \right)^{2} \qquad (4) $$

which is the Simpson diversity for incidence data. This is equivalent to the inverse Simpson concentration based on relative incidences, and is interpreted as the number of highly frequent taxa in a sample (Chao et al. 2020).

Rarefaction and extrapolation curves

Because the specimens were identified to the lowest taxonomic level and represent mixed taxonomic levels, as is common in zooplankton studies (e.g., Schartau et al. 2021; Gutierrez et al. 2022), the biodiversity indices were calculated using these levels and the terminology was updated to reflect these terms (e.g., “taxonomic richness” was used in place of “species richness”). For each site, sample-based rarefaction and extrapolation curves were constructed to explore how taxa diversity increases with sampling effort. For sample-based rarefaction, data within each sample (i.e., zooplankton tow) are first converted to incidences (i.e., presence-absence). For richness, a taxa accumulation curve is then created by randomly selecting samples, and plotting the total number of taxa detected (*y*-axis) as a function of sample size(*x*-axis). When the process of randomly resampling is repeated multiple times, the resulting plot is referred to as a rarefaction curve, which represents the statistical average of multiple taxa accumulation curves (Chiarucci et al. 2008). At first, the curve generally rises steeply as each new sample results in new taxa being observed. As more samples are analyzed, the slope often levels off as fewer new taxa are encountered. These curves can also be extrapolated to show the predicted change in diversity beyond what was collected (Chao et al. 2014).

Rarefaction curves therefore provide important information for monitoring programs. First, taxa richness is largely affected by sampling effort, since more samples will result in new taxa being encountered (Colwell et al. 2012). Richness is typically not comparable among sites with a different number of samples obtained, since the differences between sites may be more reflective of sampling effort, rather than true differences in richness (Colwell et al. 2012). Rarefaction therefore offers a means to standardize datasets to enable these comparisons (Chao et al. 2014). Second, these curves can also be used to visualize how much new information is gained (i.e., new taxa observed) with additional sampling. For

example, if the taxa accumulation curve reaches or nears an asymptote (i.e., few new taxa are being observed with each sample obtained), collecting more samples beyond this point may not be best use of resources, as little new information is gained. Predicted taxa richness within a site can also be calculated (i.e., asymptotic estimators, or Chao2 for incidence richness data; Chao 1984, 1987).

Rarefaction and extrapolation curves for richness, Shannon diversity and Simpson diversity were created, following the methods of Hsieh et al. (2016). Extrapolations were calculated and plotted up to double the sample size of each site, and 500 bootstrap replicates were used to estimate the 95% confidence intervals. These were not extrapolated further, as the extrapolations become less reliable beyond this point (Chao et al., 2014). Asymptotic estimators (i.e., the predicted diversity value in the bay) were calculated for each of the Hill numbers, with 95% confidence intervals (see Chao et al. 2014 for derivations). Often, monitoring programs base the required sampling effort on taxa richness alone (Chao et al. 2009); however, the rarefaction curves are provided for Shannon and Simpson diversity as they provide additional biodiversity information for each site (Chao et al. 2014; Chao et al. 2020). Sampling completeness was then calculated for richness as the ratio of observed to estimated richness to assess the extent of undetected diversity, and an additional graph was created to visualize the change in sampling completeness with increasing sampling effort. For brevity, only text descriptions for richness and its associated metrics (e.g., asymptotic richness and completeness) are included. Statistics are provided for the Shannon and Simpson indices in graphical and tabular format for a comprehensive analysis of biodiversity trends, but are not discussed in detail. In addition, this represents the first baseline study of diversity of zooplankton in coastal bivalve aquaculture sites in Canada. A fixed and absolute sampling target is therefore not provided, as these targets are often arbitrary (e.g., Chacoff et al., 2012). Instead, graphs visualizing the change in sampling completeness for each additional tow were provided, up to double the sampling size. These graphs are provided as guidance for developing optimal sampling plans in future years, recognizing that more samples are required to capture a greater number of rare taxa, which may play important roles in ecosystem functioning (Cao et al. 1998). We also recommend recreating these rarefaction curves in subsequent years as more data are added, to ensure these patterns remain representative. All rarefaction and extrapolation curves were generated using the iNEXT package (Hsieh et al. 2016).

While sample-based rarefaction is generally conducted using a standardized area or volume (Gotelli and Colwell 2001), this is not feasible for samples collected with zooplankton tows, as it is difficult to obtain a similar volume of water in each sample. To account for the differences in water volume filtered, the *x*-axes of each graph were rescaled to reflect the representative water volume filtered and analyzed from each sample. To obtain this value, the water volume of the sample was multiplied by the *fraction analyzed* (see *Equation 1*). This representative water volume provides a more comparable measure of effort among sites than a “zooplankton tow”. Some R packages have arguments to directly incorporate these differences in water volume for each sample (e.g., the *weights* argument in the *specaccum* function from the R *vegan* package; Oksanen et al. 2022; applied in Bessey et al. 2020). However, setting the weights argument does not affect the shape of the interpolated curve, only the associated error (Oksanen et al. 2022). Therefore, although the iNEXT package does not currently have these capabilities, we still used it for this work due to its more robust calculations for extrapolations (Chao et al. 2014), and integrated use with Hill Numbers. However, we did not proceed with significance testing among sites (e.g., if richness is significantly different among sites), which is often evaluated using overlapping confidence intervals (Chao et al. 2014; Chao et al. 2020), since these would therefore be affected by differences in water volume.

2.6.2 Objective 2: Characterizing patterns in zooplankton community structure among regions, months, and sites

As an initial graphical approach to visualize biodiversity patterns, Venn diagrams were constructed to show the number and percent overlap of taxa among sites for each region. The Venn diagrams were reflective of the true sampling effort, and sites with a greater number of samples may therefore show a greater number of taxa (Colwell et al. 2012). The Venn diagrams were created using the *Venn* and *process_data* functions from the *ggVennDiagram* package (Gao 2022), and the outputs were visualized using the *ggplot* function from the *ggplot2* package (Wickham 2016).

Next, as a measure to graphically display sample similarity based on zooplankton composition, ordinations were constructed using two-dimensional non-metric multidimensional scaling (NMDS). NMDS ordinations visually display information in a similarity or distance matrix (Borg and Groenen 2005), and samples with similar zooplankton composition (i.e., taxa and their abundance), are visualized closer together, while more dissimilar samples are located further apart. Various ordinations were therefore created to examine sample similarity at various spatial scales, including:

1. An NMDS with all sampling data, to visualize similarities and differences in composition among regions;
2. An NMDS ordination for regions exhibiting a high degree of overlap (identified in the ordination above), to visualize which sites are responsible for the similarity; and
3. Separate NMDS ordinations for each region, to visually examine trends among sites (for Maritimes and Gulf regions) or months (for Pacific and Newfoundland data).

Ordinations were constructed using a Bray-Curtis dissimilarity matrix of square root transformed abundance data (i.e., counts per sample were converted to ind m^{-3} in seawater following *Equation 1*.) The overall goodness-of-fit is provided by the Kruskall's stress (1964) which measures how well the square root transformed Bray-Curtis dissimilarity matrix can be displayed in two dimensions. Values range from 0 to 1 with values closer to 0 indicating a better fit (Clarke 1993). Ordinations were created using the *metaMDS* function from the *vegan* package (Oksanen et al. 2022).

Tests for homogeneity of multivariate dispersion were conducted among regions, sites, and months. These tests evaluate the null hypothesis of no differences in dispersion between each observation and the group's spatial median, an alternative form for the group centroid (Anderson 2006a). If tests in multivariate dispersion are significant, a significant result from the permutational multivariate analysis of variance (PERMANOVA, explained in more detail below) may therefore be the result of differences in multivariate dispersion (Anderson 2006a). However, tests for homogeneity of multivariate dispersion provide useful information on the biodiversity of communities in their own right, and multivariate dispersion has been suggested as a measure of beta diversity (Anderson et al. 2006b). Tests were run using the *betadisper* function from the *vegan* package in R, with the *permutest* function to determine significance (Oksanen et al. 2022). Pairwise comparisons of group mean dispersions were assessed using *permutest.betadisper* to test for differences between individual regions or sites. Boxplots were then created to visualize the distances of each observation to the spatial median for each group.

PERMANOVA was then used to test the significance of groups (i.e., regions, sites, and/or months, as specified above) with the *adonis2* function. PERMANOVA tests the null hypothesis that centroids of all groups are equivalent using the chosen dissimilarity matrix (Anderson 2017). The resulting test statistic is a *pseudo-F* statistic, where larger values indicate a more pronounced separation among groups (Anderson 2017). When significant, pairwise comparisons between each individual group were conducted using the *pairwise.adonis2* function from the *pairwiseAdonis* package (Arbizu 2017). The function for pairwise comparisons similarly returns *pseudo-F* values, which were converted to *pseudo-t*

values by taking the square root of the *pseudo-F* value (Anderson 2008). While *pseudo-F* values can be used, *pseudo-t* values are instead presented as they provide a more natural statistic for these comparisons, and are a direct analogue to *t*-values in standard univariate post-hoc testing (Anderson 2008). PERMANOVA and tests for homogeneity of multivariate dispersion were performed on a Bray-Curtis dissimilarities matrix of square root transformed abundance data, and significance was determined with 9999 permutations of the input data.

Lastly, when significant ($P<0.05$) differences were identified by the pairwise PERMANOVAs, similarity percentage (SIMPER) analysis was used to identify the zooplankton taxa that contributed most to the dissimilarities between significant groups. SIMPER was run using the *simper* function from the *vegan* package (Oksanen et al. 2022).

2.6.3 Objective 3: Characterizing the role of tide phase and station on zooplankton composition

As an initial approach to explore the role of tide phase and stations on zooplankton composition, relative abundance charts were created to show the percent breakdown of the zooplankton taxa for each sample. Samples were grouped by both tide phase and station as facets (panels) using the *facet_nested* function from the *ggh4x* library (Brand 2022). To enable visual comparisons and avoid displaying too many classes, a maximum of eight classes were displayed; therefore, the top seven most abundant taxa in each bay were displayed; all other taxa were combined into the category “Other”.

Next, a similar approach to the previous objective was pursued to explore patterns in zooplankton composition using multivariate statistics. NMDS ordinations were constructed for each site using the Bray-Curtis dissimilarities of square root transformed abundance, and samples were displayed with colour and symbols to explore the role of station and tide phase, respectively.

Within several sites, the effect of tide phase and station on zooplankton composition was evaluated using PERMANOVAs. However, when the number of observations is low, there may not be enough unique permutations to make statistical inferences (Anderson 2008; Oksanen et al. 2022). Following the guidance of Anderson et al. (2008), models were not constructed for bays which would result in PERMANOVAs with <100 unique permutations, since at this level, the smallest possible P-value obtained is 1/100 = 0.01; a common threshold for significance testing. For a balanced design with *a* groups and *n* samples per group, the number of distinct outcomes (i.e., unique permutations) for the PERMANOVA *Pseudo-F* statistic is $(an)!/[a!(n!)^a]$ (Clarke 1993). Accordingly, for *post-hoc* testing, two groups of five samples would be the lowest number of samples per group when 100 unique permutations are used as a cutoff (since $(10)!/[2!(5!)^2] = 126$ unique permutations, whereas two groups of four would give $(8)!/[2!(4!)^2] = 70$ unique permutations.) Although there are other approaches to test for significance with lower sample sizes (e.g., Monte Carlo permutations; Anderson and Robinson 2003), these were not pursued since zooplankton distributions are highly patchy (Folt and Burns 1999; O’Brien and Oakes 2020), and focusing on the results of significance testing on such few samples may not lead to ecologically relevant conclusions.

PERMANOVAs were therefore run in sites with at least two groups of five for the *post-hoc* testing (e.g., at least five samples per station, or individual tide phase). Tests were therefore performed on data from Argyle, St. Peters, the August 2020 and June 2021 sampling months from the Pacific region, and for October 2021 from Newfoundland. The effects of tide phase, station, and their two-way interaction on mesozooplankton composition were evaluated by treating variables as factors (with levels High Tide or Low Tide, and station labels according to Appendix 1), which were added sequentially to the model. Tide effects were only tested using samples collected from high and low tide, and not those from mid-

rising or mid-falling tide phases. *Post-hoc* pairwise comparisons were then conducted using the *pairwise.adonis2* function, for factors determined as significant by the PERMANOVA.

For the same sites and months where PERMANOVAs were conducted, tests for homogeneity of multivariate group dispersion were also run prior to each PERMANOVA to evaluate the effects of both tide phase and station. These analyses are restricted to one-way tests (Robertson et al. 2013; Oksanen et al. 2022); therefore, separate models were run to evaluate the effects of tide and station. As in objective 2, these were conducted using 9999 permutations on Bray-Curtis dissimilarities of square root transformed abundance. Lastly, SIMPER analysis was conducted for each significantly ($P<0.05$) distinct group, as identified by the *post-hoc* pairwise PERMANOVA tests, to identify taxa most responsible for the difference in groupings.

As an additional measure to evaluate the role of tides on mesozooplankton communities, two-sample t-tests were conducted to test for differences in abundance, and the three Hill Numbers (i.e., taxa richness, Shannon diversity, and Simpson diversity) between high and low tide phases. Shannon diversity was calculated as the exponential of the Shannon index, and Simpson diversity was represented as the inverse Simpson index (Jost 2006), using values calculated from the *diversity* function in the *vegan* package (Oksanen et al. 2022). Tests were conducted for stations within different sites that had at least three samples for each tide phases, which therefore included: Inner, Mid and Outer stations in Lemmens August 2020, the Mid station for Lemmens June 2021, the Outer station for Sober Island, the Inner, Mid and Outer stations at St. Peters, and the Outer station for South Arm October 2021. Tests were conducted using the *t.test* function from the *lsr* R package (Navarro 2015).

3 RESULTS

3.1 Overview of images per site

The final taxa list (following minor adjustments outlined in Appendix 4) included 70 unique taxa, comprising 1 species, 28 genera, 8 families, 11 orders, 2 suborders, 2 infraorders, 6 classes, 1 superclass, 2 subclasses, 1 subphylum, 7 phyla, and 1 paraphyletic group. Overall, 384,593 individual zooplankton images were identified by the macro-FlowCam including 47,605 from the Pacific region, 60,786 from the Maritimes region, 173,225 from the Gulf region, and 102,977 from Newfoundland (Table 2).

Table 2. Number of mesozooplankton (0.25 mm - 5.00 mm) images identified by the macro-FlowCam for each site and sampling period.

Region	Site	Count
Pacific	Lemmens August 2020	14,127
	Lemmens March 2021	1,999
	Lemmens June 2021	20,016
	Lemmens September 2021	11,463
	Total	**47,605**
Maritimes	Argyle	17,526
	Country Harbour	9,849
	Sober Island	18,763
	Whitehead	14,648
	Total	**60,786**
Gulf	Cocagne	24,510
	Malpeque	17,572
	St Peters	131,143
	Total	**173,225**
Newfoundland	South Arm (all data)	**102,977**
All data	**Total (all regions)**	**384,593**

3.2 Objective 1: Determining the optimal sampling effort per site

3.2.1 Pacific region

In Lemmens Inlet, taxa richness was highest in September 2021 (39) and similar in August 2020 (35) and June 2021 (35) (Fig. 2, Table 3). The rarefaction and extrapolation curves continued to increase for August 2020 and September 2021 up to double the sample size,

and these months had asymptotic richness estimates of 39.25 and 44.73, respectively (Fig. 2, Table 3). The extrapolations appeared to level off for June 2021, which had a richness estimate of 35.47 (Fig. 2, Table 3). Sampling completeness based on richness values was 89.17% (August 2020), 98.67% (June 2021), and 87.19% (September 2021) (Table 3).

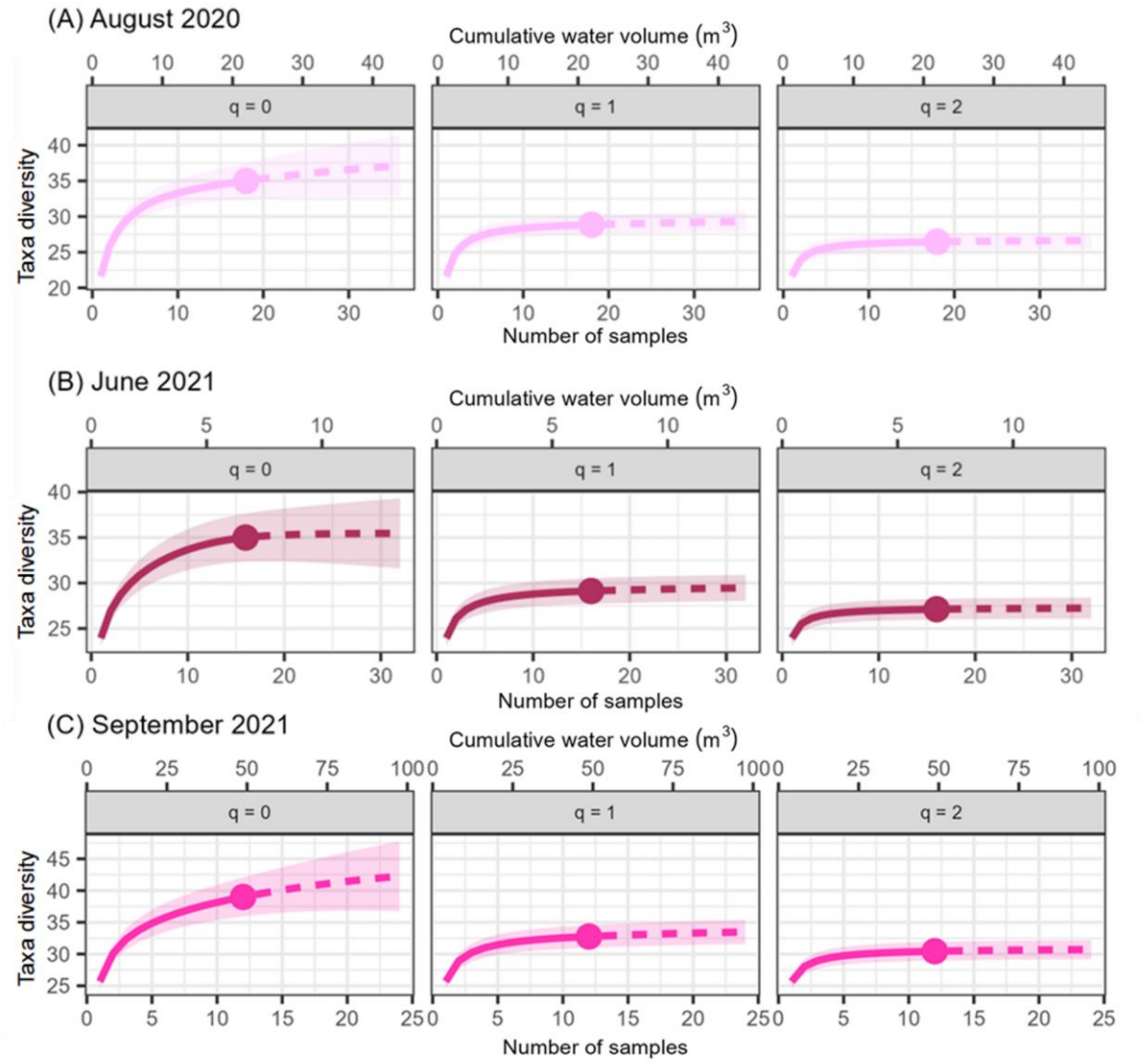

Figure 2. Sample-based rarefaction (solid line) and extrapolation (dashed line) of mesozooplankton taxa richness (q = 0), Shannon diversity (q = 1), and Simpson diversity (q = 2) for sampling months within Lemmens Inlet (Pacific region). Extrapolations were plotted up to double the sample size. The cumulative water volume on the secondary (upper) *x*-axis shows the representative volume of water analyzed per sample, accounting for subsampling and fractions analyzed by the taxonomist (i.e., Rep. vol. in Table 3). Each sample includes the combined data from two separate zooplankton tows. 500 bootstrap replicates were used to estimate the 95% confidence intervals (shaded area), although the true confidence intervals are likely to be larger, given the variability in water volume per tow (Oksanen et al. 2022). Data from March 2021 (*n* = 2) are not shown.

Table 3. Sample-based rarefaction statistics for sampling months within Lemmens Inlet (Pacific region). Tow volume (tow vol., m^3) represents the average volume of water sampled from the zooplankton tows. For the Pacific region, one sample includes the total volume from two combined tows. The percent analyzed corresponds to the average percentage of the sample analyzed by a taxonomist. The representative volume (rep. vol) denotes the amount

of seawater analyzed, accounting for subsampling and fractions analyzed by the taxonomist (see section 2.6.1 in the main text). Observed is the observed diversity value, Estimate is the estimated (i.e., asymptotic) diversity, and Completeness (%) represents the ratio of the observed to estimated values (calculated for richness only). Data from March 2021 (*n* = 2) were not included in the analysis.

Month	Tow vol. (m^3) (sd)	Analyzed (%) (sd)	Rep. vol. (m^3)	Diversity	Observed	Estimate	Completeness
Aug 2020	10.35 (1.86)	46.80 (16.25)	1.21	Taxa richness	35.00	39.25	89.17%
				Shannon diversity	28.85	29.56	
				Simpson diversity	26.47	26.82	
Jun 2021	15.21 (4.38)	11.02 (4.03)	0.42	Taxa richness	35.00	35.47	98.67%
				Shannon diversity	29.12	29.61	
				Simpson diversity	27.12	27.36	
Sept 2021	19.76 (4.41)	79.81 (27.34)	3.54	Taxa richness	39.00	44.73	87.19%
				Shannon diversity	32.76	33.91	
				Simpson diversity	30.44	30.97	

3.2.2 Maritimes region

In the Maritimes region, observed and estimated (in brackets) taxa richness was 26 (33.47) in Argyle, 31 (36.00) in Country Harbour, 28 (33.50) in Sober Island, and 27 (27.15) in Whitehead (Fig. 3, Table 4). The curves continued to increase when extrapolated up to double the sample size for Argyle, Country Harbour, and Sober Island, which had sampling completeness of 77.68%, 86.11% and 83.58%, respectively (Fig. 3, Table 4). The extrapolations appeared to level off for Whitehead, which had the highest sampling completeness of 99.45% (Fig. 3, Table 4).

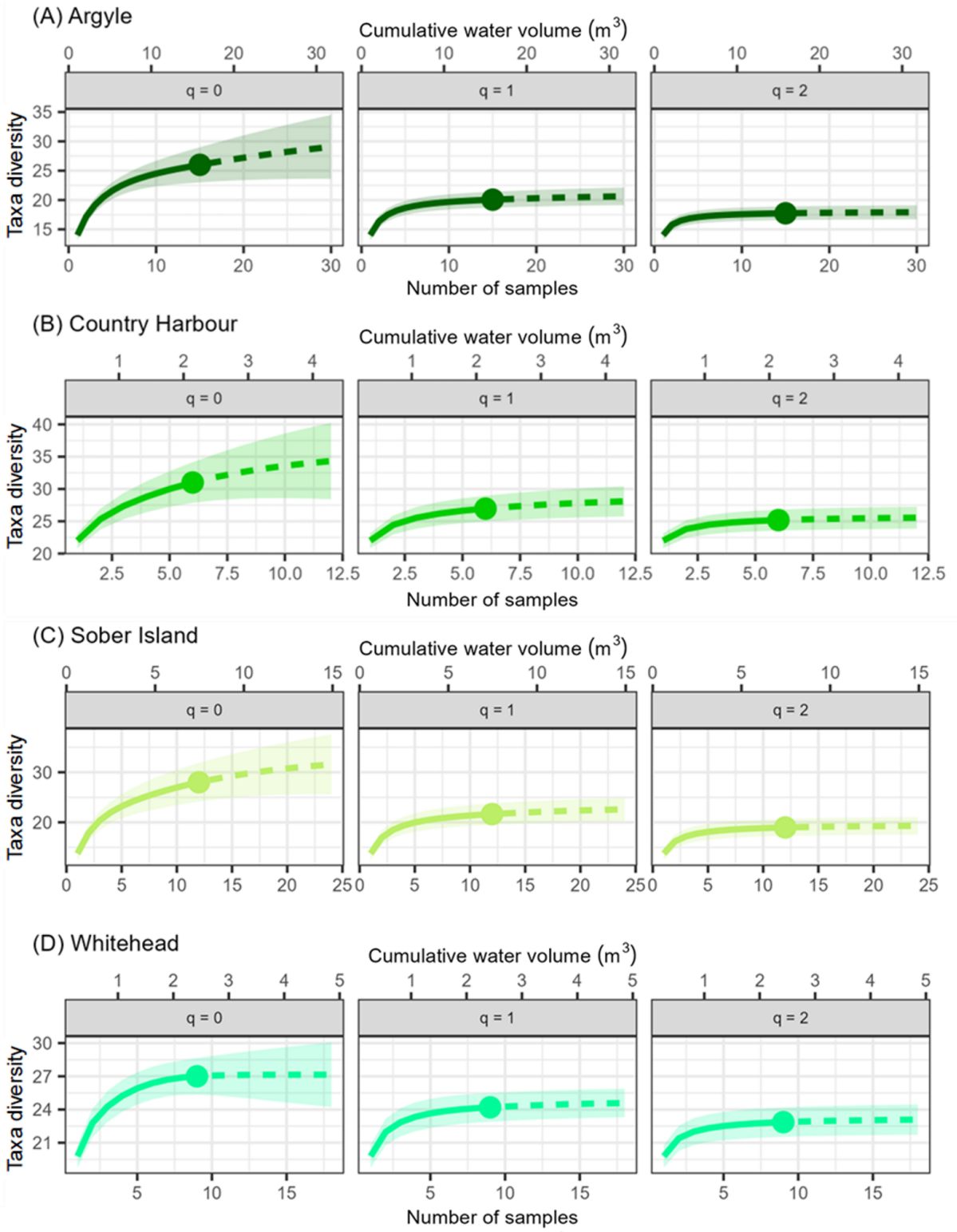

Figure 3. Sample-based rarefaction (solid line) and extrapolation (dashed line) of mesozooplankton taxa richness (q = 0), Shannon diversity (q = 1), and Simpson diversity (q = 2) for sites within the Maritimes region. Extrapolations were plotted up to double the sample size. The cumulative water volume on the secondary (upper) *x*-axis shows the representative volume of water analyzed per sample, accounting for subsampling and fractions analyzed by the taxonomist (i.e., Rep. vol. in Table 4). 500 bootstrap replicates were used to estimate the 95% confidence intervals (shaded area), although the true confidence intervals are likely to be larger, given the variability in water volume per sample (Oksanen et al. 2022).

Table 4. Sample-based rarefaction statistics for sites within the Maritimes region. Tow volume (tow vol., m^3) represents the average volume of water sampled from the zooplankton tows. The percent analyzed corresponds to the average percentage of the sample analyzed by a taxonomist. The representative volume (rep. vol) denotes the amount of seawater analyzed, accounting for subsampling and fractions analyzed by the taxonomist (see section 2.6.1 in the main text). Observed is the observed diversity value, Estimate is the estimated (i.e., asymptotic) diversity., and Completeness (%) represents the ratio of the observed to estimated values (calculated for richness only).

Site	Tow vol. (m^3) (sd)	Analyzed (%) (sd)	Rep. vol. (m^3)	Diversity	Observed	Estimate	Completeness
Argyle	5.31 (4.51)	90.40 (20.32)	1.20	Taxa richness	26.00	33.47	77.68%
				Shannon diversity	20.06	21.05	
				Simpson diversity	17.74	18.08	
Country Harbour	4.06 (0.87)	34.24 (32.70)	0.35	Taxa richness	31.00	36.00	86.11%
				Shannon diversity	26.96	28.72	
				Simpson diversity	25.18	25.93	
Sober Island	7.18 (3.37)	35.29 (28.08)	0.63	Taxa richness	28.00	33.50	83.58%
				Shannon diversity	21.64	23.17	
				Simpson diversity	18.97	19.65	
Whitehead	2.38 (0.76)	47.51 (24.68)	0.28	Taxa richness	27.00	27.15	99.45%
				Shannon diversity	24.20	24.75	
				Simpson diversity	22.86	23.31	

3.2.3 Gulf region

In the Gulf region, observed and estimated (in brackets) taxa richness was 26 (37.25) in Cocagne, 31 (37.00) in Malpeque, and 35 (35.54) in St. Peters (Fig. 4, Table 5). The curves continued to increase when extrapolated up to double the sample size for Cocagne and Malpeque, which had sampling completeness of 68.80% and 83.78%, respectively (Fig. 4,

Table 5). The extrapolations appeared to level off for St. Peters, which had the highest sampling completeness of 98.48% (Fig. 4, Table 5).

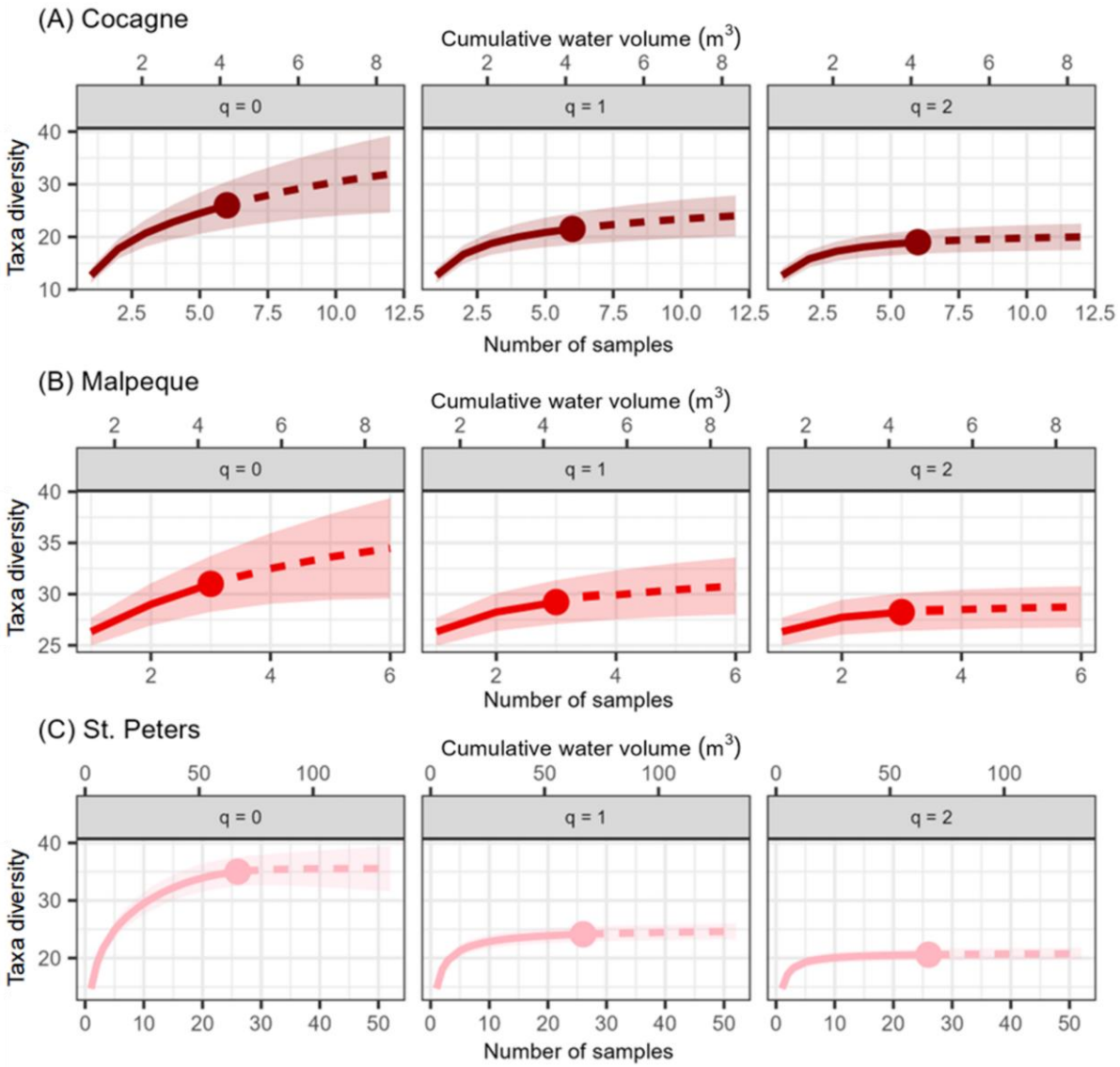

Figure 4. Sample-based rarefaction (solid line) and extrapolation (dashed line) of mesozooplankton taxa richness (q = 0), Shannon diversity (q = 1), and Simpson diversity (q = 2) for sites within the Gulf region. Extrapolations were plotted up to double the sample size. The cumulative water volume on the secondary (upper) *x*-axis shows the representative volume of water analyzed per sample, accounting for subsampling and fractions analyzed by the taxonomist (i.e., Rep. vol. in Table 5). 500 bootstrap replicates were used to estimate the 95% confidence intervals (shaded area), although true confidence intervals are likely to be larger, given the variability in water volume per sample (Oksanen et al. 2022).

Table 5. Sample-based rarefaction statistics for sites within the Gulf region. Tow volume (tow vol., m^3) represents the average volume of water sampled from the zooplankton tows. The percent analyzed corresponds to the average percentage of the sample analyzed by a taxonomist. The representative volume (rep. vol) denotes the amount of seawater analyzed, accounting for subsampling and fractions analyzed by the taxonomist (see section 2.6.1 in the main text). Observed is the observed diversity value, Estimate is the estimated (i.e.,

asymptotic) diversity, and Completeness (%) represents the ratio of the observed to estimated values (calculated for richness only).

Site	Tow vol. (m^3) (sd)	Analyzed (%) (sd)	Rep. vol. (m^3)	Diversity	Observed	Estimate	Completeness
Cocagne	12.76 (2.89)	24.86 (37.41)	0.79	Taxa richness	26.00	37.25	68.80%
				Shannon diversity	21.51	25.87	
				Simpson diversity	19.00	21.11	
Malpeque	34.98 (6.55)	16.75 (3.04)	1.46	Taxa richness	31.00	37.00	83.78%
				Shannon diversity	29.22	31.75	
				Simpson diversity	28.24	29.30	
St. Peters	73.86 (14.62)	13.22 (10.7)	2.44	Taxa richness	35.00	35.54	98.48%
				Shannon diversity	24.14	24.86	
				Simpson diversity	20.59	20.92	

3.2.4 Newfoundland region

In Newfoundland, observed and estimated (in brackets) taxa richness was 28 (50.05) in September 2020 and 32 (35.67) in October 2021 (Fig. 5, Table 6). The curves continued to increase when extrapolated up to double the sample size for both months, which had sampling completeness of 55.94% and 89.71%, respectively (Fig. 5, Table 6).

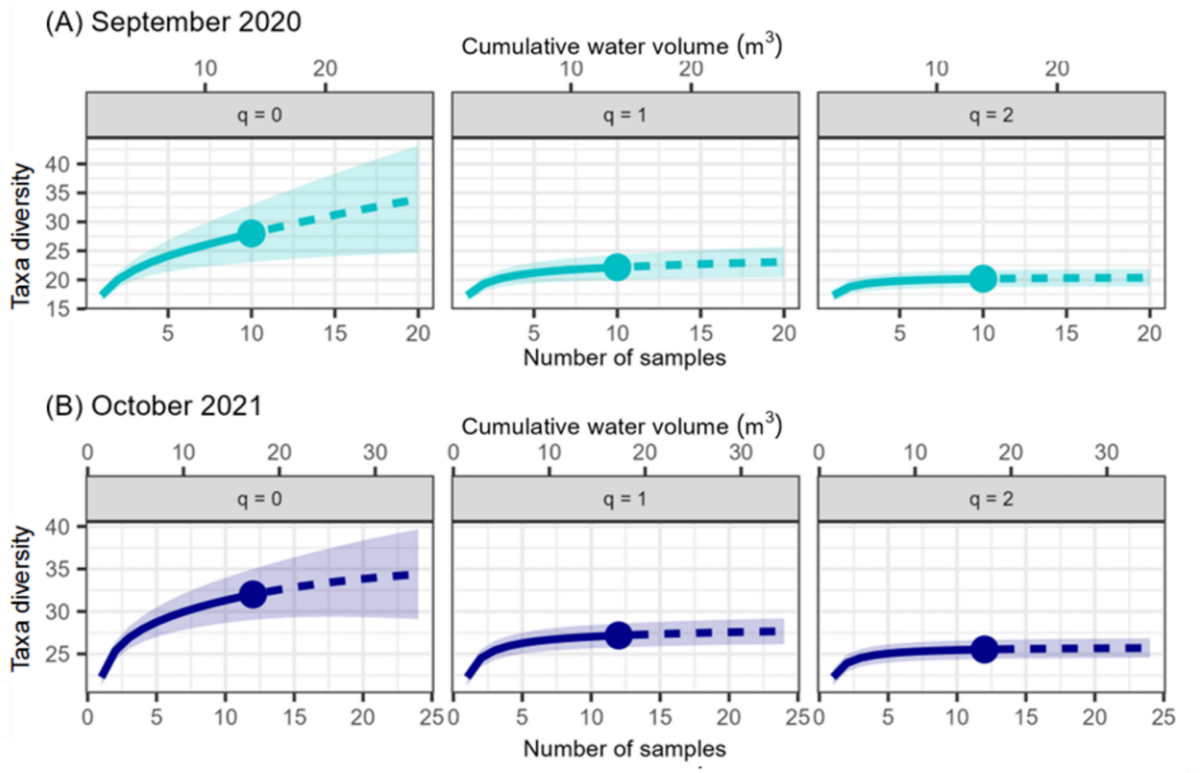

Figure 5. Sample-based rarefaction (solid line) and extrapolation (dashed line) of mesozooplankton taxa richness (q = 0), Shannon diversity (q = 1), and Simpson diversity (q = 2) for two sampling months within South Arm (Newfoundland region). Extrapolations were plotted up to double the sample size. The cumulative water volume on the secondary (upper) *x*-axis shows the representative volume of water analyzed per sample, accounting for subsampling and fractions analyzed by the taxonomist (i.e., Rep. vol. in Table 6). 500 bootstrap replicates were used to estimate the 95% confidence intervals (shaded area), although true confidence intervals are likely to be larger, given the variability in water volume per sample (Oksanen et al., 2022).

Table 6. Sample-based rarefaction statistics for sampling months within South Arm, Newfoundland. Tow volume (tow vol., m^3) represents the average volume of water sampled from the zooplankton tows. The percent analyzed corresponds to the average percentage of the sample analyzed by a taxonomist. The representative volume (rep. vol) denotes the amount of seawater analyzed, accounting for subsampling and fractions analyzed by the taxonomist (see section 2.6.1 in the main text). Observed is the observed diversity value, Estimate represents the estimated (i.e., asymptotic) diversity, and Completeness (%) represents the ratio of the observed to estimated values (calculated for richness only).

Site	Tow vol. (m^3) (sd)	Analyzed (%) (sd)	Rep. vol. (m^3)	Diversity	Observed	Estimate	Completeness
Sept 2020	5.54 (2.37)	100.00 (0.00)	1.39	Taxa richness	28.00	50.05	55.94%
				Shannon diversity	22.17	24.10	
				Simpson diversity	20.18	20.56	
Oct 2021	8.83 (0.43)	65.11 (5.59)	1.44	Taxa richness	32.00	35.67	89.71%
				Shannon diversity	27.17	27.96	
				Simpson diversity	25.52	25.87	

3.2.5 All regions

Sampling completeness varied for each site, with the highest values observed in Whitehead (99.45%, Maritimes region), Lemmens June 2021 (98.67%, Pacific), and St. Peters (98.48%, Gulf), which were obtained from collecting 9, 16 and 26 samples, respectively (Fig. 6). With the exception of Argyle (Maritimes) and South Arm September 2020 (Newfoundland), a high degree of sampling completeness of (e.g., 80%) could be reached by collecting 10 or fewer samples, while 90% completeness could be reached with 20 or fewer samples (Fig. 6). For Argyle, a sampling completeness of 80% could be obtained with ~17 samples, while >30 samples (i.e., beyond the extrapolation range) would be required to reach 90% completeness (Fig. 6). For South Arm, >20 samples would be required to reach 80% or 90% completeness (Fig. 6).

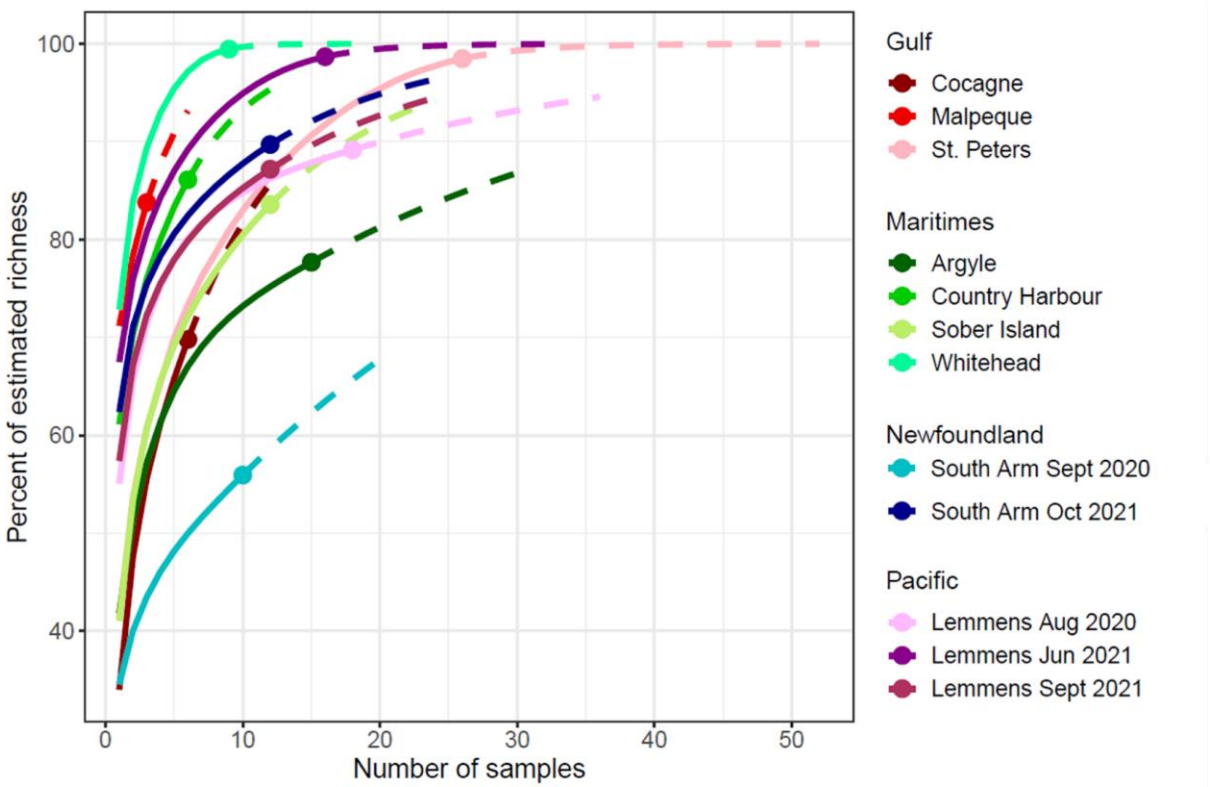

Figure 6. Sample-based rarefaction (solid line) and extrapolation (dashed line) curves for all sites collected as part of the Aquaculture Monitoring Program. The y-axis represents the sampling completeness, or the richness of each site divided by its asymptotic estimate (i.e., Chao2 estimator), to visualize how many samples are required to obtain a select percentage of the estimated richness within each site.

3.3 Objective 2: Characterizing patterns in zooplankton community structure among regions, months, and sites

3.3.1 Regional comparisons

Overall, a large percentage of taxa were observed in all sampling months in the Pacific region (46.34%) (Fig. 7). 42.50% of taxa were observed in all sites in the Maritimes and 46.34% were shared in the Gulf regions (Fig. 7). The March and June 2021 sampling months from Lemmens Inlet had no unique taxa, while the highest number of unique taxa per site or sampling month was 4, which occurred in Country Harbour (Maritimes region), Cocagne (Gulf region) and September 2021 in Lemmens Inlet (Pacific region).

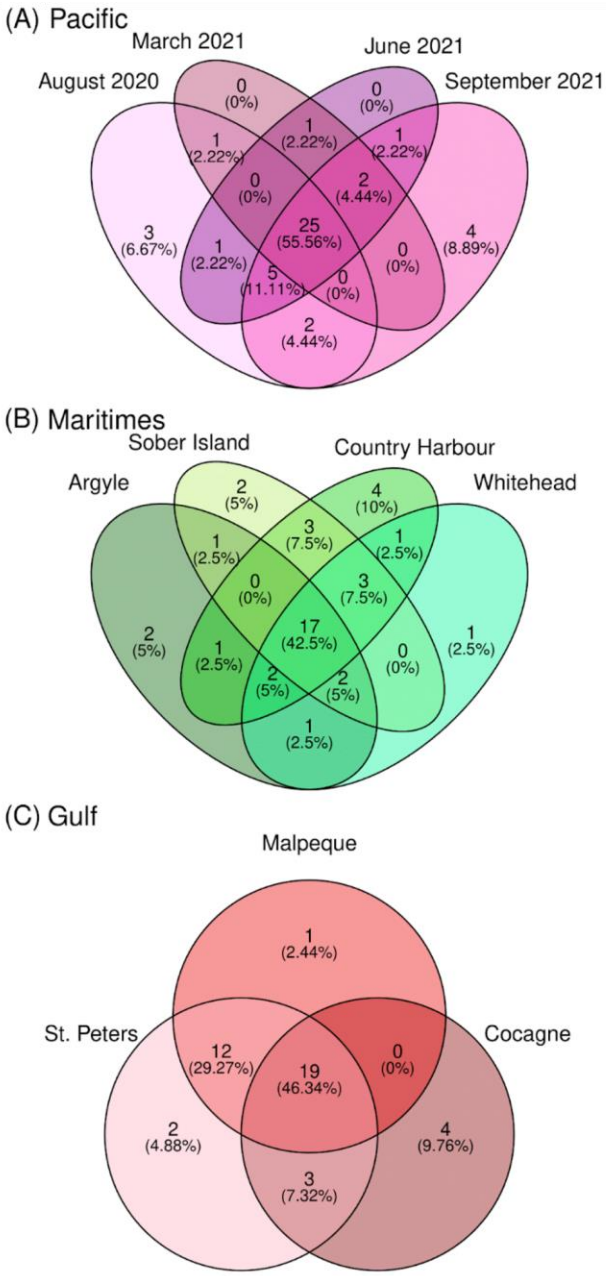

Figure 7. Venn diagrams showing the overlap in the observed number of zooplankton taxa for (A) sampling months within the Pacific region, (B) sites within the Maritimes region, and (C) sites within the Gulf region. Venn diagrams were not constructed for data collected within the Newfoundland region.

The NMDS ordination constructed using all data collected shows groupings based on AMP regions (Fig. 8A). Broadly, data from the Gulf region exhibit high variability and show some degree of overlap with the Maritimes region. Samples from the Pacific and Newfoundland regions are generally distinct and occupy the upper right and lower right portions of the NMDS ordination, respectively (Fig. 8A). When coloured based on sampling month (Fig. 8B), some temporal patterns emerge. Samples from the Gulf and Maritimes (collected from July to September) do not appear to group based on sampling month, but samples from the Pacific region appear to transition somewhat chronologically, moving from June to August to September to March (left to right) on the NMDS. An approximate cyclical progression by month was observed in the samples from the Newfoundland region (Fig. 8B).

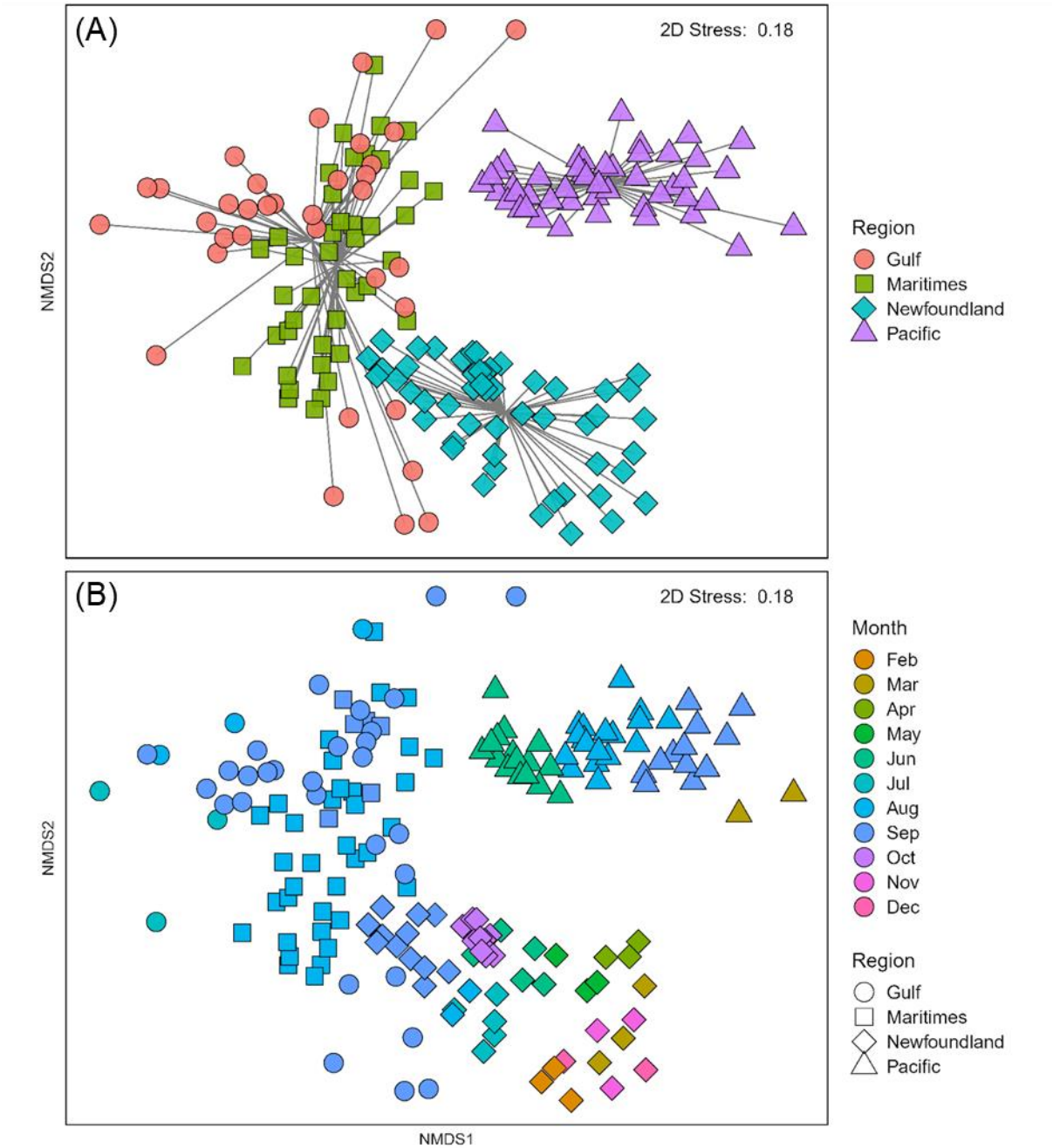

Figure 8. Two-dimensional non-metric multidimensional scaling ordination showing similarity in mesozooplankton (0.25 mm - 5.00 mm) assemblage structure for samples collected as part of the Aquaculture Monitoring Program (AMP). The ordination in (A) represents samples coloured by AMP region, and (B) shows samples coloured by collection month. AMP regions in both ordinations are denoted by symbols. The ordinations were constructed using a Bray-Curtis dissimilarity matrix of square root transformed mesozooplankton abundance (ind m^{-3}). Grey lines in (A) show the connections between each sample and the centroid of its corresponding AMP region.

Because of the high degree of overlap between the samples from the Maritimes and Gulf regions (Fig. 8), a second NMDS ordination was constructed to visualize which sites were similar between the regions (Fig. 9). The data from St. Peters show a high degree of dispersion, while samples from Cocagne and Malpeque are more separated (Fig. 9). Generally, the Gulf samples surrounded the Maritimes samples in the ordination, rather than being directly mixed (Fig. 9).

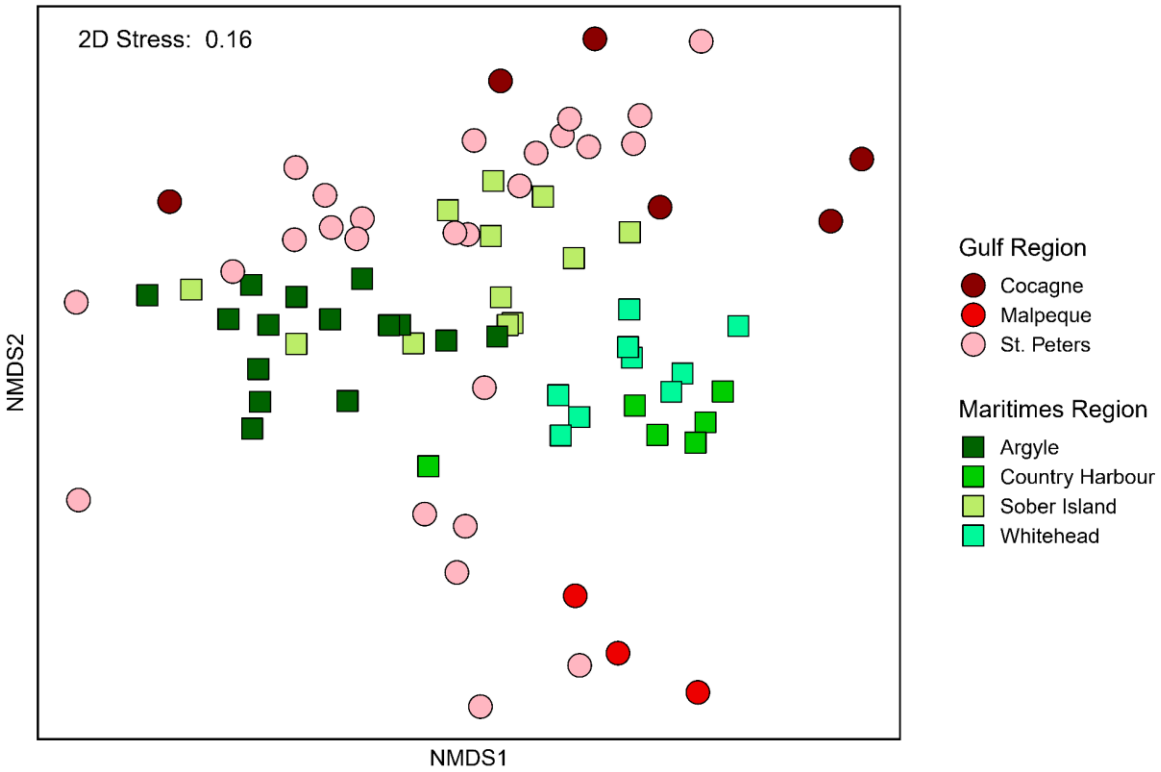

Figure 9. Two-dimensional non-metric multidimensional scaling ordination showing similarity in mesozooplankton (0.25 mm - 5.00 mm) assemblage structure for samples from the Gulf (circles) and Maritimes (squares) region collected as part of the Aquaculture Monitoring Program (AMP). Colours represent the sampling site (e.g., bay or inlet) within each region. The ordination was constructed using a Bray-Curtis dissimilarity matrix of square root transformed mesozooplankton abundance (ind m^{-3}).

When data from all regions were analyzed, significant differences in multivariate dispersion were observed among regions ($F_{3, 174}$ = 6.031 *P*(perm) = 0.002) (Table 7, Fig. 10). Pairwise comparisons revealed that samples from the Gulf were significantly higher (P<0.05) in multivariate dispersion relative to other regions (Table 7, Fig. 10). Samples from the Maritimes, Newfoundland, and Pacific regions were not significantly different in multivariate dispersion (Table 7, Fig. 10).

The PERMANOVA indicated statistically significant differences in mesozooplankton assemblage structure among regions (*pseudo-*$F_{3, 174}$ = 45.179, *P*(perm) = 0.0001), and region (treated as a factor) explained 43.79% of the variation in the data (Table 8). Pairwise comparisons revealed significant differences (P<0.05) in assemblage structure between all regions, and differences between the Pacific and Newfoundland (*pseudo-t* = 8.321, largest *t*-value) and Pacific and Maritimes (*pseudo-t* = 8.143) were the greatest, while differences between the Gulf and Maritimes were the lowest (*pseudo-t* = 3.172, lowest *t*-value) (Table 8).

The SIMPER analysis also identified that regions with the greatest geographic separation had higher overall average dissimilarity (av. dissim.) than regions closer in distance (Table 9). In particular, the mesozooplankton communities of the Pacific and Gulf regions were identified as the most different in assemblage structure (av. dissim. 74.67%) while the Maritimes and Gulf were identified as the least different (av. dissim. 58.38%). Various taxa

were responsible for the differences in composition between regions and the list of the top five are presented in Table 9.

Table 7. Summary of the multivariate homogeneity of group dispersions analysis of mesozooplankton (0.25 mm - 5.00 mm) assemblage structure between regions within the Aquaculture Monitoring Program. Results are based on a Bray-Curtis dissimilarity matrix of square root transformed mesozooplankton abundance (ind m^{-3}). The analysis was followed by *a posteriori* pairwise comparisons between individual regions.

Source	df	SS	MS	F	P(perm)
Region	**3**	**0.191**	**0.064**	**6.031**	**0.0002**
Residuals	174	1.834	0.011		
Total	177	2.025			

Comparison	t	P(perm)
Gulf - Maritimes	**2.802**	**0.0052**
Gulf - Newfoundland	**3.307**	**0.0009**
Gulf - Pacific	**3.446**	**0.0011**
Maritimes - Newfoundland	0.813	0.4118
Maritimes - Pacific	1.085	0.2825
Newfoundland - Pacific	0.256	0.7974

df: degrees of freedom; SS: sum of squares; MS: mean sum of squares; F: F-statistic, P(perm): significance by 9999 permutations; t: t-value from Student's t-test. Significant effects are shown in bold (P(perm < 0.05)).

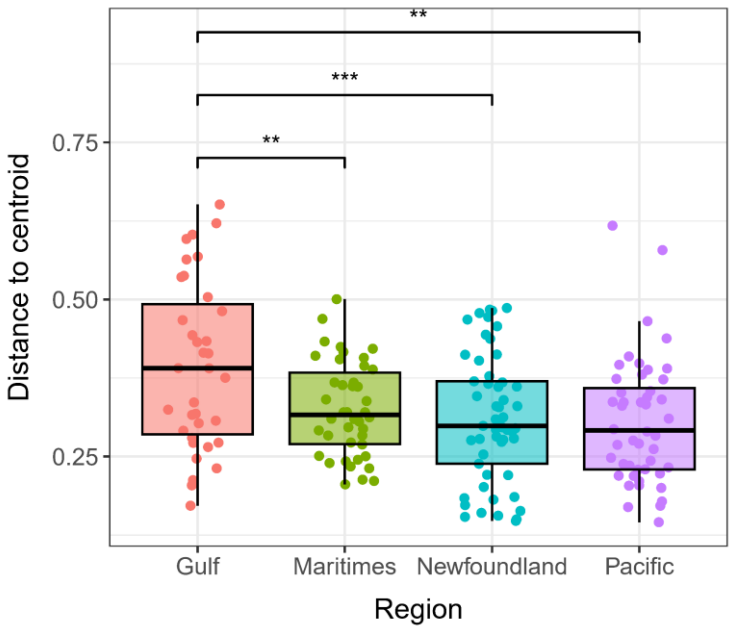

Figure 10. Boxplots depicting the distance of samples to the centroid of the corresponding region within the Aquaculture Monitoring Program (AMP). Results were obtained from the multivariate homogeneity of group dispersions analysis, based on a Bray-Curtis dissimilarity matrix of square root transformed mesozooplankton (0.25 mm - 5.00 mm) abundance (ind m^{-3}). Boxes show the first, second and third quartiles, and are coloured to represent AMP regions. Vertical lines extending from the boxes indicate the minimum and maximum values up to 1.5 times the interquartile range. Jittered points represent the values for individual samples. *P(perm)<0.05, **P(perm)<0.01, ***P(perm)<0.001; i.e., significance obtained from pairwise comparisons between regions using 9999 permutations of the input data.

Table 8. Permutational Multivariate Analysis of Variance (PERMANOVA) results based on a Bray-Curtis dissimilarity matrix of square root transformed mesozooplankton (0.25 mm - 5.00 mm) abundance (ind m^{-3}) for regions within the Aquaculture Monitoring Program. The analysis was followed by *a posteriori* pairwise comparisons between individual regions. Pseudo-t values for the pairwise comparisons were calculated as the square root of the Pseudo-F statistic generated from the *pairwise.adonis2* R function (Arbizu, 2020).

Source	df	SS	MS	R^2	Pseudo-F	P(perm)
Region	**3**	**16.465**	**5.488**	**43.787**	**45.179**	**0.0001**
Residuals	174	21.137	0.121	56.213		
Total	177	37.602		100.000		
Comparison					Pseudo-t	P(perm)
Gulf - Maritimes					**3.172**	**0.0001**
Gulf - Newfoundland					**6.332**	**0.0001**
Gulf - Pacific					**6.650**	**0.0001**
Maritimes - Newfoundland					**6.642**	**0.0001**
Maritimes - Pacific					**8.143**	**0.0001**
Newfoundland - Pacific					**8.321**	**0.0001**

df: degrees of freedom; SS: sum of squares; MS: mean sum of squares; R^2: coefficient of variation; Pseudo-F: F statistic by permutation, P(perm): significance by 9999 permutations; Pseudo-t: t-value by permutation. Significant effects are shown in bold (P(perm < 0.05)).

Table 9. Similarity percentage (SIMPER) analysis to identify the top five mesozooplankton (0.25 mm - 5.00 mm) taxa that contribute most to the average Bray-Curtis dissimilarities between regions. Values in the second column (average) represent the percent contribution of each taxon to average between-group dissimilarity, and overall average dissimilarity (av. dissim., %) represents the sum of these values. The third column (cont., %) is based on average (second column), but adjusted to sum to 100%, and the fourth column represents the cumulative contribution (c. cont) of these values. The fifth and sixth columns represent the average abundance of each taxon within each region (square root transformed, ind m^{-3}). The permutation *p*-value represents the probability of getting a larger or equal average contribution based on 999 random permutations of input data. Note that the full list of contributions from all taxa is not shown, so the sum of each entry from average (column 2)

may not equal the overall average dissimilarity, and the cumulative contribution (column 4) may not reach 100%.

Taxa	Average	Cont.	C. cont.	Av. abund. (I)	Av. abund. (II)	P(perm)
Av. dissim.: 58.38%				Maritimes	Gulf	
Acartia spp.	14.12	24.18	24.18	51.54	59.58	0.040
Evadne spp.	4.55	7.79	31.97	14.18	2.86	0.082
Copepoda (nauplii)	4.40	7.54	39.51	0.28	11.91	0.001
Centropages spp.	3.39	5.81	45.32	10.03	5.23	0.001
Podon/Pleopsis spp.	3.19	5.47	50.79	5.88	10.73	0.138
Av. dissim.: 72.14%				Newfoundland	Gulf	
Acartia spp.	16.36	22.68	22.68	19.42	59.58	0.001
Temora spp.	6.57	9.11	31.79	17.72	3.62	0.001
Pseudocalanus spp.	5.61	7.77	39.56	13.68	0.71	0.001
Copepoda (nauplii)	4.58	6.35	45.91	1.69	11.91	0.001
Evadne spp.	4.54	6.29	52.2	11.27	2.86	0.051
Av. dissim.: 74.67%				Pacific	Gulf	
Acartia spp.	18.29	24.49	24.49	15.08	59.58	0.001
Cirripedia (larvae)	5.33	7.14	31.63	15.43	2.22	0.001

Taxa	Average	Cont.	C. cont.	Av. abund. (I)	Av. abund. (II)	P(perm)
Copepoda (nauplii)	4.56	6.11	37.74	1.37	11.91	0.001
Oikopleura spp.	4.50	6.02	43.77	11.87	0.28	0.001
Podon/Pleopsis spp.	3.81	5.11	48.87	9.59	10.73	0.001

Av. dissim.: 64.08%				Maritimes	Newfoundland	
Acartia spp.	13.95	21.77	21.77	51.54	19.42	0.034
Temora spp.	6.19	9.66	31.43	6.71	17.72	0.001
Pseudocalanus spp.	5.54	8.65	40.08	2.38	13.68	0.001
Evadne spp.	5.10	7.96	48.03	14.18	11.27	0.001
Centropages spp.	3.19	4.98	53.01	10.03	2.08	0.001

Av. dissim.: 72.69%				Maritimes	Pacific	
Acartia spp.	16.41	22.57	22.57	51.54	15.08	0.001
Cirripedia (larvae)	5.91	8.13	30.70	0.40	15.43	0.001
Oikopleura spp.	4.73	6.51	37.21	0.15	11.87	0.001
Evadne spp.	4.35	5.99	43.19	14.18	5.57	0.181
Eurytemora spp.	3.24	4.46	47.65	9.40	0.00	0.001

Av. dissim.: 70.24%				Newfoundland	Pacific	

Temora spp.	8.37	11.92	11.92	17.72	0.00	0.001
Pseudocalanus spp.	6.22	8.86	20.78	13.68	0.69	0.001
Acartia spp.	6.18	8.79	29.57	19.42	15.08	1.000
Cirripedia (larvae)	6.00	8.54	38.12	1.10	15.43	0.001
Evadne spp.	4.28	6.09	44.21	11.27	5.57	0.223

3.3.2 Comparisons among sites or months

Pacific region

The NMDS ordinations for Pacific data showed that the samples exhibited distinct groupings based on month (Fig. 11). The sampling months (treated as factor) exhibited statistically significant differences in multivariate dispersion ($F_{2, 43}$ = 5.351 *P*(perm) = 0.0092) (Table 10, Fig. 12). Multivariate dispersion was significantly lower in June 2021 compared to August 2020 (*t* = -3.021, *P*(perm) = 0.0027) and was also significantly lower in June 2021 compared to September 2021 (*t* = -3.413, *P*(perm) = 0.0014) (Table 10). Data from August 2020 and September 2021 were not significantly different in multivariate dispersion (*t* = 0.327, *P*(perm) = 0.7604) (Table 10).

PERMANOVA indicated significant differences in mesozooplankton assemblage structure between sampling months for data collected in Lemmens Inlet (*pseudo*-$F_{3, 174}$ = 45.179, *P*(perm) = 0.0001) (Table 11). While the relative magnitude of differences were not evident in the NMDS (Fig. 11), pairwise comparisons indicated that June 2021 and September 2021 samples differed most with respect to mesozooplankton assemblage structure (*pseudo-t* = 7.027, *P*(perm) = 0.001), followed by August 2020 and June 2021 (*pseudo-t* = 5.142, *P*(perm) = 0.001), and the lowest differences were observed between August 2020 and September 2021 (*t* = 3.089, *P*(perm) = 0.001) (Table 11).

Similar to the pairwise PERMANOVA results, SIMPER analysis found the overall average dissimilarity was highest between September 2021 and June 2021 (av. dissim. 56.76%) and lowest between September 2021 and August 2020 (av. dissim. 41.37%) (Table 12). Cirripedia (barnacle larvae) was the taxon most responsible for differences in August 2020 (lower average abundance) to June 2021 (higher average abundance) (Table 12). *Acartia* spp. was the taxon most responsible for the differentiations between September 2021 (lower) and August 2020 (higher), and also for September 2021 (lower) and June 2021 (higher) (Table 12).

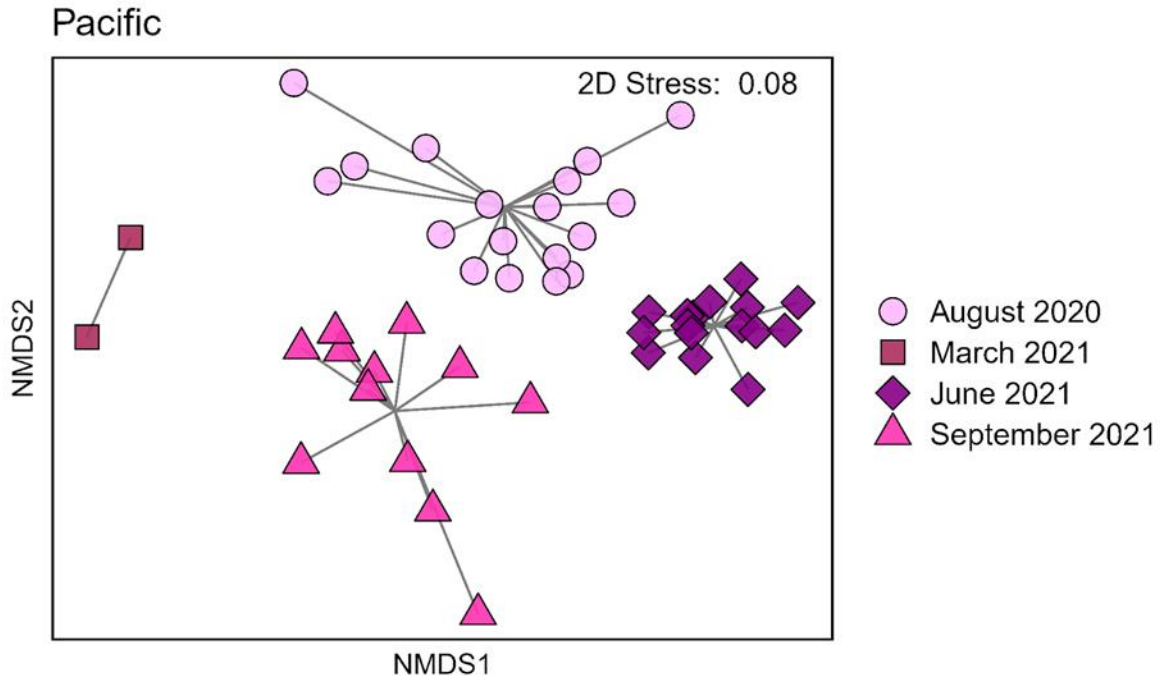

Figure 11. Two-dimensional non-metric multidimensional scaling ordination showing similarity in mesozooplankton (0.25 mm - 5.00 mm) assemblage structure for samples collected from different months within Lemmens Inlet (Pacific region). The ordination was constructed using a Bray-Curtis dissimilarity matrix of square root transformed mesozooplankton abundance (ind m^{-3}). Grey lines show the connections between each sample and the centroid of its corresponding month.

Table 10. Summary of the multivariate homogeneity of group dispersions analysis between sampling months within Lemmens Inlet (Pacific region). Results are based on a Bray-Curtis dissimilarity matrix of square root transformed mesozooplankton (0.25 mm - 5.00 mm) abundance (ind m^{-3}). Data from March 2021 (n = 2) were not included in the analysis.

Source	df	SS	MS	F	P(perm)
Month	**2**	**0.052**	**0.026**	**5.351**	**0.0092**
Residuals	43	0.207	0.005		
Total	45	0.259			
				t	P(perm)
June 2021 - Aug 2020				**-3.021**	**0.0027**
Aug 2020- September 2021				0.327	0.7604
June 2021- September 2021				**-3.413**	**0.0014**

df: degrees of freedom; SS: sum of squares; MS: mean sum of squares; F: F-statistic, P(perm): significance by 9999 permutations. Significant effects are shown in bold (P(perm < 0.05)).

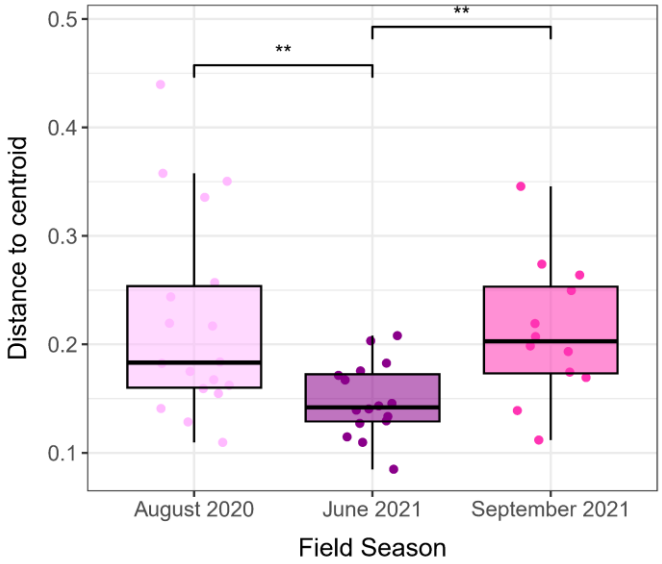

Figure 12. Boxplots depicting the distance of samples to the centroid of the corresponding sampling months within the Pacific region (Lemmens Inlet). Results were obtained from the multivariate homogeneity of groups dispersions analysis based on a Bray-Curtis dissimilarity matrix of square root transformed mesozooplankton (0.25 mm - 5.00 mm) abundance (ind m^{-3}). Boxes show the first, second and third quartiles, and lines extending from the boxes indicate the minimum and maximum values up to 1.5 times the interquartile range. Jittered points represent the values for individual samples. *P(perm)<0.05, **P(perm)<0.01, ***P(perm)<0.001; i.e., significance obtained from pairwise comparisons between regions using 9999 permutations of the input data. Data from March 2021 (*n* = 2) are not shown.

Table 11. Summary of the Permutational Multivariate Analysis of Variance (PERMANOVA) between sampling months within the Pacific region (Lemmens Inlet). Results are based on a Bray-Curtis dissimilarity matrix of square root transformed mesozooplankton (0.25 mm - 5.00 mm) abundance (ind m^{-3}), and was followed by *a posteriori* pairwise comparisons between individual months. Pseudo-t values for the pairwise comparisons were calculated as the square root of the Pseudo-F statistic generated from the *pairwise.adonis2* R function (Arbizu, 2020). Data from March 2021 (*n* = 2) were not included in the analysis.

Source	df	SS	MS	R^2	Pseudo-F	P(perm)
Month	**2**	**2.273**	**1.137**	**53.879**	**25.117**	**0.0001**
Residual	43	1.946	0.045	46.121		
Total	45	4.219		100.000		

Comparison	Pseudo-t	P(perm)
Aug. 2020 – Sept. 2021	**3.089**	**0.0001**
Aug. 2020 - Jun. 2021	**5.142**	**0.0001**
Jun. 2021 – Sept. 2021	**7.027**	**0.0001**

df: degrees of freedom; SS: sum of squares; MS: mean sum of squares; R^2: coefficient of variation; Pseudo-F: F statistic by permutation, P(perm): significance by 9999 permutations; Pseudo-t: t-value by permutation. Significant effects are shown in bold (P(perm < 0.05)).

Table 12. Similarity percentage (SIMPER) analysis to identify the top five mesozooplankton (0.25 mm - 5.00 mm) taxa that contribute most to the average Bray-Curtis dissimilarities between sampling months within the Pacific region (Lemmens Inlet). Values in the second column (average) represent the percent contribution of each taxon to average between-group dissimilarity, and overall average dissimilarity (av. dissim., %) represents the sum of these values. The third column (cont., %) is based on average (second column), but adjusted to sum to 100%, and the fourth column represents the cumulative contribution (c. cont) of these values. The fifth and sixth columns represent the average abundance of each taxon within each region (square root transformed, ind m^{-3}). The permutation *p*-value represents the probability of getting a larger or equal average contribution based on 999 random permutations of input data. Note that the full list of contributions from all taxa is not shown, so the sum of each entry from average (column 2) may not equal the overall average dissimilarity, and the cumulative contribution (column 4) may not reach 100%.

Taxa	Average	Cont.	C. cont.	Av. abund. (I)	Av. abund. (II)	P(perm)
Av. dissim.: 44.58%				Aug 2020	Jun 2021	
Cirripedia (larvae)	6.92	15.51	15.51	10.92	29.39	0.0010
Acartia spp.	6.59	14.79	30.30	10.81	29.46	0.0020
Oikopleura spp.	4.59	10.30	40.60	8.11	20.74	0.0030
Fritillaria spp.	2.93	6.58	47.18	2.15	10.14	0.0010
Evadne spp.	2.16	4.85	52.02	4.63	10.21	0.4940
Av. dissim.: 41.37%				Sept 2021	Aug 2020	
Acartia spp.	4.63	11.20	11.20	3.82	10.81	0.9880
Echinodermata (larvae)	3.63	8.77	19.96	5.65	7.45	0.0020
Podon/Pleopsis spp.	3.50	8.46	28.42	4.59	10.00	0.0320
Cirripedia (larvae)	3.40	8.21	36.64	5.72	10.92	1.0000
Oikopleura spp.	2.62	6.33	42.96	7.45	8.11	1.0000

Taxa	Average	Cont.	C. cont.	Av. abund. (I)	Av. abund. (II)	P(perm)
Av. dissim.: 56.76%				Sept 2021	Jun 2021	
Acartia spp.	10.31	18.16	18.16	3.82	29.46	0.0010
Cirripedia (larvae)	9.73	17.14	35.30	5.72	29.39	0.0010
Oikopleura spp.	5.44	9.59	44.89	7.45	20.74	0.0010
Podon/Pleopsis spp.	3.82	6.72	51.61	4.59	14.04	0.0050
Evadne spp.	3.53	6.22	57.83	1.66	10.21	0.0010

Maritimes region

The NMDS ordinations for the Maritimes data showed distinct groupings of samples by sites (Fig. 13). Sites were not significantly different in their multivariate dispersion ($F_{3,38}$ = 1.205, *P*(perm) = 0.3135) (Table 13, Fig. 14). PERMANOVA indicated statistically significant differences in mesozooplankton assemblage structure among sites (*pseudo*-$F_{3, 38}$ = 20.172, *P*(perm) = 0.0001) and Sites (treated as a factor) explained 61.427% of the variation in the data (Table 14). Pairwise comparisons indicated greatest differences between sites that were most geographically separated (largest *t* values), and lowest differences between nearby sites (lowest *t* values) (Table 14). For instance, the largest differences in assemblage structure were observed between Whitehead and Argyle (*t* = 6.183, *P*(perm) = 0.0004; most geographically separated), and the lowest differences were between Country Harbour and Whitehead (*t* = 2.754, *P*(perm) = 0.004; least geographically separated) (Table 14).

SIMPER analysis also revealed larger differences in the overall average dissimilarity between regions with greater geographic separation than those nearby (Table 15). The taxa most responsible for differences between sites were either *Evadne* spp., *Acartia* spp., or Hydrozoa (medusa) (Table 15).

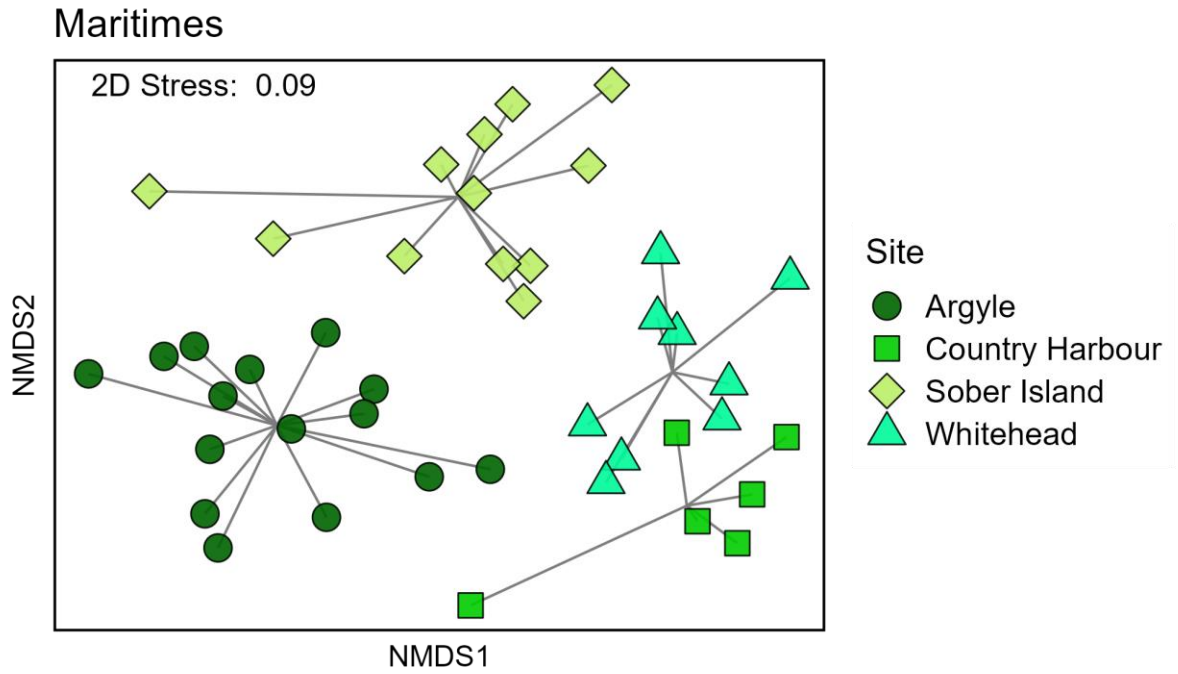

Figure 13. Two-dimensional non-metric multidimensional scaling ordination showing similarity in mesozooplankton (0.25 mm - 5.00 mm) assemblage structure for samples collected from sites within the Maritimes region. The ordination was constructed using a Bray-Curtis dissimilarity matrix of square root transformed mesozooplankton abundance (ind m^{-3}). Grey lines show the connections between each sample and the centroid of its corresponding site.

Table 13. Summary of the multivariate homogeneity of group dispersions analysis of mesozooplankton (0.25 mm - 5.00 mm) assemblage structure between sites within the Maritimes region, sampled as part of the Aquaculture Monitoring Program. Results are based on a Bray-Curtis dissimilarity matrix of square root transformed mesozooplankton abundance (ind m^{-3}).

Source	df	SS	MS	F	P(perm)
Site	3	0.026	0.009	1.205	0.3135
Residuals	38	0.272	0.007		
Total	41	0.298			

df: degrees of freedom; SS: sum of squares; MS: mean sum of squares; F: F-statistic, P(perm): significance by 9999 permutations.

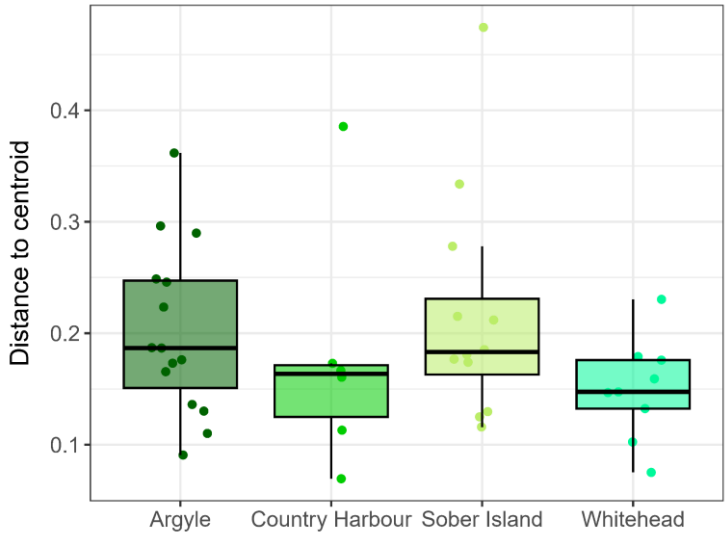

Figure 14. Boxplots depicting the distance of samples to the centroid of the corresponding site within the Maritimes region. Results were obtained from the multivariate homogeneity of groups dispersions analysis based on a Bray-Curtis dissimilarity matrix of square root transformed mesozooplankton (0.25 mm - 5.00 mm) abundance (ind m^{-3}). Boxes show the first, second and third quartiles, and lines extending from the boxes indicate the minimum and maximum values up to 1.5 times the interquartile range. Jittered points represent the values for individual samples.

Table 14. Summary of the Permutational Multivariate Analysis of Variance (PERMANOVA) between sites within the Maritimes region. Results are based on a Bray-Curtis dissimilarity matrix of square root transformed mesozooplankton (0.25 mm - 5.00 mm) abundance (ind m^{-3}), and was followed by *a posteriori* pairwise comparisons between individual sites. Pseudo-t values for the pairwise comparisons were calculated as the square root of the Pseudo-F statistic generated from the *pairwise.adonis2* R function (Arbizu, 2020).

Source	df	SS	MS	R^2	Pseudo-F	P(perm)
Site	**3**	**2.875**	**0.958**	**61.427**	**20.172**	**0.0001**
Residual	38	1.805	0.048	38.573		
Total	41	4.680		100.000		

	Pseudo-t	P (perm)
Argyle - Country Harbour	**5.118**	**0.0001**
Argyle - Sober Island	**4.055**	**0.0001**
Argyle - Whitehead	**6.183**	**0.0001**
Country Harbour - Sober Island	**3.461**	**0.0002**
Country Harbour - Whitehead	**2.754**	**0.0004**
Sober Island - Whitehead	**4.100**	**0.0001**

df: degrees of freedom; SS: sum of squares; MS: mean sum of squares; R^2: coefficient of variation; Pseudo-F: F statistic by permutation, P(perm): significance by 9999 permutations; Pseudo-t: t-value by permutation. Significant effects are shown in bold (P(perm < 0.05)).

Table 15. Similarity percentage (SIMPER) analysis to identify the top five mesozooplankton (0.25 mm - 5.00 mm) taxa that contribute most to the average Bray-Curtis dissimilarities between sites within the Maritimes region. Values in the second column (average) represent the percent contribution of each taxon to average between-group dissimilarity, and overall average dissimilarity (av. dissim., %) represents the sum of these values. The third column (cont., %) is based on average (second column), but adjusted to sum to 100%, and the fourth column represents the cumulative contribution (c. cont) of these values. The fifth and sixth columns represent the average abundance of each taxon within each region (square root transformed, ind m^{-3}). The permutation *p*-value represents the probability of getting a larger or equal average contribution based on 999 random permutations of input data. Note that the full list of contributions from all taxa is not shown, so the sum of each entry from average (column 2) may not equal the overall average dissimilarity, and the cumulative contribution (column 4) may not reach 100%.

Taxa	Average	Cont.	C. cont.	Av. abund. (I)	Av. abund. (II)	P(perm)
Av. dissim.: 60.78%				Country Harbour	Argyle	
Evadne spp.	10.16	16.71	16.71	34.67	1.84	0.0001
Acartia spp.	8.58	14.12	30.83	57.18	32.10	0.9233
Eurytemora spp.	6.21	10.21	41.04	24.41	4.24	0.0001
Temora spp.	6.12	10.07	51.11	20.64	2.72	0.0001
Gastropoda (larvae/Limacina)	4.63	7.62	58.74	17.26	3.03	0.0001
Av. dissim.: 47.31%				Sober Island	Argyle	
Acartia spp.	18.10	38.25	38.25	61.58	32.10	0.0001
Evadne spp.	7.43	15.70	53.95	14.87	1.84	0.0001
Centropages spp.	2.22	4.68	58.63	3.37	6.76	0.9993

Taxa	Average	Cont.	C. cont.	Av. abund. (I)	Av. abund. (II)	P(perm)
Pseudodiaptomus spp.	2.12	4.49	63.12	1.70	5.22	0.0001
Eurytemora spp.	1.94	4.09	67.21	1.32	4.24	1.0000
Av. dissim.: 57.75%				Whitehead	Argyle	
Acartia spp.	11.88	20.57	20.57	66.78	32.10	0.2138
Hydrozoa (medusa)	8.75	15.14	35.71	26.13	0.39	0.0001
Evadne spp.	6.24	10.81	46.52	20.16	1.84	0.0254
Centropages spp.	6.18	10.70	57.22	24.96	6.76	0.0001
Eurytemora spp.	5.03	8.71	65.93	18.76	4.24	0.0007
Av. dissim.: 50.46%				Country Harbour	Sober Island	
Acartia spp.	7.02	13.91	13.91	57.18	61.58	0.9917
Eurytemora spp.	6.34	12.56	26.46	24.41	1.32	0.0002
Evadne spp.	5.78	11.46	37.93	34.67	14.87	0.2161
Temora spp.	5.37	10.64	48.57	20.64	2.78	0.0001
Gastropoda (larvae/Limacina)	4.03	7.98	56.55	17.26	3.03	0.0003

Taxa	Average	Cont.	C. cont.	Av. abund. (I)	Av. abund. (II)	P(perm)
Av. dissim.: 36.48%				Country Harbour	Whitehead	
Hydrozoa (medusa)	5.04	13.82	13.82	2.55	26.13	0.0143
Acartia spp.	4.46	12.23	26.04	57.18	66.78	0.9999
Evadne spp.	3.62	9.92	35.96	34.67	20.16	0.9857
Centropages spp.	3.36	9.22	45.19	9.17	24.96	0.4105
Temora spp.	2.56	7.03	52.21	20.64	9.30	0.3495
Av. dissim.: 46.95%				Whitehead	Sober Island	
Hydrozoa (medusa)	7.78	16.58	16.58	26.13	0.16	0.0001
Acartia spp.	7.58	16.15	32.73	66.78	61.58	0.9916
Centropages spp.	6.46	13.77	46.50	24.96	3.37	0.0001
Eurytemora spp.	5.29	11.27	57.77	18.76	1.32	0.0002
Evadne spp.	2.59	5.51	63.28	20.16	14.87	1.0000

Gulf region

The NMDS ordinations for the Gulf data showed separations of samples by site, although samples from St. Peters were intermixed with samples from Cocagne and Malpeque (Fig. 15). Cocagne and St. Peters were not significantly different in their multivariate dispersion ($F_{1,30}$ = 0.035, *P*(perm) = 0.8545) (Table 16, Fig. 16). PERMANOVA indicated statistically significant differences in mesozooplankton assemblage structure between these two sites (*pseudo*-$F_{1, 30}$ = 5.460, *P*(perm) = 0.0005), and site (treated as a factor) explained 15.40% of the variation in the data (Table 17). Data from Malpeque were not included in statistical testing due to the lower sample size (*n* = 3).

The SIMPER analysis revealed an overall average dissimilarity of 63.09% between Cocagne and St. Peters, and *Acartia* spp. was the taxon most responsible for differentiating between the two sites (higher average abundance in Cocagne, lower in St. Peters) (Table 18).

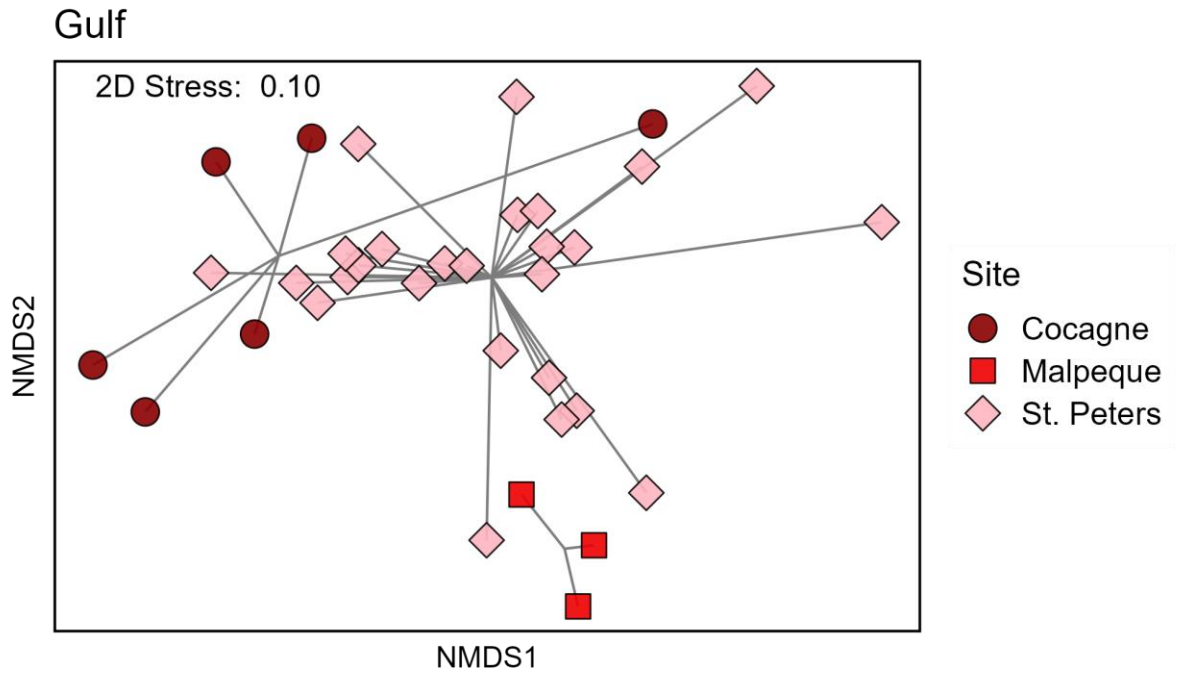

Figure 15. Two-dimensional non-metric multidimensional scaling ordination showing similarity in mesozooplankton (0.25 mm - 5.00 mm) assemblage structure for samples collected from sites within the Gulf region. The ordination was constructed using a Bray-Curtis dissimilarity matrix of square root transformed mesozooplankton abundance (ind m^{-3}). Grey lines show the connections between each sample and the centroid of its corresponding site.

Table 16. Summary of the multivariate homogeneity of group dispersions analysis of mesozooplankton (0.25 mm - 5.00 mm) assemblage structure between sites (St. Peters and Cocagne) within the Gulf region. Results are based on a Bray-Curtis dissimilarity matrix of square root transformed mesozooplankton abundance (ind m^{-3}), and the analysis was followed by *a posteriori* pairwise comparisons between individual sites. Data from Malpeque were not included in the analysis (n = 3).

Source	df	SS	MS	F	P(perm)
Site	1	0.001	0.001	0.035	0.8545
Residuals	30	0.640	0.021		
Total	31	0.641			

df: degrees of freedom; SS: sum of squares; MS: mean sum of squares; F: F-statistic, P(perm): significance by 9999 permutations.

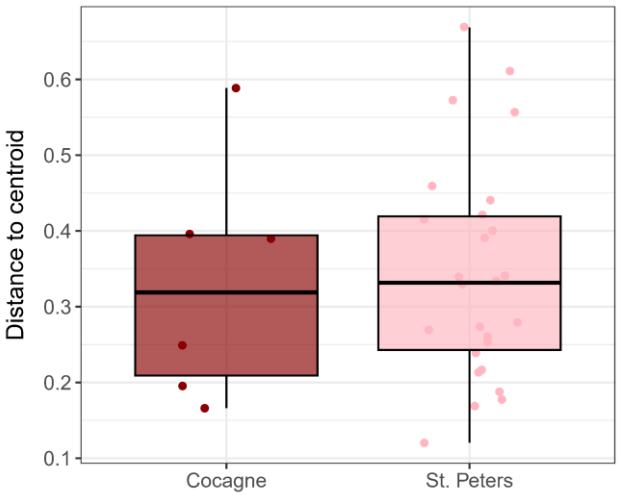

Figure 16. Boxplots depicting the distance of samples to the centroid of the corresponding site within the Gulf region. Results were obtained from the multivariate homogeneity of groups dispersions analysis based on a Bray-Curtis dissimilarity matrix of square root transformed mesozooplankton (0.25 mm - 5.00 mm) abundance. Boxes show the first, second and third quartiles, and lines extending from the boxes indicate the minimum and maximum values up to 1.5 times the interquartile range. Jittered points represent the values for individual samples. Data for Malpeque are not included (*n* = 3).

Table 17. Summary of the Permutational Multivariate Analysis of Variance (PERMANOVA) between sites (St. Peters and Cocagne) within the Gulf region. Results are based on a Bray-Curtis dissimilarity matrix of square root transformed mesozooplankton (0.25 mm - 5.00 mm) abundance (ind m^{-3}), and was followed by *a posteriori* pairwise comparisons between individual sites. Pseudo-t values for the pairwise comparisons were calculated as the square root of the Pseudo-F statistic generated from the *pairwise.adonis2* R function (Arbizu, 2020). Data from Malpeque were not included in the analysis (*n* = 3).

Source	df	SS	MS	R^2	Pseudo-t	P(perm)
Site	**1**	**0.775**	**0.775**	**15.398**	**5.460**	**0.0005**
Residual	30	4.258	0.142	84.602		
Total	34	5.033		100.00		

df: degrees of freedom; SS: sum of squares; MS: mean sum of squares; R^2: coefficient of variation; Pseudo-t: t-value by permutation, P(perm): significance by 9999 permutations. Significant effects are shown in bold (P(perm < 0.05)).

Table 18. Similarity percentage (SIMPER) analysis to identify the top five mesozooplankton (0.25 mm - 5.00 mm) taxa that contribute most to the average Bray-Curtis dissimilarities between sites within the Gulf region. Values in the second column (average) represent the percent contribution of each taxon to average between-group dissimilarity, and overall average dissimilarity (av. dissim., %) represents the sum of these values. The third column (cont., %) is based on average (second column), but adjusted to sum to 100%, and the fourth column represents the cumulative contribution (c. cont) of these values. The fifth and sixth columns represent the average abundance of each taxon within each region (square root transformed, ind m^{-3}). The permutation *p*-value represents the probability of getting a larger or equal average contribution based on 999 random permutations of input data. Note

that the full list of contributions from all taxa is not shown, so the sum of each entry from average (column 2) may not equal the overall average dissimilarity, and the cumulative contribution (column 4) may not reach 100%.

Taxa	Average	Cont.	C. cont.	Av. abund. (I)	Av. abund. (II)	P(perm)
Av. dissim.: 63.09%				Cocagne	St. Peters	
Acartia spp.	23.53	37.31	37.31	115.68	51.65	0.005
Copepoda (nauplii)	4.64	7.36	44.67	0.48	14.59	0.837
Centropages spp.	4.14	6.56	51.23	18.20	1.81	0.008
Podon/Pleopsis spp.	3.89	6.16	57.39	1.00	12.92	0.852
Pseudodiaptomus spp.	3.45	5.47	62.87	9.34	10.26	0.661

Newfoundland region

Data collection in Newfoundland focused largely on providing highly-detailed temporal data by collecting samples in multiple months (Table 1). Results for this section therefore follow a slightly different format in comparison to those from the other regions above, to reflect these efforts. First, a relative abundance chart was created to show the changes in taxonomic composition from June 2021 to July 2022. Next, an NMDS ordination was constructed as an additional means to show these changes. Data from September 2020 was also included in the NMDS. Tests for significance in multivariate assemblage structure were not conducted between all of these sampling months and Venn diagrams were also not constructed due to the large number of sampling months. Analyses focused on examining the role of tide phase and station for the September 2020 (n = 10) and October 2021 (n = 12) datasets are included in Section 3.3.4.

From June 2021 to July 2022, samples comprised a variety of taxa, and generally, *Acartia* spp., *Evadne* spp., *Temora* spp., and *Pseudocalanus* spp. comprised the largest portions of each taxa (Fig. 17). Shifts in the relative abundance were observed between months, and occasionally, taxa comprised a large portion of the sample during certain months (e.g., *Fritillaria* spp. in April and May 2022), and then decreased in relative abundance (Fig. 17).

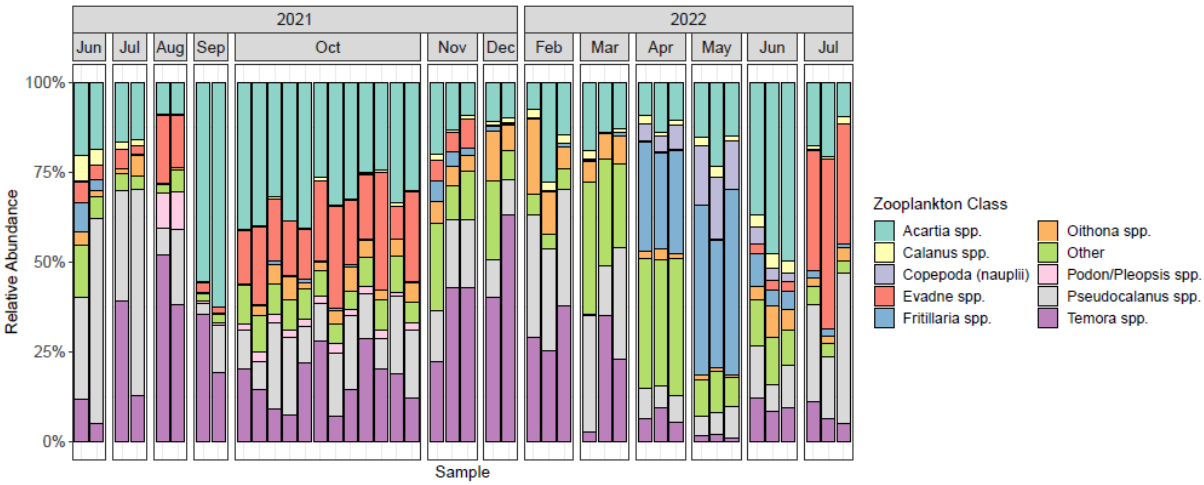

Figure 17. Relative abundance bar charts showing the zooplankton composition of individual samples collected from June 2021 through July 2022 in South Arm (Newfoundland region). The top nine most common taxa are identified, while the remaining taxa are grouped into an “Other” category.

The NMDS ordination of temporal data from South Arm (Newfoundland region) shows a cyclical progression in taxonomic composition, which moves in an approximate clockwise pattern between months (Fig. 18). Data collected in the same months, regardless of year, are grouped together, indicating similar assemblage structure (e.g., samples from June 2021 and June 2022 are not distinct from each other) (Fig. 18). Large shifts in composition are observed between certain time months (e.g., October to November), while smaller shifts are observed between other time periods (e.g., June to July) (Fig. 18).

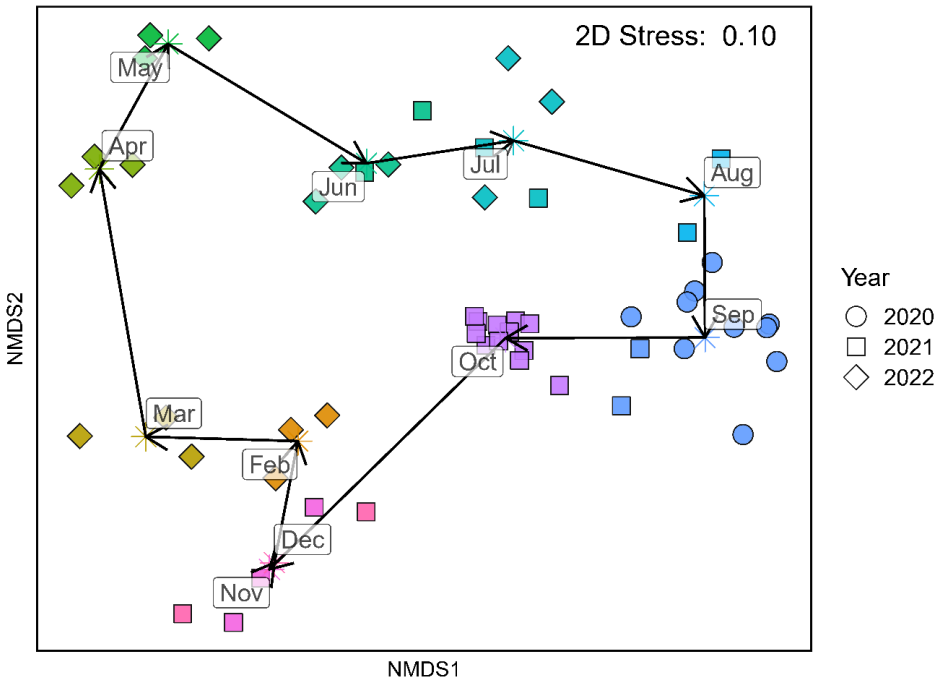

Figure 18. Two-dimensional non-metric multidimensional scaling ordination showing similarity in mesozooplankton (0.25 mm - 5.00 mm) composition from monthly samples collected in South Arm, Newfoundland. Samples are shown in colour to represent sampling months, and shapes indicate sampling year. Arrows connect the months chronologically, and the asterisks represent the centroid of sampling months, regardless of year (e.g., June of all

data, July of all data, etc.) The ordination was constructed using a Bray-Curtis dissimilarity matrix of square root transformed mesozooplankton abundance (ind m^{-3}).

3.4 Objective 3: Characterizing the role of tide phase and stations on zooplankton composition

3.4.1 Pacific region

In Lemmens Inlet, for each month, the total abundance was distributed over several classes with no clear dominance by any taxa (Fig. 19). However, in general, the differences in the relative abundance of taxa were more noticeable between months, than within specific stations or tide phases at a specific site (Fig. 19), as also shown in section 3.3.2. Further analyses were thus conducted independently for each sampling month.

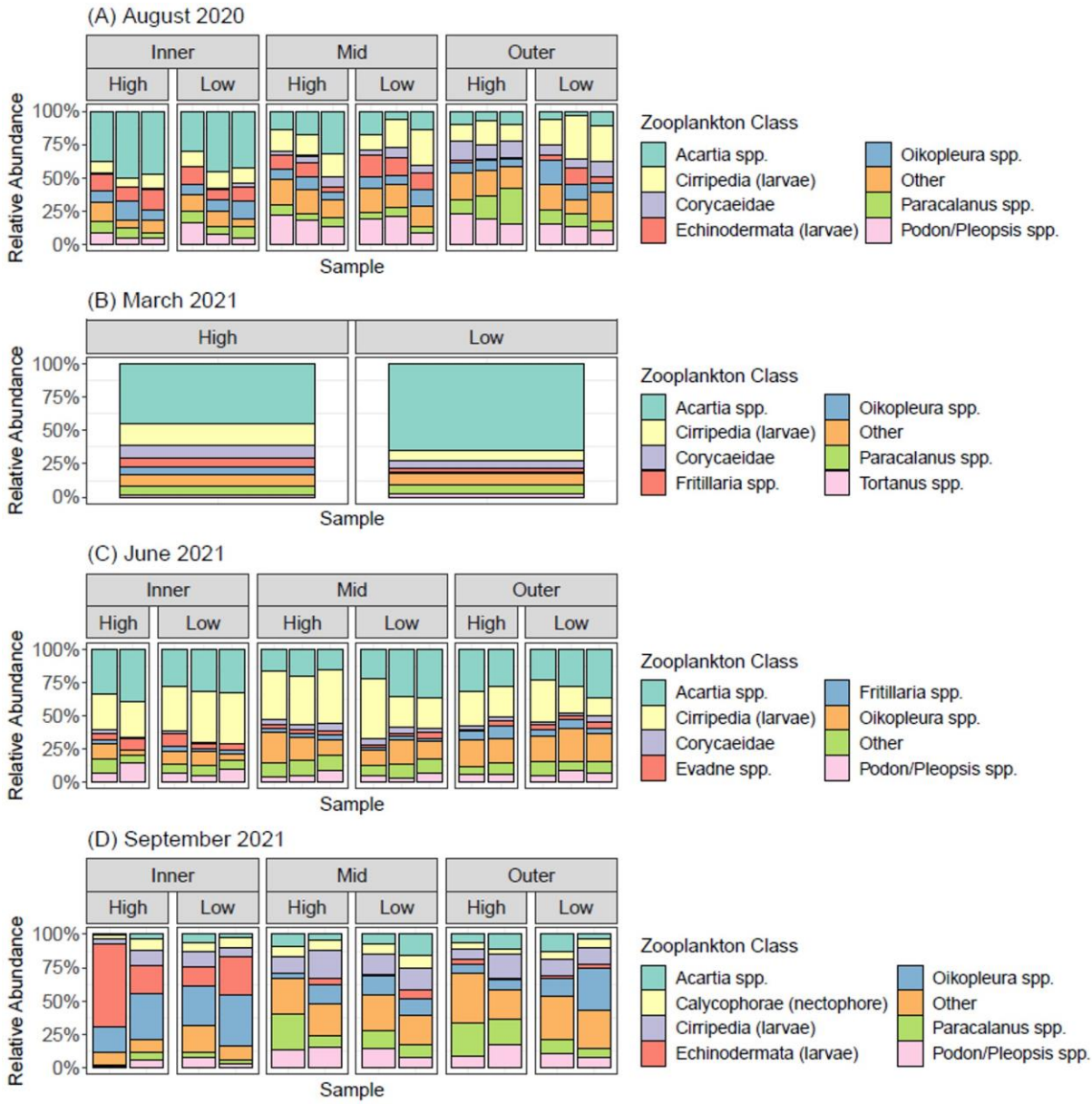

Figure 19. Relative abundance bar charts showing zooplankton composition of individual samples for different sampling months from Lemmens Inlet of the Pacific region. For each month, the top seven most common taxa are identified, while the remaining taxa are grouped into an “Other” category; therefore, the resulting colour scheme may differ among

charts. The top panel in each subplot indicates station labels as denoted in Fig. 1, and sub-panels refer to tide phases including high tide (High) and low tide (Low).

Each NMDS ordination separated by sampling months from Lemmens Inlet showed unique patterns (Fig. 20). In August 2020, clear groupings based on station were apparent, and the samples transitioned from Outer to Mid to Inner stations when moving from the lower left to upper right regions of the NMDS (Fig. 20A). In June 2021, the Mid stations formed somewhat of a distinct grouping, while the Outer and Inner stations were intermixed (Fig. 20B). In September 2021, samples from the Inner station were separated on the ordination from the Mid and Outer stations, which exhibited overlap (Fig. 20C). No months showed any obvious groupings based on tide phase (Fig. 20A-C).

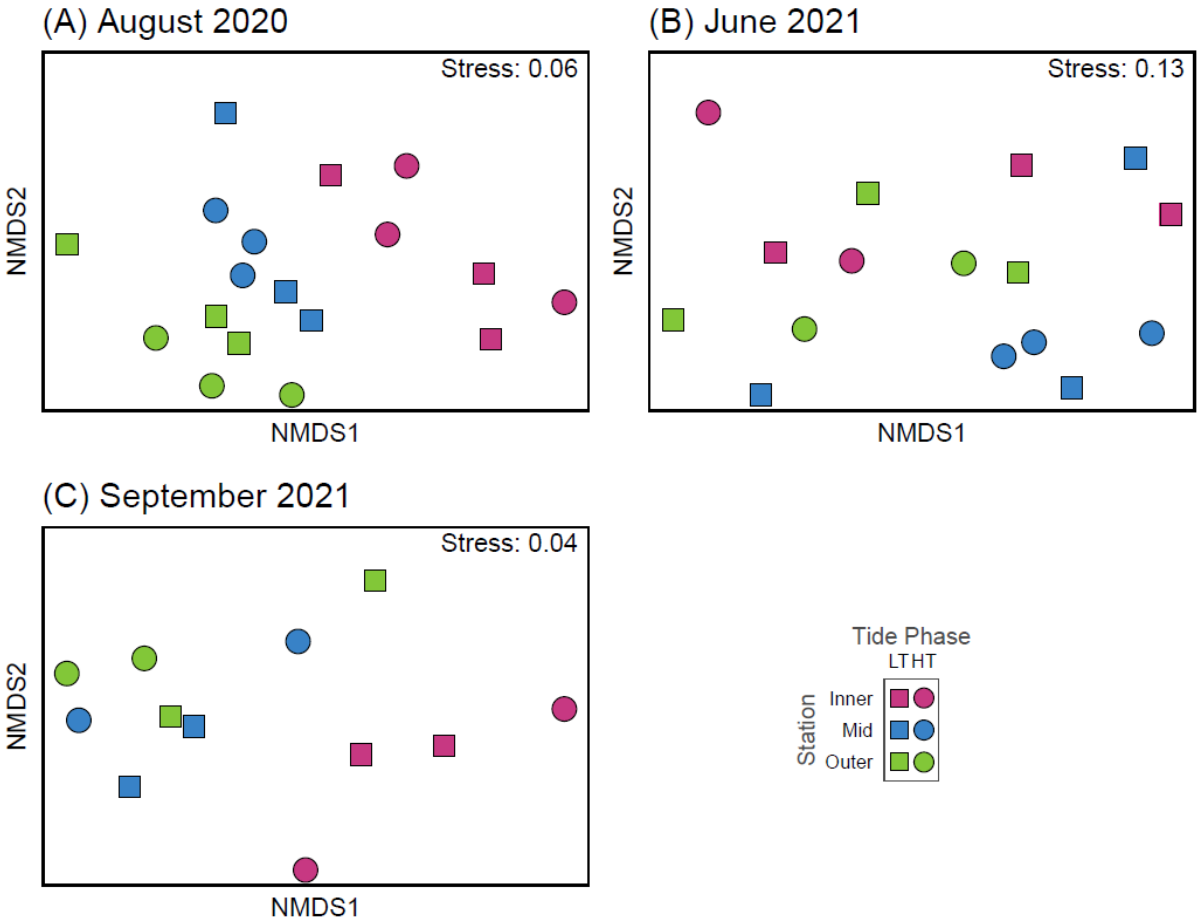

Figure 20. Two-dimensional non-metric multidimensional scaling ordination showing similarity in mesozooplankton (0.25 mm - 5.00 mm) assemblage structure from different sampling months within Lemmons Inlet of the Pacific Region, including (A) August 2020, (B) June 2021, and (C) September 2021. Each ordination was constructed using a Bray-Curtis dissimilarity matrix of square root transformed mesozooplankton abundance (ind m^{-3}). Symbol shapes indicate tide phases, and colours represent the sampling location (station) within each bay, as denoted in Fig. 1. Ordinations for data collected in March 2021 (n = 2) were not created.

Lemmens August 2020 - Tide and station effects

No significant differences in multivariate dispersion were observed between the tide phases ($F_{1, 16}$ = 0.038, P(perm) = 0.8515) or among stations ($F_{2, 15}$ = 0.743, P(perm) = 0.4981) for

the August 2020 data from Lemmens Inlet (Table 19, Fig. 21). The PERMANOVA indicated no difference in mesozooplankton assemblage structure between the tide phases (PERMANOVA *pseudo-*$F_{1, 12}$ = 0.929, *P*(perm) = 0.3893) (Table 20). However, significant differences in mesozooplankton assemblage structure were observed between stations (PERMANOVA *pseudo-*$F_{2,12}$ = 7.977, *P*(perm) = 0.0002) and explained 52.49% of the variation in the data (Table 20). Pairwise comparisons revealed significant differences in assemblage structure between all stations, with the strongest differences between samples from the Inner and Outer stations (*pseudo-t* = 3.470, *P*(perm) = 0.0021) and Inner and Mid stations (*pseudo-t* = 3.033, *P*(perm) = 0.0020) (Table 20). Weaker, but statistically significant differences were observed between samples from the Mid and Outer stations (*pseudo-t* = 1.594, *P*(perm) = 0.0213) (Table 20).

SIMPER analysis similarly found the greatest differences in mesozooplankton composition between the Outer and Inner stations (av. dissim. 43.95%), then Mid and Inner (av. dissim.: 37.19%), and the Outer and Mid were the least different (av. dissim. 25.92%) (Table 21). *Podon/Pleopsis* spp. were the taxa most responsible for the differentiation between Mid (higher) and Inner (lower) stations, Corycaeidae for Outer (higher) and Inner (lower) stations, and Echinodermata larvae for Outer (lower) and Mid (higher) stations (Table 21).

Table 19. Summary of multivariate homogeneity of group dispersions analysis for samples in Lemmens Inlet for the August 2020 dataset (Pacific region), showing the effect of tide and station (run as separate tests) on mesozooplankton (0.25 mm - 5.00 mm) assemblage structure. Results are based on a Bray-Curtis dissimilarity matrix of square root transformed mesozooplankton abundance (ind m^{-3}).

Source	df	SS	MS	F	P(perm)
Tide	1	0.000	0.000	0.038	0.8515
Residuals	16	0.166	0.010		
Total	17	0.166	0.010		
Station	2	0.004	0.002	0.743	0.4981
Residuals	15	0.041	0.003		
Total	17	0.045	0.005		

df: degrees of freedom; SS: sum of squares; MS: mean sum of squares; F: F-statistic, P(perm): significance by 9999 permutations.

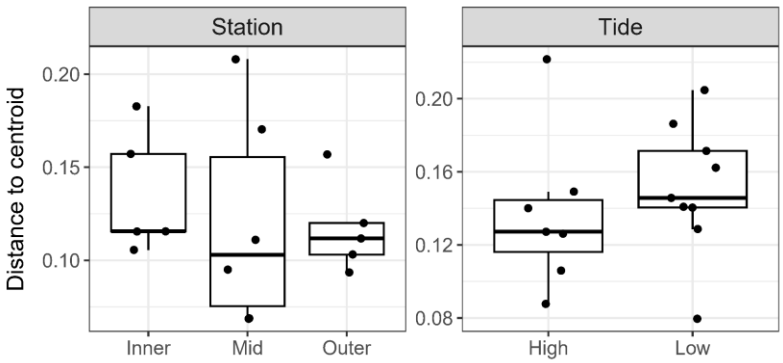

Figure 21. Boxplots depicting the distance of samples to the centroid of the corresponding station (left) or tide phase (right) for data collected in August 2020 in Lemmens Inlet (Pacific

region). Results were obtained from the multivariate homogeneity of groups dispersions analysis based on a Bray-Curtis dissimilarity matrix of square root transformed mesozooplankton (0.25 mm - 5.00 mm) abundance. Boxes show the first, second and third quartiles, and lines extending from the boxes indicate the minimum and maximum values up to 1.5 times the interquartile range. Jittered points represent the values for individual samples.

Table 20. Summary of the Permutational Multivariate Analysis of Variance (PERMANOVA) showing the effect of tide, station, and their interaction in Lemmens Inlet for the August 2020 dataset (Pacific region). Results are based on a square root transformed Bray-Curtis dissimilarity matrix of mesozooplankton (0.25 mm - 5.00 mm) abundance (ind m^{-3}), and was followed by *a posteriori* pairwise comparisons between individual stations. Pseudo-t values for the pairwise comparisons were calculated as the square root of the Pseudo-F statistic generated from the *pairwise.adonis2* R function (Arbizu, 2020).

Source	df	SS	MS	R^2	Pseudo-F	P(perm)
Tide	1	0.031	0.031	3.058	0.929	0.3893
Station	**2**	**0.592**	**0.265**	**52.490**	**7.977**	**0.0002**
Tide*Station	2	0.050	0.025	4.969	0.755	0.5952
Residual	12	0.398	0.033	39.483		
Total	17	1.008	0.059	100.000		
Comparison (stations)					Pseudo-t	P(perm)
Inner - Mid					**3.033**	**0.0020**
Inner - Outer					**3.470**	**0.0021**
Mid - Outer					**1.594**	**0.0213**

df: degrees of freedom; SS: sum of squares; MS: mean sum of squares; R^2: coefficient of variation; Pseudo-F: F statistic by permutation, P(perm): significance by 9999 permutations; Pseudo-t: t-value by permutation. Significant effects are highlighted in bold (P(perm < 0.05)).

Table 21. Similarity percentage (SIMPER) analysis to identify the top five mesozooplankton (0.25 mm - 5.00 mm) taxa that contribute most to the average Bray-Curtis dissimilarities between stations in Lemmens Inlet (Pacific region) in August 2020. Values in the second column (average) represent the percent contribution of each taxon to average between-group dissimilarity, and overall average dissimilarity (av. dissim., %) represents the sum of these values. The third column (cont., %) is based on average (second column), but adjusted to sum to 100%, and the fourth column represents the cumulative contribution (c. cont) of these values. The fifth and sixth columns represent the average abundance of each taxon within each region (square root transformed, ind m^{-3}). The permutation *p*-value represents the probability of getting a larger or equal average contribution based on 999 random permutations of input data. Note that the full list of contributions from all taxa is not shown, so the sum of each entry from average (column 2) may not equal the overall average dissimilarity, and the cumulative contribution (column 4) may not reach 100%.

Taxa	Average	Cont.	C. cont.	Av. abund. (I)	Av. abund. (II)	P(perm)
Av. dissim.: 37.19%				Mid	Inner	
Podon/Pleopsis spp.	4.20	11.29	11.29	11.97	5.21	0.0024
Cirripedia (larvae)	3.78	10.16	21.45	12.02	5.94	0.0425
Corycaeidae	3.17	8.52	29.97	6.62	1.42	0.0207
Acartia spp.	2.35	6.32	36.29	11.93	11.93	0.1364
Evadne spp.	2.32	6.25	42.54	5.73	1.97	0.0011
Av. dissim.: 43.95%				Outer	Inner	
Corycaeidae	4.83	10.99	10.99	10.07	1.42	0.0001
Cirripedia (larvae)	4.78	10.87	21.85	14.80	5.94	0.0003
Podon/Pleopsis spp.	4.29	9.75	31.61	12.83	5.21	0.0016
Paracalanus spp.	3.61	8.21	39.82	11.59	5.05	0.0001
Evadne spp.	2.38	5.42	45.24	6.17	1.97	0.0004
Av. dissim.: 25.92%				Outer	Mid	
Echinodermata (larvae)	2.41	9.28	9.28	6.26	9.56	0.1874
Paracalanus spp.	2.11	8.14	17.42	11.59	6.93	0.4815
Acartia spp.	1.99	7.66	25.08	8.57	11.93	0.5593
Cirripedia (larvae)	1.94	7.47	32.56	14.80	12.02	0.9877
Corycaeidae	1.50	5.80	38.35	10.07	6.62	0.9995

Lemmens June 2021 - Tide and station effects

In the Lemmens Inlet June 2021 data, no significant differences in multivariate dispersion were observed between tide phases ($F_{1, 14}$ = 0.412, *P*(perm) = 0.5291) or among stations ($F_{2, 13}$ = 0.291, *P*(perm) = 0.7518) (Table 22, Fig. 22). PERMANOVA found no significant differences in zooplankton assemblage structure between the tide phases (*pseudo*-$F_{1, 10}$ = 0.451, *P*(perm) = 0.8749), although a significant effect of station was observed (*pseudo*-$F_{2,10}$ = 12.123, *P*(perm) = 0.048) and explained 26.12% of the variation in the data (Table 23). Pairwise comparisons found statistically significant differences in composition between Inner and Mid stations (*pseudo-t* = 1.617, *P*(perm) = 0.0354) (Table 23). Similar to the NMDS (Fig. 20B), no significant differences were observed between the Inner and Outer stations in the inlet (*t* = 1.338, *P*(perm) = 0.1198) (Table 23).

SIMPER analysis revealed an overall average dissimilarity of 37.19% between Inner and Mid stations, with *Acartia* spp. as the taxon most responsible for the differentiation between the two (higher average abundances in Inner, lower in Mid) (Table 24).

Table 22. Summary of the multivariate homogeneity of group dispersions analysis for samples in Lemmens Inlet for the June 2021 dataset (Pacific region), showing the effect of tide and station (run as separate tests) on mesozooplankton (0.25 mm - 5.00 mm) assemblage structure. Results are based on a Bray-Curtis dissimilarity matrix of square root transformed mesozooplankton abundance (ind m^{-3}).

Source	df	SS	MS	F	P(perm)
Tide	1	0.001	0.001	0.412	0.5291
Residuals	14	0.021	0.001		
Total	15	0.022	0.002		
Station	2	0.001	0.001	0.291	0.7518
Residuals	13	0.023	0.002		
Total	15	0.024	0.002		

df: degrees of freedom; SS: sum of squares; MS: mean sum of squares; F: F-statistic, P(perm): significance by 9999 permutations.

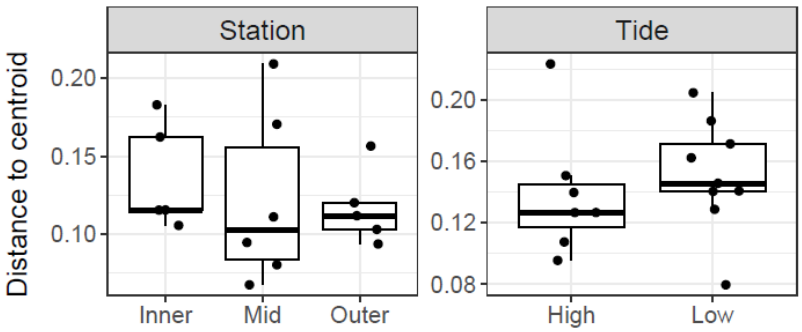

Figure 22. Boxplots depicting the distance of samples to the centroid of the corresponding station (left) or tide phase (right) for data collected in June 2021 in Lemmens Inlet (Pacific region). Results were obtained from the multivariate homogeneity of groups dispersions analysis based on a Bray-Curtis dissimilarity matrix of square root transformed mesozooplankton (0.25 mm - 5.00 mm) abundance. Boxes show the first, second and third

quartiles, and lines extending from the boxes indicate the minimum and maximum values up to 1.5 times the interquartile range. Jittered points represent the values for individual samples.

Table 23. Summary of Permutational Multivariate Analysis of Variance (PERMANOVA) showing the effect of tide, station, and their interaction in Lemmens Inlet for the June 2021 dataset (Pacific region). Results are based on a square root transformed Bray-Curtis dissimilarity matrix of mesozooplankton (0.25 mm - 5.00 mm) abundance (ind m^{-3}), and was followed by *a posteriori* pairwise comparisons between individual bays. Pseudo-t values for the pairwise comparisons were calculated as the square root of the Pseudo-F statistic generated from the *pairwise.adonis2* R function (Arbizu, 2020).

Source	df	SS	MS	R^2	Pseudo-F	P(perm)
Tide	1	0.010	0.010	2.777	0.451	0.8749
Station	**2**	**0.096**	**0.048**	**26.115**	**2.123**	**0.0410**
Tide*Station	2	0.035	0.018	9.591	0.780	0.6584
Residual	10	0.226	0.023	61.516		
Total	15	0.368	0.025	100.000		

Comparison (stations)	Pseudo-t	P(perm)
Inner - Mid	**1.617**	**0.0354**
Inner - Outer	1.338	0.1198
Mid - Outer	1.614	0.0518

df: degrees of freedom; SS: sum of squares; MS: mean sum of squares; R^2: coefficient of variation; Pseudo-F: F statistic by permutation, P(perm): significance by 9999 permutations; Pseudo-t: t-value by permutation. Significant effects are highlighted in bold (P(perm < 0.05).

Table 24. Similarity percentage (SIMPER) analysis to identify the top five mesozooplankton (0.25 mm - 5.00 mm) taxa that contribute most to the average Bray-Curtis dissimilarities between stations in Lemmens Inlet (Pacific region) in June 2021. Values in the second column (average) represent the percent contribution of each taxon to average between-group dissimilarity, and overall average dissimilarity (av. dissim., %) represents the sum of these values. The third column (cont., %) is based on average (second column), but adjusted to sum to 100%, and the fourth column represents the cumulative contribution (c. cont) of these values. The fifth and sixth columns represent the average abundance of each taxon within each region (square root transformed, ind m^{-3}). The permutation *p*-value represents the probability of getting a larger or equal average contribution based on 999 random permutations of input data. Note that the full list of contributions from all taxa is not shown, so the sum of each entry from average (column 2) may not equal the overall average dissimilarity, and the cumulative contribution (column 4) may not reach 100%.

Taxa	Average	Cont.	C. cont.	Av. abund. (I)	Av. abund. (II)	P(perm)
Av. dissim.: 37.19%				Inner	Mid	
Acartia spp.	3.43	14.58	14.58	33.33	24.27	0.0455
Cirripedia (larvae)	2.00	8.51	23.09	32.67	28.11	0.4187
Evadne spp.	1.93	8.20	31.29	14.06	7.23	0.0002
Oikopleura spp.	1.84	7.80	39.09	16.10	19.62	0.9185
Podon/Pleopsis spp.	1.61	6.86	45.96	16.67	11.00	0.0489

3.4.2 Maritimes region

For all sites within the Maritimes region, *Acartia* spp. was the most abundant taxon in every sample. Specifically, the relative proportional abundance of *Acartia* spp. per sample ranged from 61.9-96.3% in Argyle (Fig. 23A), 41.6-54.97% in Country Harbour (Fig. 23B), 74.8-97.7% in Sober Island (Fig. 23C), and 50.6-75.6% in Whitehead (Fig. 23D). Generally, the differences in the relative abundance of taxa were more noticeable between sites, than within specific stations or tide phases at a specific site, as also shown in section 3.3.2. Further analyses were thus conducted independently for each site.

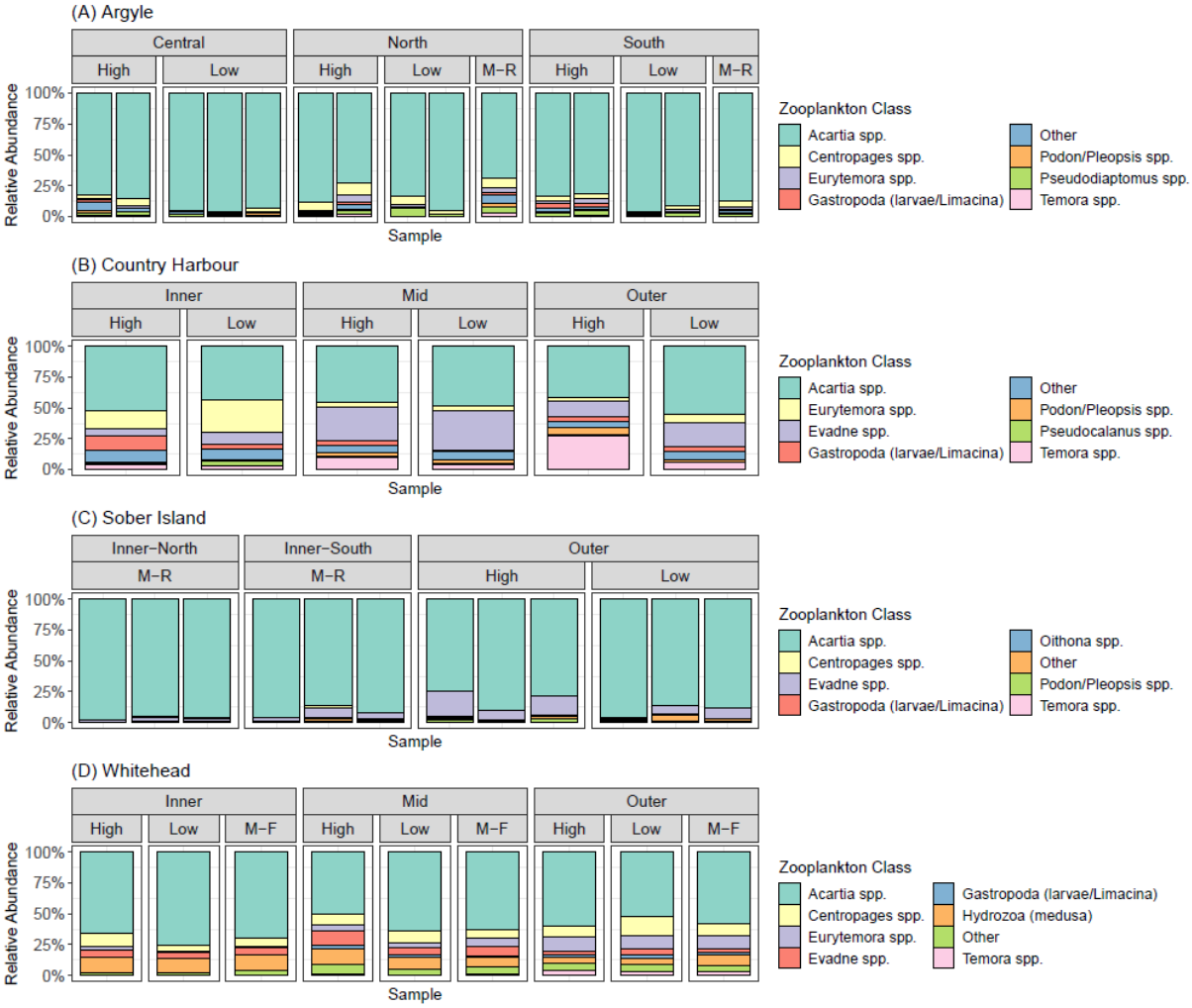

Figure 23. Relative abundance bar charts showing the zooplankton composition of individual samples from sites within the Maritimes region. For each site, the top seven most common taxa are identified, while the remaining taxa are grouped into an “Other” category; therefore, the corresponding colour scheme may differ among charts. The top panel in each subplot indicates station labels as denoted in Fig 1, and sub-panels refer to tide phases including high tide (High), low tide (Low), mid-falling (M-F), and mid-rising (M-R).

In general, NMDS ordinations for individual sites in the Maritimes region showed groupings by station and in some instances, tide phase (Fig. 24). For Argyle, High tide samples were separated from Low tide samples and occupied the lower right, and upper portions of the NMDS, respectively (Fig 23A). Samples from the Mid-Rising tide phase were intermixed within the High tide samples. In addition, when moving from left to right on the *x*-axis of the NMDS, samples generally transitioned from Outer to Inner to Mid stations, although there was overlap among the station types.

For Country Harbour, the near-zero stress on the NMDS ordinations indicates that multiple unique solutions may exist, and re-running the code may generate slightly different ordinations (Fig. 24B). In the ordination, samples appeared to generally group by station, as Inner station samples were located in the top right of the NMDS, Outer station data were in the middle of the ordination, and Mid station samples were located in the bottom right. One sample (Outer station, High tide) appeared as an outlier in comparison, and was located on the left-hand side of the NMDS. There were no clear groupings by tide phase in the ordination.

For Sober Island, the NMDS showed groupings of samples by station, although deciphering between station and tide effects is complicated by the lack of repeated sampling at different tide phases (Fig. 24C). In particular, the Inner and Mid stations were only sampled during Mid-Rising tides, and the Outer station was sampled only at High and Low tide. However, in general, the outer station samples were grouped in the upper left quadrant of the NMDS, samples from the Inner station were located in the bottom left, and Mid station samples were in the lower-right quadrant. The lack of clear separation between Low and High tide data at the Outer station indicates the mesozooplankton composition is likely not different between these tide phases. Mid-rising tides were distinct from the other tide phases, and those from the Inner-North stations were distinct from the Inner-South.

The NMDS for Whitehead showed differences in mesozooplankton composition among stations (Fig. 24D). Moving from top left to bottom right of the NMDS, the samples transition from Inner to Mid, then Outer stations. An effect of the tide phase may be present, since the High tide samples from all stations were located in the bottom left portion of the NMDS, which were separated from the intermixed Low Tide and Mid-Falling samples.

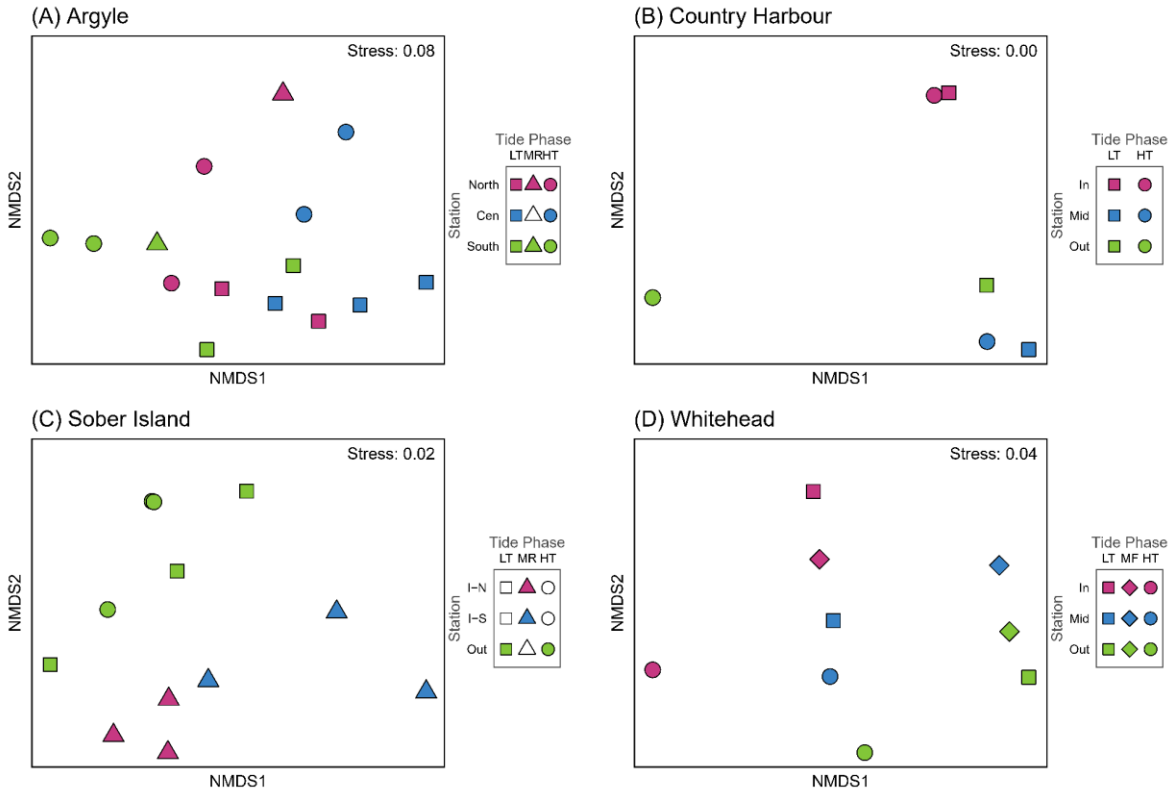

Figure 24. Two-dimensional non-metric multidimensional scaling ordination showing similarity in mesozooplankton (0.25 mm - 5.00 mm) assemblage structure for sites sampled within the Maritimes region, including (A) Argyle, (B) Country Harbour, (C) Sober Island Oyster, and (D) Whitehead. Each ordination was constructed using a Bray-Curtis dissimilarity matrix of square root transformed mesozooplankton abundance (ind m^{-3}). Symbol shapes indicate tide phases (LT: low tide, MR: mid-rising; MF: Mid-Falling, HT: high tide), and colours represent the sampling location (station) within each site, as denoted in Fig. 1. Legend items shown in white indicate that samples were not obtained for that specific tide phase and station combination.

Argyle - Tide and station effects

In Argyle, no significant differences in multivariate dispersion were observed between tide phases ($F_{1, 11}$ = 2.105, *P*(perm) = 0.1714) or among stations ($F_{2, 12}$ = 0.552, *P*(perm) = 0.6013) (Table 25, Fig. 25). PERMANOVA indicated a significant effect of tide phase (*pseudo*-$F_{1,7}$ = 7.624, *P*(perm) = 0.0023) that explained 29.41% of the variation in mesozooplankton assemblage structure (Table 26). In addition, a significant Station effect was also observed (PERMANOVA *pseudo*-$F_{2,7}$ = 4.501, *P*(perm) = 0.0107) and explained 34.72% of the variation in mesozooplankton assemblage structure (Table 26). Pairwise comparisons revealed significant differences in assemblage structure between the Central and South stations (*pseudo-t* = 2.212, *P*(perm) = 0.0239) (Table 26). These findings agree with the NMDS ordinations, which also showed a visual separation between these stations (Fig. 24A).

SIMPER analysis identified *Acartia* spp. as the taxon most responsible for differentiating between High tide and Low tide samples (av. dissim. 32.4%) (Table 27). The average abundance of *Acartia* spp. was lower in samples from Low tide than samples at High tide. *Acartia* spp. was also identified as the taxon most responsible for differentiating between Central and South stations (av. dissim.: 35.55%) (Table 27). The average abundance of *Acartia* spp. was lower in the Central than the South station (Table 27).

Table 25. Summary of the multivariate homogeneity of group dispersions analysis for Argyle (Maritimes region), showing the effect of tide and station (run as separate tests) on mesozooplankton (0.25 mm - 5.00 mm) assemblage structure. Results are based on a Bray-Curtis dissimilarity matrix of square root transformed mesozooplankton abundance (ind m^{-3}). Data with a Mid-Rising tide phase (*n* = 2) were excluded from the analysis.

Source	df	SS	MS	F	P(perm)
Tide	1	0.010	0.010	2.105	0.1714
Residuals	11	0.054	0.005		
Total	12	0.064	0.015		
Station	2	0.004	0.002	0.552	0.6013
Residuals	10	0.036	0.004		
Total	12	0.040	0.006		

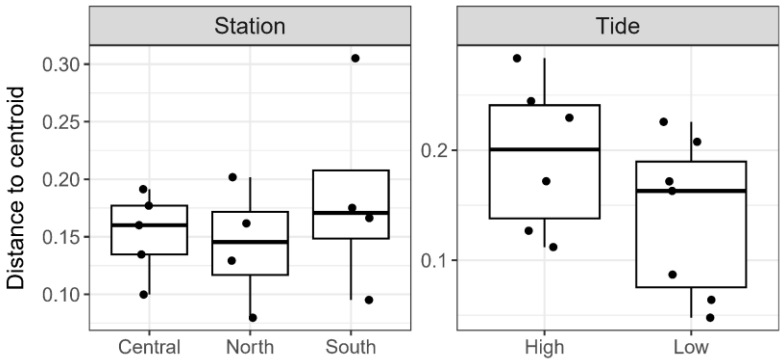

Figure 25. Boxplots depicting the distance of samples to the centroid of the corresponding station (left) or tide phase (right) for data collected in Argyle (Maritimes region). Results were obtained from the multivariate homogeneity of groups dispersions analysis based on a Bray-Curtis dissimilarity matrix of square root transformed mesozooplankton (0.25 mm - 5.00 mm) abundance. Boxes show the first, second and third quartiles, and lines extending from the

boxes indicate the minimum and maximum values up to 1.5 times the interquartile range. Jittered points represent the values for individual samples.

Table 26. Summary of the Permutational Multivariate Analysis of Variance (PERMANOVA) showing the effect of tide, station, and their interaction in Argyle (Maritimes region). Results are based on a square root transformed Bray-Curtis dissimilarity matrix of mesozooplankton (0.25 mm - 5.00 mm) abundance (ind m^{-3}), and was followed by *a posteriori* pairwise comparisons between individual stations. Pseudo-t values for the pairwise comparisons were calculated as the square root of the Pseudo-F statistic generated from the *pairwise.adonis2* R function (Arbizu, 2020). Data with a Mid-Rising tide phase (*n* = 2) were excluded from the analysis; therefore, pairwise comparisons are not shown for tide effects since there are only two levels (high tide and low tide) in the main PERMANOVA.

Source	df	SS	MS	R^2	Pseudo-F	P(perm)
Tide	1	0.171	0.171	29.407	7.624	**0.0023**
Station	2	0.202	0.101	34.721	4.501	**0.0107**
Tide*Station	2	0.052	39.387	8.870	1.150	0.3456
Residual	7	0.157	0.022	27.002		
Total	12	0.582	0.0485	100.000		
Comparison (stations)					Pseudo-t	P(perm)
Central - South					**2.212**	**0.0239**
Central - North					1.767	0.0687
South - North					1.040	0.3464

df: degrees of freedom; SS: sum of squares; MS: mean sum of squares; R^2: coefficient of variation; Pseudo-F: F statistic by permutation, P(perm): significance by 9999 permutations; Pseudo-t: t-value by permutation. Significant effects are shown in bold (P(perm < 0.05).

Table 27. Similarity percentage (SIMPER) analysis to identify the top five mesozooplankton (0.25 mm - 5.00 mm) taxa that contribute most to the average Bray-Curtis dissimilarities between tide phases (HT: high tide, LT: low tide) and stations in Argyle (Maritimes region). Tests were only conducted between significantly different (P<0.05) stations or tide phases identified in the pairwise PERMANOVA results. Values in the second column (average) represent the percent contribution of each taxon to average between-group dissimilarity, and overall average dissimilarity (av. dissim., %) represents the sum of these values. The third column (cont., %) is based on average (second column), but adjusted to sum to 100%, and the fourth column represents the cumulative contribution (c. cont) of these values. The fifth and sixth columns represent the average abundance of each taxon within each region (square root transformed, ind m^{-3}). The permutation *p*-value represents the probability of getting a larger or equal average contribution based on 999 random permutations of input data. Note that the full list of contributions from all taxa is not shown, so the sum of each entry from average (column 2) may not equal the overall average dissimilarity, and the cumulative contribution (column 4) may not reach 100%.

Taxa	Average	Cont.	C. cont.	Av. abund. (I)	Av. abund. (II)	P(perm)
Av. dissim.: 32.40%				LT	HT	
Acartia spp.	8.37	25.83	25.83	30.17	35.39	0.4408
Centropages spp.	3.60	11.11	36.94	4.66	8.90	0.0458
Gastropoda (larvae/Limacina)	3.19	9.84	46.78	0.82	5.59	0.0019
Eurytemora spp.	2.58	7.96	54.74	2.55	6.01	0.0175
Pseudodiaptomus spp.	2.16	6.67	61.41	4.36	6.28	0.4932
Av. dissim.: 35.55%				Central	South	
Acartia spp.	12.45	35.01	35.01	24.72	42.05	0.0038
Gastropoda (larvae/Limacina)	3.38	9.51	44.52	0.99	6.05	0.0353
Centropages spp.	3.05	8.58	53.10	3.81	7.91	0.5788
Eurytemora spp.	2.58	7.26	60.36	2.25	6.15	0.131
Pseudodiaptomus spp.	2.54	7.15	67.51	3.40	7.22	0.1988

3.4.3 Gulf region

For sites within the Gulf region, *Acartia* spp. was usually the most abundant taxon in each sample, with relative abundances of 69.1 - 96.3% in Cocagne (Fig. 26A) and 61.2 - 99.3% in St. Peters (Fig. 26C). Exceptions were seen in Malpeque where samples collected in fall stormy weather were dominated by *Evadne* spp. (Central station, 40.4%), or *Fritillaria* spp. (North 19.8% and South 18.6% stations) (Fig. 26B) and in St. Peters where Bivalvia larvae could also occasionally comprise the largest portion of the relative abundance (up to 59.4%) (Fig. 26C). Further analyses were performed independently for each site as it was the most structuring factor of Gulf data (see section 3.3.2).

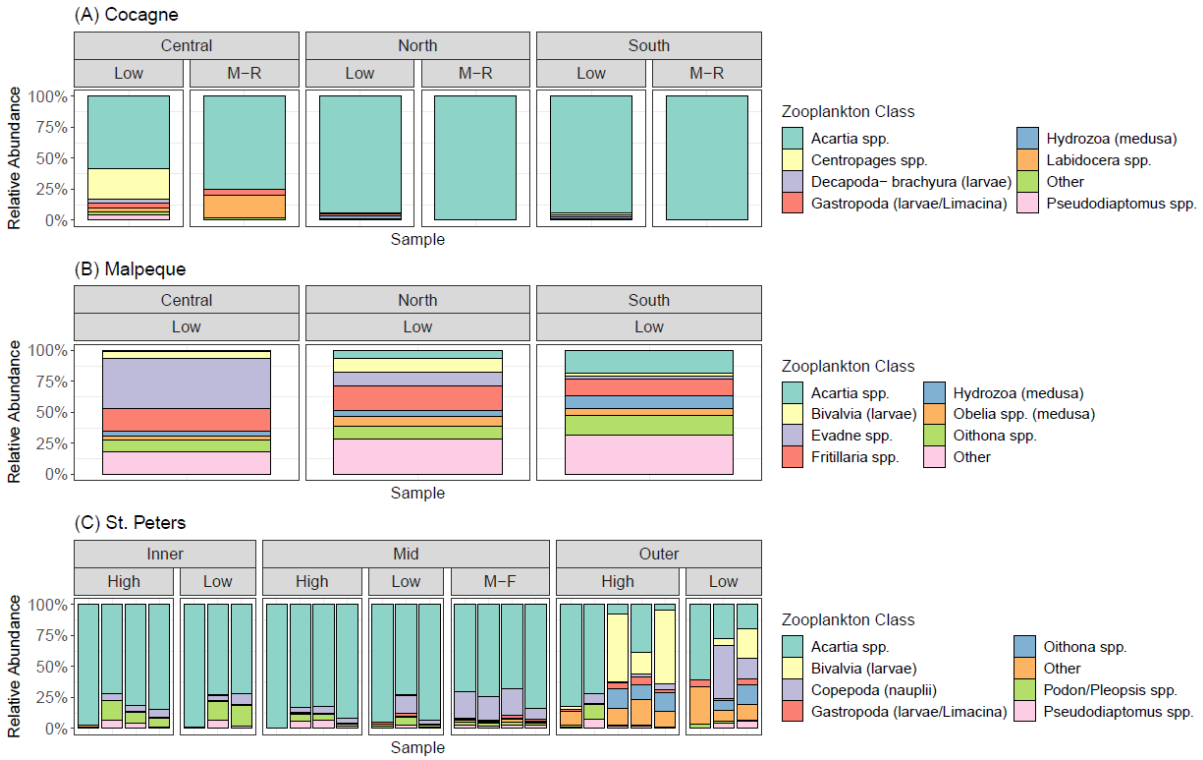

Figure 26. Relative abundance bar charts showing the zooplankton composition of individual samples from sites within the Gulf region. For each site, the top seven most common taxa are identified, with all other taxa grouped into an “Other” category; therefore, the resulting colour scheme may differ among charts. The top panel in each subplot indicates station labels as denoted in Fig. 1, and sub-panels refer to tide phases including high tide (High), low tide (Low), mid-falling (M-F), and mid-rising (M-R).

For Cocagne, the ordination shows a separation between July (left-hand side of NMDS) and August (mid/right) samples, indicating a possible difference in composition between the two sampling months (Fig. 27A). However, the near-zero stress indicates multiple equally-valid ordinations may be possible, although running the code multiple times generally resulted in similar patterns being displayed (Fig 26A). By default, this also shows differences in composition between Low (July) and Mid-Rising (August) tide phases, since samples were only collected at one tide phase per month (Fig. 27A). No obvious trends are apparent in the NMDS ordination for Malpeque due to low sample size (n = 3, Fig. 27B). For St. Peters, there is no obvious grouping by tide phase in the NMDS ordination (Fig. 27C). However, samples are somewhat grouped by station, and the Outer station samples are generally located in the upper portions of the NMDS, while samples from the Mid and Inner stations are intermixed in the lower portion of the NMDS (Fig. 27C).

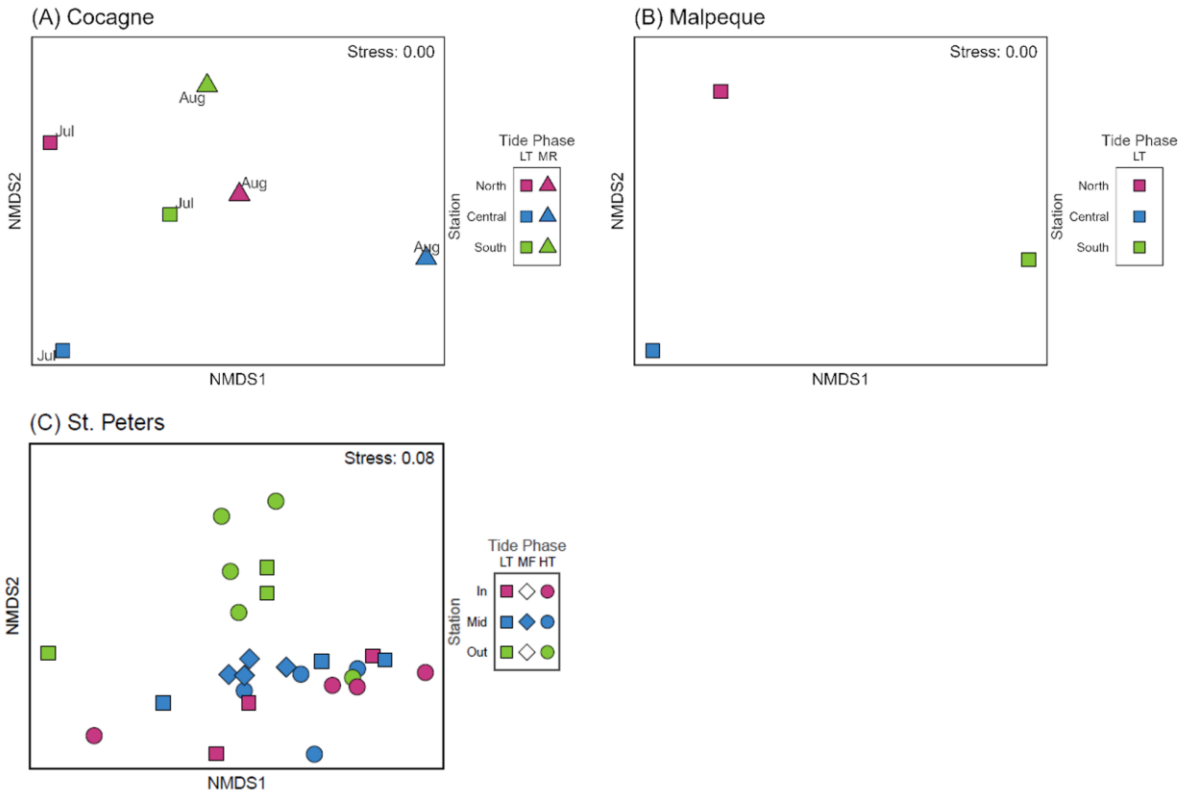

Figure 27. Two-dimensional non-metric multidimensional scaling ordination showing similarity in mesozooplankton (0.25 mm - 5.00 mm) assemblage structure for samples collected within the Gulf region, including (A) Cocagne, (B) Malpeque, and (C) St. Peters. Each ordination was constructed using a Bray-Curtis dissimilarity matrix of square root transformed mesozooplankton abundance (ind m^{-3}). Symbol shapes indicate tide phases (LT: low tide and HT: high tide), and colours represent the sampling station within each bay, as denoted in Fig. 1. Text labels in (A) represent sampling months (Jul: July and Aug: August), since samples in Cocagne were obtained in more than one field season. Legend items shown in white indicate that samples were not obtained for that specific tide phase and station combination.

St. Peters - Tide and station effects

In St. Peters, there were no significant differences in multivariate dispersion between the tide phases ($F_{1, 20}$ = 0.051, *P*(perm) = 0.8232) or stations ($F_{2, 19}$ = 0.183, *P*(perm) = 0.8309) (Table 28, Fig. 28). PERMANOVA did not identify significant differences in zooplankton assemblage structure between tide phases (*pseudo*-$F_{1,16}$ = 0.793, *P*(perm) = 0.5130) (Table 29). A significant Station effect was observed (PERMANOVA *pseudo*-$F_{2,16}$ = 3.026, *P*(perm) = 0.0081) and explained 25.5% of the variation in mesozooplankton assemblage structure (Table 29). Pairwise comparisons revealed statistically significant differences in assemblage structure between the Outer and Inner stations (*pseudo-t* = 2.098, *P*(perm) = 0.0037) and between Outer and Mid stations (*pseudo-t* = 2.140, *P*(perm) = 0.0036) (Table 29).

SIMPER analysis identified *Acartia* spp. as the taxon most responsible for differentiating between Outer and Inner stations (av. dissim.: 61.46%) (Table 30). The average abundance of *Acartia* spp. was lower in samples from the Outer stations and higher in samples from the Inner stations. *Acartia* spp. was also identified as the taxon most responsible for differentiating between Outer and Mid stations (av. dissim.: 53.93%). The average abundance of *Acartia* spp. was lower in samples from the Outer stations and higher in samples from the Mid stations.

Table 28. Summary of the multivariate homogeneity of group dispersions analysis for St. Peters (Gulf region), showing the effect of tide and station (run as separate tests) on mesozooplankton (0.25 mm - 5.00 mm) assemblage structure. Results are based on a Bray-Curtis dissimilarity matrix of square root transformed mesozooplankton abundance (ind m^{-3}). Data with a mid-falling tide phase (*n* = 4) were removed from the analysis.

Source	df	SS	MS	F	P(perm)
Tide	1	0.001	0.001	0.051	0.8232
Residuals	20	0.475	0.024		
Total	21	0.476	0.025		
Station	2	0.011	0.006	0.183	0.8309
Residuals	19	0.592	0.031		
Total	21	0.603	0.037		

df: degrees of freedom; SS: sum of squares; MS: mean sum of squares; F: F-statistic, P(perm): significance by 9999 permutations.

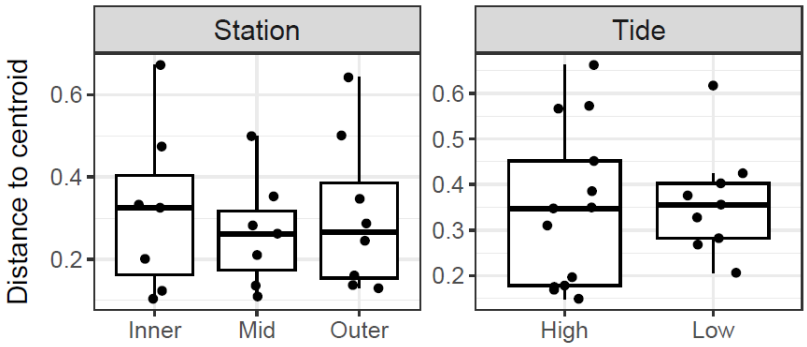

Figure 28. Boxplots depicting the distance of samples to the centroid of the corresponding station (left) or tide phase (right) for data collected in St. Peters (Gulf region). Results were obtained from the multivariate homogeneity of groups dispersions analysis based on a Bray-Curtis dissimilarity matrix of square root transformed mesozooplankton (0.25 mm - 5.00 mm) abundance. Boxes show the first, second and third quartiles, and lines extending from the boxes indicate the minimum and maximum values up to 1.5 times the interquartile range. Jittered points represent the values for individual samples. Data with a mid-falling tide phase (*n* = 4) are not shown.

Table 29. Summary of Permutational Multivariate Analysis of Variance (PERMANOVA) showing the effect of tide, station, and their interaction in St. Peters Bay (Gulf region). Results are based on a square root transformed Bray-Curtis dissimilarity matrix of mesozooplankton (0.25 mm - 5.00 mm) abundance (ind m^{-3}), followed by *a posteriori* pairwise comparisons between individual stations. t-values for the pairwise comparisons were calculated as the square root of the Pseudo-F statistic generated from the *pairwise.adonis2* R function (Arbizu, 2020). Data with a mid-falling tide phase (*n* = 4) were removed from the analysis.

Source	df	SS	MS	R^2	Pseudo-F	P(perm)
Tide	1	0.107	0.107	3.341	0.793	0.5130
Station	**2**	**0.817**	**0.408**	**25.500**	**3.026**	**0.0081**
Tide*Station	2	0.120	0.060	3.743	0.444	0.9094
Residual	16	2.160	0.135	67.416		
Total	21	3.203	0.153	100.000		

Comparison (stations)	Pseudo-t	P(perm)
Inner - Mid	0.612	0.8070
Inner - Outer	**2.098**	**0.0037**
Mid - Outer	**2.140**	**0.0036**

df: degrees of freedom; SS: sum of squares; MS: mean sum of squares; R^2: coefficient of variation; Pseudo-F: F statistic by permutation, P(perm): significance by 9999 permutations; Pseudo-t: t-value by permutation.t: t-value. Significant effects are shown in bold (P(perm < 0.05)).

Table 30. Similarity percentage (SIMPER) analysis to identify the top five mesozooplankton (0.25 mm - 5.00 mm) taxa that contribute most to the average Bray-Curtis dissimilarities between stations in St. Peters Bay (Gulf region). Tests were only conducted between significantly different (P<0.05) stations identified in the pairwise PERMANOVA results. Values in the second column (average) represent the percent contribution of each taxon to average between-group dissimilarity, and overall average dissimilarity (av. dissim., %) represents the sum of these values. The third column (cont., %) is based on average (second column), but adjusted to sum to 100%, and the fourth column represents the cumulative contribution (c. cont) of these values. The fifth and sixth columns represent the average abundance of each taxon within each region (square root transformed, ind m^{-3}). The permutation *p*-value represents the probability of getting a larger or equal average contribution based on 999 random permutations of input data. Note that the full list of contributions from all taxa is not shown, so the sum of each entry from average (column 2) may not equal the overall average dissimilarity, and the cumulative contribution (column 4) may not reach 100%.

Taxa	Average	Cont.	C. cont.	Av. abund. (I)	Av. abund. (II)	P(perm)
Av. dissim.: 61.46%				Outer	Inner	
Acartia spp.	15.00	24.40	24.40	30.37	67.72	0.4061
Bivalvia (larvae)	6.96	11.32	35.72	22.00	0.41	0.0046
Podon/Pleopsis spp.	6.45	10.50	46.22	7.51	24.31	0.0273

Taxa	Average	Cont.	C. cont.	Av. abund. (I)	Av. abund. (II)	P(perm)
Copepoda (nauplii)	5.13	8.35	54.57	12.75	16.49	0.6392
Oithona spp.	4.39	7.14	61.70	14.39	1.73	0.0046
Av. dissim.: 53.93%				Outer	Mid	
Acartia spp.	13.03	24.16	24.16	30.37	56.45	0.8447
Bivalvia (larvae)	6.97	12.92	37.08	22.00	2.30	0.0007
Copepoda (nauplii)	4.82	8.93	46.01	12.75	14.63	0.8805
Oithona spp.	4.36	8.09	54.10	14.39	3.03	0.0011
Hydrozoa (medusa)	2.94	5.44	59.54	8.83	0.75	0.0001

3.4.4 Newfoundland region

In South Arm, visualizations (relative abundance charts and NMDS ordinations) were created for the September 2020 and October 2021 datasets to show the potential influences of station and tide effects. For these two months, *Acartia* spp., *Evadne* spp., *Pseudocalanus* spp., and *Temora* spp. comprised the majority of each sample (Fig. 29). However, differences in the relative abundance of taxa were more noticeable between these two months than within specific stations or tide phases for each month, as also shown in Section 3.3.2. Further analyses were thus conducted independently for each month.

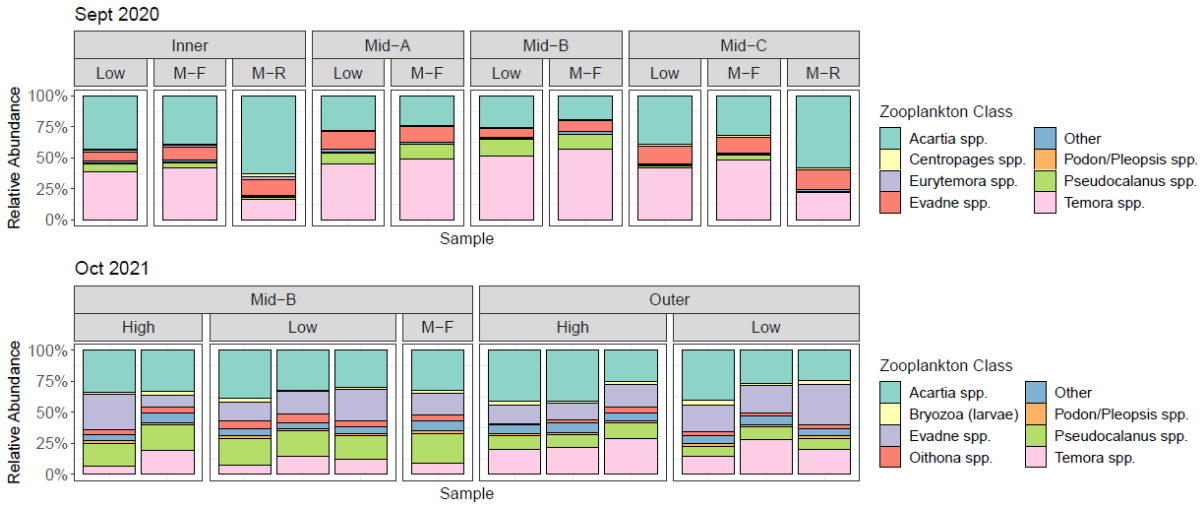

Figure 29. Relative abundance bar charts showing the zooplankton composition of individual samples from (A) September 2020 and (B) October 2021 from South Arm (Newfoundland). For each time period, the top seven most common taxa are identified, while the remaining taxa are grouped into an “Other” category; therefore, the resulting colour scheme may be different among charts. The top panel in each subplot indicates station labels as denoted in Fig. 1, and sub-panels refer to tide phases including high (High), low (Low), mid-falling (M-F), and mid-rising (M-R) tides.

The NMDS ordinations for samples collected in September 2020 from South Arm do not show groupings based on tide phase, but do show a separation by station (Fig. 30A). In October 2021, differences in composition between Outer (left-hand side of NMDS) and Mid-B stations (right) were apparent, and showed a clear separation (Fig 29B). There were no obvious groupings based on tide phase (Fig 29B).

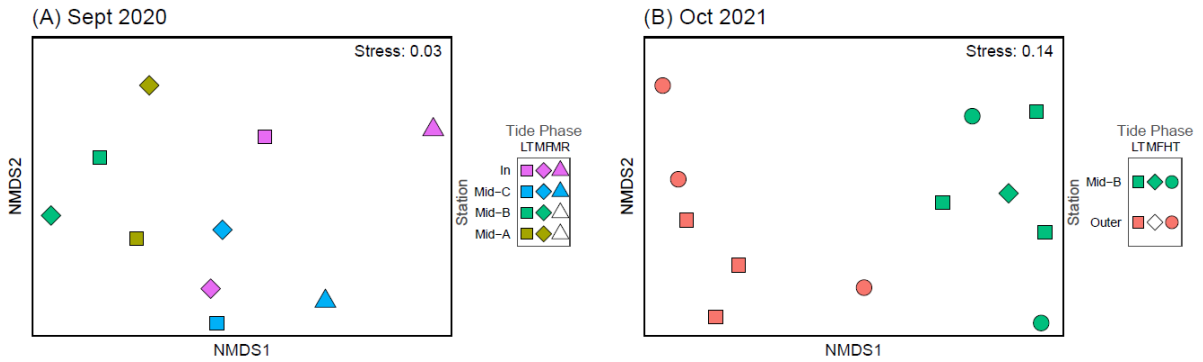

Figure 30. Two-dimensional non-metric multidimensional scaling ordination showing similarity in mesozooplankton (0.25 mm - 5.00 mm) assemblage structure for samples collected in (A) September 2020 and (B) October 2021 in South Arm, Newfoundland. Each ordination was constructed using a Bray-Curtis dissimilarity matrix of square root transformed mesozooplankton abundance (ind m^{-3}). Symbol shapes indicate tide phases (LT: low tide, MF: mid-falling, MR: mid-rising, HT: high tide), and colours represent the sampling location (station) within each bay, as denoted in Fig. 1. Legend items shown in white indicate that samples were not obtained for that specific tide phase and station combination.

South Arm October 2021 - Tide and station effects

For the October 2021 data from South Arm, no significant differences in multivariate dispersion were observed between the tide phases ($F_{1, 9}$ = 0.280, P(perm) = 0.6011) or

between stations ($F_{1, 9}$ = 0.145, *P*(perm) = 0.6955) (Table 31, Fig. 31). PERMANOVA indicated no statistically significant differences in zooplankton assemblage structure between the Low and High tide phases (PERMANOVA *pseudo*-$F_{1, 7}$ = 1.236, *P*(perm) = 0.2697), although a significant effect of station (Mid-B vs Outer) was observed (PERMANOVA *pseudo*-$F_{1,7}$ = 4.187, *p* = 0.0012), which explained 31.09% of the variation in mesozooplankton assemblage structure (Table 32).

SIMPER analysis identified *Temora* spp. as the taxon most responsible for differentiating between the Outer and Mid-B stations (av. dissim.: 18.92%) (Table 33). The average abundance of *Temora* spp. was higher in samples from the Outer station and lower in samples from the Mid-B station.

Table 31. Summary of the multivariate homogeneity of group dispersions analysis for October 2021 data collected in October 2021 in South Arm (Newfoundland region). Results show the effect of tide and station (run as separate tests) on mesozooplankton (0.25 mm - 5.00 mm) assemblage structure based on a Bray-Curtis dissimilarity matrix of square root transformed mesozooplankton abundance (ind m^{-3}). Data from the mid-falling tide phase (*n* = 1) were excluded from the analysis.

Source	df	SS	MS	F	P(perm)
Tide	1	0.000	0.000	0.280	0.6011
Residuals	9	0.003	0.000		
Total	10	0.004	0.000		
Station	1	0.000	0.000	0.145	0.6955
Residuals	9	0.003	0.000		
Total	10	0.003	0.000		

df: degrees of freedom; SS: sum of squares; MS: mean sum of squares; F: F-statistic, P(perm): significance by 9999 permutations.

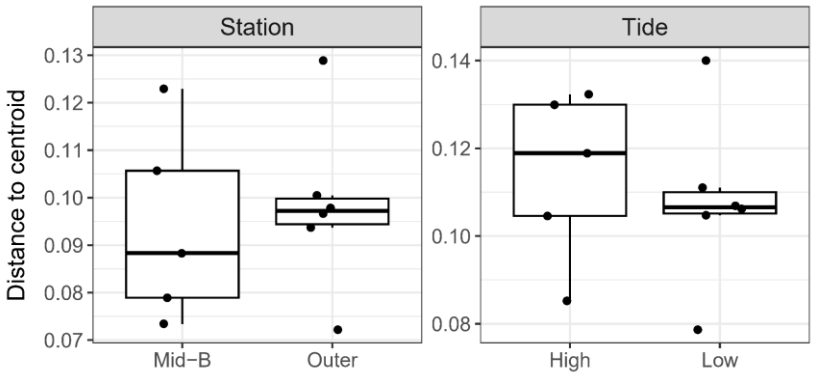

Figure 31. Boxplots depicting the distance of samples to the centroid of the corresponding station (left) or tide phase (right) for data collected in October 2021 from South Arm (Newfoundland region). Results were obtained from the multivariate homogeneity of groups dispersions analysis based on a Bray-Curtis dissimilarity matrix of square root transformed mesozooplankton (0.25 mm - 5.00 mm) abundance. Boxes show the first, second and third quartiles, and lines extending from the boxes indicate the minimum and maximum values up

to 1.5 times the interquartile range. Jittered points represent the values for individual samples. Data from the mid-falling tide phase (*n* = 1) are not shown.

Table 32. Summary of Permutational Multivariate Analysis of Variance (PERMANOVA) showing the effect of tide, station, and their interaction for samples collected in South Arm (Newfoundland region) in October 2021. Results are based on a square root transformed Bray-Curtis dissimilarity matrix of mesozooplankton (0.25 mm - 5.00 mm) abundance (ind m^{-3}). Data from the mid-falling tide phase (*n* = 1) were excluded from the analysis.

Source	df	SS	MS	R^2	Pseudo-F	P(perm)
Tide	1	0.014	0.014	9.180	1.236	0.2697
Station	**1**	**0.047**	**0.047**	**31.091**	**4.187**	**0.0012**
Tide*Station	1	0.012	0.012	7.755	1.044	0.3982
Residual	7	0.079	0.011	51.974		
Total	10	0.152	0.015	100.000		

df: degrees of freedom; SS: sum of squares; MS: mean sum of squares; R^2: coefficient of variation; Pseudo-F: F statistic by permutation, P(perm): significance by 9999 permutations. Significant effects are shown in bold (P(perm < 0.05)).

Table 33. Similarity percentage (SIMPER) analysis to identify the top five mesozooplankton (0.25 mm - 5.00 mm) taxa that contribute most to the average Bray-Curtis dissimilarities between stations in South Arm (Newfoundland region) in October 2021. Tests were only conducted between significantly different (P<0.05) stations identified in the pairwise PERMANOVA results. Values in the second column (average) represent the percent contribution of each taxon to average between-group dissimilarity, and overall average dissimilarity (av. dissim., %) represents the sum of these values. The third column (cont., %) is based on average (second column), but adjusted to sum to 100%, and the fourth column represents the cumulative contribution (c. cont) of these values. The fifth and sixth columns represent the average abundance of each taxon within each region (square root transformed, ind m^{-3}). The permutation *p*-value represents the probability of getting a larger or equal average contribution based on 999 random permutations of input data. Note that the full list of contributions from all taxa is not shown, so the sum of each entry from average (column 2) may not equal the overall average dissimilarity, and the cumulative contribution (column 4) may not reach 100%.

Taxa	Average	Cont.	C. cont.	Av. abund. (I)	Av. abund. (II)	P(perm)
Av. dissim.: 18.92%				Outer	Mid B	
Temora spp.	2.55	13.45	13.45	15.93	10.84	0.0050
Pseudocalanus spp.	1.76	9.32	22.77	10.75	14.31	0.0001

Taxa	Average	Cont.	C. cont.	Av. abund. (I)	Av. abund. (II)	P(perm)
Evadne spp.	1.54	8.13	30.90	15.25	13.81	0.5806
Oithona spp.	1.15	6.10	37.00	5.15	7.39	0.0137
Acartia spp.	1.15	6.07	43.07	19.36	18.57	0.2619

No significant differences in taxa richness were observed between high and low tide for any sites where comparisons were evaluated (Table 34).

Table 34. Results of the two-sample *t*-tests to evaluate differences in abundance, taxa richness, Shannon diversity (i.e., the exponential of the Shannon index), and Simpson diversity (i.e., the inverse Simpson index) between tide phases for select stations. Tests were conducted for stations with at least three samples per high or low tide.

Region	Site	Station	Index	Mean HT	Mean LT	df	t	95% CI	P
Pac	Lemmens Aug 2020	Outer	Abundance	949.34	1265.18	4	-0.66	[-1644.74, 1013.06]	0.545
			Richness	24.33	23.67	4	0.34	[-4.81, 6.14]	0.752
			Shannon	10.75	10.35	4	0.32	[-2.98, 3.77]	0.763
			Simpson	7.83	7.37	4	0.53	[-1.99, 2.92]	0.625
		Mid	Abundance	965.12	775.05	4	0.77	[-495, 875.13]	0.484
			Richness	21.33	23.33	4	-2.68	[-4.07, 0.07]	0.055
			Shannon	9.79	10.37	4	-1.07	[-2.10, 0.93]	0.345
			Simpson	7.37	7.66	4	-0.38	[-2.40, 1.83]	0.725

Region	Site	Station	Index	Mean HT	Mean LT	df	t	95% CI	P
		Inner	Abundance	383.19	352.07	4	0.19	[-428.5, 490.74]	0.860
			Richness	18.00	18.33	4	-0.12	[-7.74, 7.07]	0.907
			Shannon	6.46	7.18	4	-0.65	[-3.81, 2.37]	0.552
			Simpson	4.07	4.81	4	-0.83	[-3.22, 1.74]	0.455
	Lemmens Jun 2021	Mid	Abundance	2063.04	2989.06	4	-0.83	[-4017.95, 2165.92]	0.452
			Richness	25.67	23.33	4	0.89	[-4.95, 9.62]	0.424
			Shannon	7.42	6.61	4	1.57	[-0.62, 2.25]	0.191
			Simpson	4.63	4.30	4	1.01	[-0.58, 1.24]	0.369
Mar	Sober Island	Outer	Abundance	4827.65	6503.33	4	-0.44	[-12316.5, 8965.12]	0.685
			Richness	14.67	16.33	4	-0.51	[-10.83, 7.5]	0.640
			Shannon	1.99	1.64	4	1.08	[-0.54, 1.23]	0.340
			Simpson	1.49	1.23	4	1.63	[-0.18, 0.69]	0.179
Gulf	St. Peters	Outer	Abundance	4883.02	1654.59	6	1.64	[-1593.31, 8050.17]	0.152
			Richness	23.20	20.67	6	0.64	[-7.19, 12.25]	0.547
			Shannon	4.37	6.18	6	-1.26	[-5.33, 1.72]	0.256

Region	Site	Station	Index	Mean HT	Mean LT	df	t	95% CI	P
			Simpson	2.73	4.20	6	-1.29	[-4.27, 1.33]	0.246
		Mid	Abundance	5076.17	8346.50	5	-0.64	[-16490.59, 9949.94]	0.553
			Richness	10.75	11.67	5	-0.49	[-5.68, 3.85]	0.642
			Shannon	1.66	1.77	5	-0.25	[-1.22, 1]	0.810
			Simpson	1.27	1.35	5	-0.35	[-0.65, 0.49]	0.740
		Inner	Abundance	10231.73	4892.31	5	0.74	[-13243.19, 23922.04]	0.493
			Richness	10.75	10.33	5	0.15	[-6.79, 7.63]	0.888
			Shannon	1.87	1.99	5	-0.24	[-1.36, 1.13]	0.820
			Simpson	1.43	1.54	5	-0.38	[-0.83, 0.62]	0.718
NL	SE Arm Oct 2021	Outer	Abundance	1140.12	1167.82	4	-0.43	[-205.73, 150.35]	0.688
			Richness	23.33	22.00	4	0.85	[-3.01, 5.67]	0.442
			Shannon	6.20	6.30	4	-0.34	[-0.93, 0.72]	0.750
			Simpson	4.40	4.51	4	-0.30	[-1.12, 0.9]	0.777

Mean HT: average taxa richness from samples obtained at high tide, Mean LT: average taxa richness from samples obtained at low tide, df: degrees of freedom, t: t-value, CI: confidence interval, P: p-value.

4 DISCUSSION

Zooplankton play critical roles in marine food webs, and their communities are potentially altered by intensive bivalve aquaculture (Lindeman 1942; Hulot et al. 2014, 2020). This report examined the spatiotemporal dynamics of mesozooplankton assemblage structure of AMP data obtained using an innovative imaging system from nine sites, located across four DFO regions, from various sampling months, tide phases, and sampling stations. The results showed strong station effects within bays, underscoring the relevance of site-specific spatial dynamics, while tide effects were generally a less important factor for structuring mesozooplankton communities. Differences in assemblage structure were observed among monthly observations in the Pacific and Newfoundland regions, highlighting the importance of considering seasonality in future sampling. By using an optical imaging system, these results represent the first of their kind for coastal zooplankton monitoring in Canada, and will contribute to a global effort for more advanced plankton analyses using machine learning approaches (e.g., see Irisson et al. 2022). These analyses help address key knowledge gaps for effectively monitoring potential long-term ecosystem changes from bivalve aquaculture.

This report used taxa accumulation theory to quantify sampling completeness and assess the extent of undetected diversity within each site. Completeness ranged from 55.94% (South Arm, September 2020) to 99.45% (Whitehead), indicating that in general, a large portion of the estimated taxa had been sampled. Although estimated richness was generally highest in the Pacific region, high completeness was observed in multiple sites, regardless of region, including Lemmens June 2021 (98.7%, Pacific), Whitehead (99.6%, Maritimes), and St. Peters (98.6%, Gulf). For these sites, the stabilization of the slope of the rarefaction and extrapolation curves indicates that the asymptotic estimates are reliable, and the sampling effort for these sites obtained a very high proportion of the estimated diversity (Chao et al. 2014). For the remaining sites (Lemmens August 2020 and September 2021, Country Harbour, Sober Island, Cocagne, Malpeque, and South Arm), a positive slope on the rarefaction and extrapolation curves was still present when extrapolated to double the sample size; therefore, the asymptotic estimates for richness represent a lower bound (Chao et al, 2020). This often occurs for richness, as there are typically vanishingly rare taxa still to be sampled (Chao et al., 2020), and indicates that these sites have a greater number of rare taxa, which would require increased sampling effort to obtain. Rare taxa are often of interest in monitoring programs as they may make up important ecological roles and can act as indicators of human-induced environmental changes (Cao et al. 1998, 2001; Ma et al. 2022); however, it is virtually impossible to sample all taxa present, especially in hyper-diverse communities (Colwell and Coddington 1994; Gotelli and Colwell 2001; Magurran and McGill 2010). Regardless, these results indicate that a large portion of diversity was captured at each site (55.94% - 99.45%). The markedly different completeness profile for South Arm September 2020 was likely due to the high Chao2 asymptotic estimate, which can result from a large number of singletons within samples, or taxa that are only present within one sample (Chao 1984, 1987). Future work can address whether these are true biological phenomena or if a greater number of samples per site will result in asymptotic estimates closer to the observed richness value (e.g., as with the South Arm October 2021 data). Overall, these results provide important baseline information for expected trends in diversity, and present helpful guidance of potential changes to completeness if sampling effort is increased or decreased in future field campaigns.

Data collected from multiple months in the Newfoundland and Pacific regions revealed that seasonality effects are important to consider when monitoring mesozooplankton. This agrees with existing research, since zooplankton are known to exhibit seasonality in community structure, which is driven by a combination of both biological and physical factors (Neuheimer et al. 2010; Ji et al. 2010; Tommasi et al. 2013). In the Pacific region, the assemblage structure was different between each month; therefore, sampling in multiple

months will lead to better understanding of the local diversity. In Newfoundland, the year-round data collection provided a detailed characterization of mesozooplankton dynamics, and revealed a cyclical shift in mesozooplankton communities between months. In addition to providing important information of the local diversity, these results may help identify preferred months for sampling. For example, large shifts in the assemblage structure during certain time periods were visualized on the NMDS ordination (e.g., October to November, March to April) which may be related to processes such as plankton blooms or storms. Because AMP is focused on evaluating long-term trends, sampling during these time periods is likely not recommended as the mesozooplankton structure is less stable, thereby challenging the interpretation of inter-annual comparisons. By contrast, the end of June to September period exhibited more stable patterns, as indicated by the smaller changes in composition on the NMDS ordination. Sampling during these time periods is advised, as it may be easier to detect long-term changes in community structure, since the variability associated with events such as blooms or storms may be minimized. Data collected within these months may be used to test which factors drive any additional changes to community composition over time, and pose new hypotheses related to the driving forces behind these shifts. For example, climate change is expected to cause alterations to zooplankton communities by causing changes in phenology (e.g., spring and summer species occur earlier), poleward shifts in distribution to remain within an optimal temperature range, and overall reductions in body size (see Ratnarajah et al. 2023 for review). Therefore, sampling at more stable time periods may help reduce the complexity of analyzing the effects of multiple driving forces, and isolate climate change-related effects to those from bivalve aquaculture. However, zooplankton communities are often characterized by strong interannual variability (e.g., Mackas et al. 2012) and the factors influencing zooplankton communities may differ seasonally due to these annually-varying processes (Varpe 2012). Likewise, the effects of bivalve aquaculture on zooplankton communities may differ seasonally (Steeves et al. 2018), but characterizing these effects across seasons was beyond the scope of the study. More data are therefore required to characterize these patterns, and to aid in the long-term analysis of these trends, we suggest sampling from at least three separate months at each site. Although we cannot develop specific recommendations for each site due to the lack of temporal data, results from Newfoundland suggest the summer months (June to September) may be the preferred sampling months going forward. Selecting consecutive months within this time frame would likely be ideal, for a continuous monthly time series within one sampling year.

Spatial patterns within bays are important to consider in future field seasons, as indicated by the observed differences in mesozooplankton assemblage structure between stations (i.e., “station effects”) for all sites. These station effects were observed either through statistical testing (e.g., Lemmens August 2020 and June 2021, Argyle, St. Peters, South Arm October 2021) or visualized on the NMDS ordinations (all others, excluding Cocagne, n = 6, and Malpeque, n = 3, for which more samples are required for reliable conclusions). These results highlight the importance of spatial dynamics, which has implications for sampling designs. For example, collecting samples from a single station within each bay is likely insufficient, since important bay dynamics would be missed. Increasing the number of samples to characterize this variability would be recommended (discussed below in more detail). However, spatial gradients in mesozooplankton assemblage structure are known in coastal settings and are driven by a complex set of biophysical characteristics including salinity, oxygen content, nutrient levels, turbidity and temperature (Soetaert and Van Rijswijk 1993; Marques et al. 2007; Helenius et al. 2017; Usov et al. 2019). Because station effects were observed in all sites, even those with low to no aquaculture production (e.g., Argyle, Country Harbour), the differences in composition between stations are likely driven by a combination of various local factors. While analyzing patterns in spatial distributions will not provide a direct causal link to processes such as bivalve grazing (McIntire and Fajardo 2009), increasing the spatial coverage and mapping the results may help further disentangle

the role of multiple driving forces on zooplankton distributions and provide a clearer visual link to the role of bivalve aquaculture production on their communities.

Tide effects on community structure were tested to (1) define if direct grazing from bivalve aquaculture could be detected and (2) if samples collected at different tides provide different species composition and thus need to be taken into consideration within long-term operational monitoring plans. Differences in composition between tide phases (i.e., “tide effects") were generally less pronounced than station effects. Likely, the variety of ecosystems, hydrographic properties, and embayment complexity within AMP sites resulted in the lack of a uniform response to different tide phases. For example, tide effects were only significant in Argyle, which has a highly complex coastline, and is located near the Bay of Fundy. The large tidal ranges likely result in differences in composition between the time periods. As indicated by the NMDS ordinations, tide effects may be important for structuring the mesozooplankton communities in Whitehead and Sober Island, which have comparatively high bivalve production for sites in the Maritimes region (see Table 35). However, tide effects were not observed in St. Peters Bay, which has similar hydrography to Whitehead (e.g., both are enclosed, narrow channels with one point of exposure with the ocean). Potentially, tide effects may be noted in some sites as the result of diel vertical migrations of the zooplankton, which may be affected by the type of tow used. Zooplankton have been found to utilize tidal currents for retention within the system, by moving vertically between outflowing surface water and inflowing deeper water (e.g. Wooldridge and Erasmus 1980; Schlacher and Wooldridge 1995). Although we attempted to minimize these effects by sampling the entire (or nearly the entire) water column, this is more difficult to achieve in shallow sites, where horizontal or oblique tows were obtained. For sites where tide effects were not observed, other factors were likely more important than tides for structuring the zooplankton communities, and monitoring the two tides will not greatly improve the description of the mesozooplankton community. A detailed understanding of the water flow within these sites may therefore help supplement future data analysis. Spatially-explicit hydrodynamic models exist for several of the sites (see Table 1 for references) and this pre-existing knowledge of the ecosystem could supplement future data analysis. For example, the outputs of seston or zooplankton depletion from the coupled biological-physical models could be compared against the collected AMP data in future work. A qualitative modeling approach may highlight critical ecological processes and interactions that could be disrupted by the presence of farms (Forget et al. 2020). There is also empirical evidence of shellfish aquaculture impacts on phytoplankton at bay-scale (Cranford et al. 2008), and Gianasi et al. (2023) showed that high mussel production decreases phytoplankton concentration to a point that it negatively impacts zooplankton survival, including important commercial species in a series of laboratory experiments. There is thus a potential food-web interaction through zooplankton depletion (i.e. direct grazing and competition) showed by theoretical models and experiments. However, in natural environments, it is unclear if bivalve aquaculture may significantly impact zooplankton communities due to unpredictable large-scale ecosystem complexity, such as interactions between nutrient availability, renewal rates for phyto- and zooplankton, niche partitioning, and environmental/stochastic variability. The development of a monitoring program for aquaculture will provide a more holistic view of ecosystem dynamics, species diversity, interactions, and changes in Canadian bivalve aquaculture sites.

Overall, these results suggest that station effects generally play a larger role in defining the zooplankton assemblage structure at each site than tide effects. We therefore recommend collecting samples at a greater number of stations from each site, to better understand these spatial dynamics. For example, samples could be obtained from 20 stations (i.e., 1 sample from each station, in 1 day, with no replicates), spread approximately evenly throughout each site, which would likely provide high sampling completeness as indicated from the taxa accumulation curves. In addition, 20 samples is also similar to the original goal of 18 samples per site (i.e., 1 sample from 3 stations from both high and low tide over 3 days = 1 x

3 x 2 x 3 = 18 samples), and could be obtained with the other pelagic properties already being collected. Although the rarefaction and extrapolation curves level off before 20 samples for some sites (e.g., Whitehead), it is generally recommended to oversample in the initial stages of monitoring programs, and reduce the number of samples in the future if necessary (Hoffman et al. 2011). For sites with confirmed tide effects (Argyle), possible tide effects (e.g., Sober Island, Whitehead), or not enough samples to draw conclusions (e.g., Country Harbour, Cocagne, Malpeque), the tide phase should still be considered when sampling. It would be recommended to test the tidal effect again, or sample at a single tide phase if this is logistically possible, to ensure data from multiple tide phases do not add additional variability to the dataset. For the remaining sites (St. Peters, South Arm, Lemmens), we have no evidence to suggest tide phases affect the mesozooplankton communities, and samples can therefore be obtained at any time during the day. Table 35 is provided below to summarize the sampling completeness, the presence of tide and station effects, and if seasonality (i.e., monthly sampling) had been considered. In absence of carrying capacity indicators consistently estimated across sites, an additional classification was assigned to each bay, indicating the potential vulnerability to aquaculture impacts on zooplankton composition. This represents a qualitative measure combining bivalve aquaculture production and bay hydrodynamics to evaluate the risk of effects on mesozooplankton community structure from bivalve grazing. Simple models could provide proper quantitative grazing pressure evaluations (Comeau et al. 2023) and should be considered to further characterize AMP sites.

Table 35. Summary table of results and sampling advice for sites and/or sampling months, collected as part of the Aquaculture Monitoring Program. Vulnerability represents a qualitative classification assigned to each bay, indicating the potential combined effects of bivalve aquaculture production and bay hydrodynamics on mesozooplankton community structure. Completeness represents the ratio of the observed to expected richness, derived from the sample-based rarefaction and extrapolation analyses. For the Station effect and Tide effect columns, “Yes” indicates statistically significant ($P<0.05$) effects of each variable were observed from PERMANOVA, while “No” indicates a significant effect was not observed. “Likely” indicates mesozooplankton assemblage structure is different among Tide phases or Stations, as visualized from the non-metric multidimensional scaling (NMDS) ordinations, but the sample sizes were too low for significance testing. “Unlikely” indicates an obvious effect was not visualized on the NMDS, and the sample sizes were also too low for significance testing. “Unknown” indicates the sample size was too low to allow for trends to be observed from either significance testing (PERMANOVA) or multivariate ordinations (NMDS).

Region	Site	Vulnerability	Completeness	Station effect	Tide effect	Seasonality
Pac	Lemmens (Aug 2020)	Low	89.17%	Yes	No	Yes
	Lemmens (June 2021)		98.67%	Yes	No	
	Lemmens (Sept 2021)		87.19%	Likely	Unlikely	
Mar	Argyle	Low	77.68%	Yes	Yes	No data
	Country Harbour	Low	86.11%	Likely	Unlikely	

Region	Site	Vulnerability	Completeness	Station effect	Tide effect	Seasonality
	Sober Island	High	83.58%	Likely	Likely	
	Whitehead	High	99.45%	Likely	Likely	
Gulf	Cocagne	Medium	68.80%	Unknown	Unknown	In progress*
	Malpeque	Medium	83.78%	Unknown	Unknown	
	St. Peters	High	98.48%	Yes	No	
Nfld	South Arm (Sept 2020)	Low	55.94%	Likely	Unlikely	Yes
	South Arm (Oct 2021)		89.71%	Yes	No	

*Seasonal data from Bouctouche, New Brunswick, were collected in 2022 and will be analyzed at a later date.

While this report provides guidance on best practices to monitoring mesozooplankton communities, further examination of trends in both the size-spectra and community structure will provide a comprehensive understanding of potential ecosystem effects such as food web alterations due to bivalve aquaculture. In that purpose, the findings in this report provide complementary results to a related departmental project that focuses on size-spectra changes in mesozooplankton using this same dataset. Additionally, while the macro-FlowCam may vastly reduce the time spent identifying plankton, thereby reducing the cost of analysis per sample (Benfield et al. 2007; Álvarez et al. 2014), these procedures also require an evaluation to identify benefits and disadvantages of the methods, and assess the reliability or confidence of the data (Jakobsen and Carstensen 2011; Álvarez et al. 2014). Taxa were also identified and enumerated using traditional microscopy for approximately 90 AMP samples, and comparing counts of the mesozooplankton taxa between the macro-FlowCam and traditional microscopy is a crucial step to ensure a reliable long-term monitoring program. Previous studies have found good agreement between zooplankton counts derived between these two methods although it is noted the taxonomic resolution provided by FlowCam is generally coarser (Le Bourg et al. 2015; Kydd et al. 2018; Detmer et al. 2019; Hrycik et al. 2019). These future comparisons will help develop local information for Canadian waters, evaluate if any corrections to FlowCam counts need to be made, and determine if any patterns such as community-level observations vary between the approaches. Furthermore, this work will also help refine precise sampling targets and document any differences in sampling completeness by the two methods, due to the potential differences in detecting rare taxa (Le Bourg et al. 2015; Stanislawczyk et al. 2018). In addition, plankton data were simultaneously collected at AMP sites for two different size fractions, which were then enumerated with the micro-FlowCam (plankton in the 50 - 600 um range) and by flow cytometry (0.2 - 20 um). Although bivalves are known to ingest mesozooplankton (Lehane and Davenport 2002; Wong and Levinton 2006; Ezgeta-Balić et al. 2012), these smaller size fractions are of particular interest, since bivalves are known to selectively filter for smaller particles during feeding (Lehane and Davenport 2002, 2006). These therefore represent key properties to be analyzed when considering potential bivalve-environment interactions. Future work will apply similar methods to those used in this report to analyze the spatiotemporal variations in these size fractions. Interpreting patterns in the zooplankton communities in these different size fractions will also help optimize future sampling strategies, and propose adjustments based on factors such as sample completeness, seasonality, stations, and tides. Continued sampling of zooplankton over a

range of aquaculture production levels may also further help develop carrying capacity models, by analyzing variations in grazing intensity (Grant et al. 2005; Ibarra et al. 2014; Han et al. 2017). In addition, these datasets will provide baseline data for analyzing potential effects under various climate change scenarios. Incorporating a combination of datasets and analysis approaches will provide greater knowledge of the possible effects of bivalve aquaculture on zooplankton communities.

5 CONCLUSION

The results obtained in this report provide a nationally-consistent spatiotemporal assessment of zooplankton community characterstics in coastal Canadian aquaculture lease areas. Samples were collected from an extensive, nation-wide monitoring program, and this report helps inform science-based recommendations to transition towards an optimal AMP operational phase to monitor long-term ecosystem effects from bivalve aquaculture. These results underscored the importance of considering seasonality, since large changes in mesozooplankton assemblage structure were observed between sampling months. Sampling during multiple (e.g., three) consecutive months is recommended, as this may, in the long term, help differentiate climate change-related shifts in mesozooplankton community structure, to those potentially resulting from bivalve aquaculture. In addition, differences in mesozooplankton composition were observed between stations at each site, while differences were often less pronounced or not detected between tide phases. For national consistency, we recommend increasing the number of stations to a higher number (e.g., 20) to better understand the bay-scale dynamics, and only one sample per station would be required (i.e., no replicates). These results and guidance are part of a long-term monitoring approach to further characterize effects from bivalve aquaculture using a nationally-consistent sampling strategy. Understanding these dynamics through an effective sampling design will address key knowledge gaps related to the effects of the bivalve aquaculture industry on the environment.

6 ACKNOWLEDGEMENTS

Project development: David Drolet, Luc Comeau, Terri Sutherland.
Fieldwork: Kevin Chernoff, Theraesa Coyle, Brianne Kucharski, Steve R Neil, Kate Gingles, Kim Hobbs, Vanessa Oldford, Terry Bungay, Shannon Cross, Laura Steeves.
Data management: Khang Hua, Peter Kraska.
Taxonomy and FlowCam analyses: Karen Ross (Huntsman Marine Science Centre), William Chamberlain, Reegan Reid, Cassidy Bertin, Brontë Thomas, Jesslynn Shaw.
Provinces and industry fieldwork support: Charlene LeBlanc (Nova Scotia), Alix d'Entremont (Nova Scotia), Terry Mills (Newfoundland), Trevor Munro (Nova Scotia).
Reviewers: Catherine Johnson, David Drolet.
Additional support: Jackson Chu, Ruben Cordero, Myriam Lacharité, Michael Kalyn.

7 AUTHOR CONTRIBUTIONS

ALR, TG, CM, JB and RF conceived the study. ALR, JA, JB, OG, DG and TG contributed to data acquisition in the field. ALR, JA, RM, CG, TM developed the FlowCam protocol, identified plankton, and processed samples. SF, ALR, RF, TG and CM did the data analyses and interpreted results. SF, ALR, RF, TG and CM wrote the manuscript and all authors reviewed it.

8 REFERENCES

Allan, J.D. 1976. Life History Patterns in Zooplankton. Am. Nat. 110(971): 165-180.

Álvarez, E., Moyano, M., López-Urrutia, Á., Nogueira, E., and Scharek, R. 2014. Routine determination of plankton community composition and size structure: a comparison between FlowCAM and light microscopy. J. Plankton Res. 36(1): 170-184.

Anderson, M. 2008. PERMANOVA+ for PRIMER: guide to software and statistical methods. Primer-E Limited.

Anderson, M.J. 2006. Distance-Based Tests for Homogeneity of Multivariate Dispersions. Biometrics 62(1): 245-253.

Anderson, M.J. 2017. Permutational Multivariate Analysis of Variance (PERMANOVA). *In* Wiley StatsRef: Statistics Reference Online. pp. 1-15.

Anderson, M.J., Ellingsen, K.E., and McArdle, B.H. 2006. Multivariate dispersion as a measure of beta diversity. Ecol. Lett. 9(6): 683-693.

Anderson, M.J., and Robinson, J. 2003. Generalized discriminant analysis based on distances. Aust. N. Z. J. Stat. 45(3): 301-318.

Anderson, M.J., and Walsh, D.C.I. 2013. PERMANOVA, ANOSIM, and the Mantel test in the face of heterogeneous dispersions: what null hypothesis are you testing? Ecol. Monogr. 83(4): 557-574.

Angermeier, P.L., and Smogor, R.A. 1995. Estimating number of species and relative abundances in stream-fish communities: effects of sampling effort and discontinuous spatial distributions. Can. J. Fish. Aquat. Sci. 52(5): 936-949.

Arbizu, P.M. 2017. pairwiseAdonis: Pairwise Multilevel Comparison using Adonis.

Azra, M.N., Okomoda, V.T., Tabatabaei, M., Hassan, M., and Ikhwanuddin, M. 2021. The Contributions of Shellfish Aquaculture to Global Food Security: Assessing Its Characteristics From a Future Food Perspective. Front. Mar. Sci. 8(654897): 1-6.

Bacher, C., Filgueira, R., and Guyondet, T. 2016. Probabilistic approach of water residence time and connectivity using Markov chains with application to tidal embayments. J. Mar. Syst. 153: 25-41.

Batten, S.D., Abu-Alhaija, R., Chiba, S., Edwards, M., Graham, G., Jyothibabu, R., Kitchener, J.A., Koubbi, P., McQuatters-Gollop, A., Muxagata, E., Ostle, C., Richardson, A.J., Robinson, K.V., Takahashi, K.T., Verheye, H.M., and Wilson, W. 2019. A Global Plankton Diversity Monitoring Program. Front. Mar. Sci. 6(321): 1-14.

Benfield, M.C., Grosjean, P., Culverhouse, P.F., Irigoien, X., Sieracki, M.E., Lopez-Urratia, A., Dam, H.G., Hu, Q., Davis, C.S., Hansen, A., Pilkaln, C.H., Riseman, E.M., Schultz, H., Utgoff, P.E., and Gorksy, G. 2007. RAPID: Research on Automated Plankton Identification. Oceanogr. 20(2): 172-187.

Bessey, C., Jarman, S.N., Berry, O., Olsen, Y.S., Bunce, M., Simpson, T., Power, M., McLaughlin, J., Edgar, G.J., and Keesing, J. 2020. Maximizing fish detection with eDNA metabarcoding. Environ. DNA. 2(4): 493-504.

Birk, S., Chapman, D., Carvalho, L., Spears, B.M., Andersen, H.E., Argillier, C., Auer, S., Baattrup-Pedersen, A., Banin, L., and Beklioğlu, M. 2020. Impacts of multiple

stressors on freshwater biota across spatial scales and ecosystems. Nat. Ecol. Evol. 4(8): 1060-1068.

Borg, I., and Groenen, P.J.F. 2005. Springer series in statistics. Modern multidimensional scaling: Theory and applications (2nd ed.). New York, NY, US: Springer Science+ Business Media.

Brand, T. van den. 2022. ggh4x: Hacks for “ggplot2.”

Cao, Y., Larsen, D.P., and Thorne, R.S.-J. 2001. Rare species in multivariate analysis for bioassessment: some considerations. J. North Am. Benthol. Soc. 20(1): 144-153.

Cao, Y., Williams, D.D., and Williams, N.E. 1998. How important are rare species in aquatic community ecology and bioassessment? Limnol. Oceanogr. 43(7): 1403–1409.

Chacoff, N.P., Vázquez, D.P., Lomáscolo, S.B., Stevani, E.L., Dorado, J., and Padròn, B. 2012. Evaluating sampling completeness in a desert plant-pollinator network. J. Anim. Ecol. 81(1): 190-200.

Chao, A. 1984. Nonparametric estimation of the number of classes in a population. Scand. J. Stat. 11: 265-270.

Chao, A. 1987. Estimating the population size for capture-recapture data with unequal catchability. Biometrics. 43: 783-791.

Chao, A., Colwell, R.K., Lin, C.-W., and Gotelli, N.J. 2009. Sufficient sampling for asymptotic minimum species richness estimators. Ecol. 90(4): 1125-1133.

Chao, A., Gotelli, N.J., Hsieh, T.C., Sander, E.L., Ma, K.H., Colwell, R.K., and Ellison, A.M. 2014. Rarefaction and extrapolation with Hill numbers: a framework for sampling and estimation in species diversity studies. Ecol. Monogr. 84(1): 45-67.

Chao, A., Kubota, Y., Zelený, D., Chiu, C.-H., Li, C.-F., Kusumoto, B., Yasuhara, M., Thorn, S., Wei, C.-L., Costello, M.J., and Colwell, R.K. 2020. Quantifying sample completeness and comparing diversities among assemblages. Ecol. Res. 35(2): 292-314.

Chiarucci, A., Bacaro, G., Rocchini, D., and Fattorini, L. 2008. Discovering and rediscovering the sample-based rarefaction formula in the ecological literature. Community Ecol. 9(1): 121-123.

Chiu, C.-H., and Chao, A. 2014. Distance-Based Functional Diversity Measures and Their Decomposition: A Framework Based on Hill Numbers. PLoS One. 9(7): e100014.

Clarke, K.R. 1993. Non-parametric multivariate analyses of changes in community structure. Aust. J. Ecol. 18(1988): 117-143.

Colwell, R.K., Chao, A., Gotelli, N.J., Lin, S.-Y., Mao, C.X., Chazdon, R.L., and Longino, J.T. 2012. Models and estimators linking individual-based and sample-based rarefaction, extrapolation and comparison of assemblages. J. Plant Ecol. 5(1): 3-21.

Colwell, R.K. and Coddington, J.A. 1994. Estimating terrestrial biodiversity through extrapolation. Phil. Trans. R. Soc. Lond. B. 345(1311): 101-118.

Comeau, L.A., Guyondet, T., Drolet, D., Sonier, R., Clements, J.C., Tremblay, R., and Filgueira, R. 2023. Revisiting ecological carrying capacity indices for bivalve aquaculture. Aquac. 577: 739911.

Cox, K.D., Black, M.J., Filip, N., Miller, M.R., Mohns, K., Mortimor, J., Freitas, T.R., Greiter Loerzer, R., Gerwing, T.G., Juanes, F., and Dudas, S.E. 2017. Community assessment techniques and the implications for rarefaction and extrapolation with Hill numbers. Ecol. Evol. 7(24): 11213-11226.

Cranford P.J., Li W., Strand Ø., Strohmeier T. 2008 Phytoplankton depletion by mussel aquaculture: high resolution mapping, ecosystem modeling and potential indicators of ecological carrying capacity. ICES CM2008/H:12. International Council for the Exploration of the Sea, Copenhagen.

Cuffney, T.F., Bilger, M.D., and Haigler, A.M. 2007. Ambiguous taxa: effects on the characterization and interpretation of invertebrate assemblages. J. North Am. Benthol. Soc. 26(2): 286-307.

Danielsen, F., Balete, D.S., Poulsen, M.K., Enghoff, M., Nozawa, C.M., and Jensen, A.E. 2000. A simple system for monitoring biodiversity in protected areas of a developing country. Biodivers. Conserv. 9(12): 1671-1705.

Davenport, J., Smith, R.J.J.W., and Packer, M. 2000. Mussels *Mytilus edulis*: significant consumers and destroyers of mesozooplankton. Mar. Ecol. Prog. Ser. 198: 131-137.

Detmer, T.M., Broadway, K.J., Potter, C.G., Collins, S.F., Parkos, J.J., and Wahl, D.H. 2019. Comparison of microscopy to a semi-automated method (FlowCAM®) for characterization of individual-, population-, and community-level measurements of zooplankton. Hydrobiologia. 838(1): 99-110.

Domènech, M., Wangensteen, O.S., Enguídanos, A., Malumbres-Olarte, J., and Arnedo, M.A. 2022. For all audiences: Incorporating immature stages into standardised spider inventories has a major impact on the assessment of biodiversity patterns. Mol. Ecol. Resour. 22(6): 2319-2332.

Ezgeta-Balić, D., Najdek, M., Peharda, M., and Blažina, M. 2012. Seasonal fatty acid profile analysis to trace origin of food sources of four commercially important bivalves. Aquac. 334-337: 89-100.

Filgueira, R., Guyondet, T., Bacher, C., and Comeau, L.A. 2015. Informing Marine Spatial Planning (MSP) with numerical modelling: A case-study on shellfish aquaculture in Malpeque Bay (Eastern Canada). Mar. Pollut. Bull. 100(1): 200-216.

Filgueira, R., Guyondet, T., Comeau, L.A., and Grant, J. 2014. A fully-spatial ecosystem-DEB model of oyster (*Crassostrea virginica*) carrying capacity in the Richibucto Estuary, Eastern Canada. J. Mar. Syst. 136: 42-54.

Filgueira, R., Guyondet, T., Comeau, L.A., and Tremblay, R. 2016. Bivalve aquaculture-environment interactions in the context of climate change. Glob. Chang. Biol. 22(12): 3901-3913.

Filgueira, R., Guyondet, T., Thupaki, P., Sakamaki, T., and Grant, J. 2021. The effect of embayment complexity on ecological carrying capacity estimations in bivalve aquaculture sites. J. Clean. Prod. 288: 125739.

Flaherty, M., Reid, G., Chopin, T., and Latham, E. 2019. Public attitudes towards marine aquaculture in Canada: insights from the Pacific and Atlantic coasts. Aquac. Int. 27: 9-32.

Folt, C.L., and Burns, C.W. 1999. Biological drivers of zooplankton patchiness. Trends Ecol. Evol. 14(8): 300-305.

Forget, N.L, Duplisea, D.E., Sardenne, F., and McKindsey, C.W. 2020. Using qualitative networks to assess the influence of mussel culture on ecosystem dynamics. Ecol. Model. 430: 109070.

Gao, C.-H. 2022. ggVennDiagram: A “ggplot2” Implement of Venn Diagram.

Gianasi, B.L., McKindsey, C.W., Tremblay, R., Comeau, L.A. and Drolet, D., 2023. Plankton depletion by mussel grazing negatively impacts the fitness of lobster larvae. Aquaculture. 574: 739659.

Gotelli, N.J., and Colwell, R.K. 2001. Quantifying biodiversity: procedures and pitfalls in the measurement and comparison of species richness. Ecol. Lett. 4(4): 379-391.

Grant, J., Bacher, C., Cranford, P.J., Guyondet, T., and Carreau, M. 2008. A spatially explicit ecosystem model of seston depletion in dense mussel culture. J. Mar. Syst. 73(1-2): 155-168.

Grant, J., Bugden, G., Horne, E., Archambault, M.-C., and Carreau, M. 2007. Remote sensing of particle depletion by coastal suspension-feeders. Can. J. Fish. Aquat. Sci. 64(3): 387-390.

Grant, J., Cranford, P., Hargrave, B., Carreau, M., Schofield, B., Armsworthy, S., Burdett-Coutts, V., and Ibarra, D. 2005. A model of aquaculture biodeposition for multiple estuaries and field validation at blue mussel (*Mytilus edulis*) culture sites in eastern Canada. Can. J. Fish. Aquat. Sci. 62(6): 1271-1285.

Grant, J., and Pastres, R. 2019. Ecosystem models of bivalve aquaculture: implications for supporting goods and services. Goods and Services of Marine Bivalves: 507-525. Springer International Publishing.

Gutierrez, M.F., Epele, L.B., Mayora, G., Aquino, D., Mora, C., Quintana, R., and Mesa, L. 2022. Hydro-climatic changes promote shifts in zooplankton composition and diversity in wetlands of the Lower Paraná River Delta. Hydrobiologia. 849(16): 3463-3480.

Guyondet, T., Comeau, L.A., Bacher, C., Grant, J., Rosland, R., Sonier, R., and Filgueira, R. 2015. Climate Change Influences Carrying Capacity in a Coastal Embayment Dedicated to Shellfish Aquaculture. Estuaries Coasts. 38(5): 1593-1618.

Han, D., Chen, Y., Zhang, C., Ren, Y., Xue, Y., and Wan, R. 2017. Evaluating impacts of intensive shellfish aquaculture on a semi-closed marine ecosystem. Ecol. Modell. 359: 193-200.

Helenius, L.K., Leskinen, E., Lehtonen, H., and Nurminen, L. 2017. Spatial patterns of littoral zooplankton assemblages along a salinity gradient in a brackish sea: A functional diversity perspective. Estuar. Coast. Shelf Sci. 198: 400-412.

Hill, M.O. 1973. Diversity and Evenness: A Unifying Notation and Its Consequences. Ecol. 54(2): 427-432.

Hoffman, J.C., Kelly, J.R., Trebitz, A.S., Peterson, G.S., and West, C.W. 2011. Effort and potential efficiencies for aquatic non-native species early detection. Can. J. Fish. Aquat. Sci. 68(12): 2064-2079.

Holden, J.J., Collicutt, B., Covernton, G., Cox, K.D., Lancaster, D., Dudas, S.E., Ban, N.C., and Jacob, A.L. 2019. Synergies on the coast: Challenges facing shellfish aquaculture development on the central and north coast of British Columbia. Mar. Policy. 101: 108-117.

Hrycik, A.R., Shambaugh, A., and Stockwell, J.D. 2019. Comparison of FlowCAM and microscope biovolume measurements for a diverse freshwater phytoplankton community. J. Plankton Res. 41(6): 849-864.

Hsieh, T.C., Ma, K.H., and Chao, A. 2016. iNEXT: an R package for rarefaction and extrapolation of species diversity (Hill numbers). Methods Ecol. Evol. 7(12): 1451-1456.

Hulot, F.D., Lacroix, G., and Loreau, M. 2014. Differential responses of size-based functional groups to bottom-up and top-down perturbations in pelagic food webs: a meta-analysis. Oikos. 123(11): 1291-1300.

Hulot, V., Saulnier, D., Lafabrie, C., and Gaertner-Mazouni, N. 2020. Shellfish culture: a complex driver of planktonic communities. Rev. Aquac. 12(1): 33-46.

Ibarbalz, F.M., Henry, N., Brandão, M.C., Martini, S., Busseni, G., Byrne, H., Coelho, L.P., Endo, H., Gasol, J.M., Gregory, A.C., Mahé, F., Rigonato, J., Royo-Llonch, M., Salazar, G., Sanz-Sáez, I., Scalco, E., Soviadan, D., Zayed, A.A., Zingone, A., Labadie, K., Ferland, J., Marec, C., Kandels, S., Picheral, M., Dimier, C., Poulain, J., Pisarev, S., Carmichael, M., Pesant, S., Babin, M., Boss, E., Iudicone, D., Jaillon, O., Acinas, S.G., Ogata, H., Pelletier, E., Stemmann, L., Sullivan, M.B., Sunagawa, S., Bopp, L., de Vargas, C., Karp-Boss, L., Wincker, P., Lombard, F., Bowler, C., Zinger, L., Acinas, S.G., Babin, M., Bork, P., Boss, E., Bowler, C., Cochrane, G., de Vargas, C., Follows, M., Gorsky, G., Grimsley, N., Guidi, L., Hingamp, P., Iudicone, D., Jaillon, O., Kandels, S., Karp-Boss, L., Karsenti, E., Not, F., Ogata, H., Pesant, S., Poulton, N., Raes, J., Sardet, C., Speich, S., Stemmann, L., Sullivan, M.B., Sunagawa, S., and Wincker, P. 2019. Global Trends in Marine Plankton Diversity across Kingdoms of Life. Cell. 179(5): 1084-1097.e21.

Ibarra, D.A., Fennel, K., and Cullen, J.J. 2014. Coupling 3-D Eulerian bio-physics (ROMS) with individual-based shellfish ecophysiology (SHELL-E): A hybrid model for carrying capacity and environmental impacts of bivalve aquaculture. Ecol. Modell. 273: 63-78.

Irisson, J.-O., Ayata, S.-D., Lindsay, D.J., Karp-Boss, L., and Stemmann, L. 2022. Machine Learning for the Study of Plankton and Marine Snow from Images. Annu. Rev. Mar. Sci. 14(1): 277-301.

Jakobsen, H., and Carstensen, J. 2011. FlowCAM: Sizing cells and understanding the impact of size distributions on biovolume of planktonic community structure. Aquat. Microb. Ecol. 65(1): 75-87.

Ji, R., Edwards, M., Mackas, D.L., Runge, J.A., and Thomas, A.C. 2010. Marine plankton phenology and life history in a changing climate: current research and future directions. J. Plankton Res. 32(10): 1355-1368.

Johnson, W.S., and Allen, D.M. 2012. Zooplankton of the Atlantic and Gulf coasts: a guide to their identification and ecology. JHU Press.

Jost, L. 2006. Entropy and diversity. Oikos 113(2): 363-375.

Kerr, T., Clark, J.R., Fileman, E.S., Widdicombe, C.E., and Pugeault, N. 2020. Collaborative Deep Learning Models to Handle Class Imbalance in FlowCam Plankton Imagery. IEEE Access. 8: 170013-170032.

Kiørboe, T. 2009. A Mechanistic Approach to Plankton Ecology. ASLO Web Lectures 1(2): 1-91. John Wiley & Sons, Ltd.

Kosobokova, K.N., Hopcroft, R.R., and Hirche, H.-J. 2011. Patterns of zooplankton diversity through the depths of the Arctic's central basins. Mar. Biodivers. 41(1): 29-50.

Kruskal, J.B. 1964. Multidimensional scaling by optimizing goodness of fit to a nonmetric hypothesis. Psychometrika. 29(1): 1-27.

Kydd, J., Rajakaruna, H., Briski, E., and Bailey, S. 2018. Examination of a high resolution laser optical plankton counter and FlowCAM for measuring plankton concentration and size. J. Sea Res. 133: 2-10.

Lamb, J. 2005. Ecological zonation of zooplankton in the COAST study region off central Oregon in June and August 2001 with consideration of retention mechanisms. J. Geophys. Res. 110(C10): C10S15.

Lavaud, R., Guyondet, T., Filgueira, R., Tremblay, R., and Comeau, L.A. 2020. Modelling bivalve culture - Eutrophication interactions in shallow coastal ecosystems. Mar. Pollut. Bull. 157: 111282.

Le Bourg, B., Cornet-Barthaux, V., Pagano, M., and Blanchot, J. 2015. FlowCAM as a tool for studying small (80–1000 µm) metazooplankton communities. J. Plankton Res. 37(4): 666-670.

Lehane, C., and Davenport, J. 2002. Ingestion of mesozooplankton by three species of bivalve; *Mytilus edulis*, *Cerastoderma edule* and *Aequipecten opercularis*. J. Mar. Biolog. Assoc. 82(4): 615-619.

Lehane, C., and Davenport, J. 2006. A 15-month study of zooplankton ingestion by farmed mussels (*Mytilus edulis*) in Bantry Bay, Southwest Ireland. Estuar. Coast. Shelf Sci. 67(4): 645-652.

Lindeman, R.L. 1942. The Trophic-Dynamic Aspect of Ecology. Ecol. 23(4): 399-417.

Luo, J.Y., Irisson, J., Graham, B., Guigand, C., Sarafraz, A., Mader, C., and Cowen, R.K. 2018. Automated plankton image analysis using convolutional neural networks. Limnol. Oceanogr.: Methods. 16(12): 814-827.

Ma, K.C.K., McKindsey, C.W., and Johnson, L.E. 2022. Detecting Rare Species With Passive Sampling Tools: Optimizing the Duration and Frequency of Sampling for Benthic Taxa. Front. Mar. Sci. 9: 809327.

Maar, M., Nielsen, T., and Petersen, J. 2008. Depletion of plankton in a raft culture of *Mytilus galloprovincialis* in Ría de Vigo, NW Spain. II. Zooplankton. Aquat. Biol. 4: 127-141.

Mackas, D.L., Pepin, P., and Verheye, H. 2012. Interannual variability of marine zooplankton and their environments: Within- and between-region comparisons. Prog. Oceanogr. 97-100: 1-14.

Magurran, A.E., and McGill, B.J. 2010. Biological diversity: frontiers in measurement and assessment. OUP Oxford.

Marques, S.C., Pardal, M.A., Pereira, M.J., Gonçalves, F., Marques, J.C., and Azeiteiro, U.M. 2007. Zooplankton distribution and dynamics in a temperate shallow estuary. Hydrobiologia 587: 213-223.

McIntire, E.J.B., and Fajardo, A. 2009. Beyond description: the active and effective way to infer processes from spatial patterns. Ecol. 90(1): 46-56.

Navarro, D. 2015. Learning statistics with R: A tutorial for psychology students and other beginners. (Version 0.6). University of New South Wales, Sydney, Australia.

Neuheimer, A.B., Gentleman, W.C., Pepin, P., and Head, E.J.H. 2010. Explaining regional variability in copepod recruitment: Implications for a changing climate. Prog. Oceanogr. 87(1-4): 94-105.

O'Brien, T.D., and Oakes, S.A. 2020. Visualizing and exploring zooplankton spatio-temporal variability. *In* Zooplankton Ecology. CRC Press. pp. 192-224.

Oksanen, J., Simpson, G.L., Blanchet, F.G., Kindt, R., Legendre, P., Minchin, P.R., O'Hara, R.B., Solymos, P., Stevens, M.H.H., Szoecs, E., Wagner, H., Barbour, M., Bedward, M., Bolker, B., Borcard, D., Carvalho, G., Chirico, M., Caceres, M.D., Durand, S., Evangelista, H.B.A., FitzJohn, R., Friendly, M., Furneaux, B., Hannigan, G., Hill, M.O., Lahti, L., McGlinn, D., Ouellette, M.-H., Cunha, E.R., Smith, T., Stier, A., Braak, C.J.F.T., and Weedon, J. 2022. vegan: Community Ecology Package.

Olsen, A.R., Sedransk, J., Edwards, D., Gotway, C.A., Liggett, W., Rathbun, S., Reckhow, K.H., and Yyoung, L.J. 1999. Statistical Issues for Monitoring Ecological and Natural Resources in the United States. Environ. Monit. Assess. 54(1): 1-45.

Orenstein, E.C., Ayata, S., Maps, F., Becker, É.C., Benedetti, F., Biard, T., de Garidel-Thoron, T., Ellen, J.S., Ferrario, F., Giering, S.L.C., Guy-Haim, T., Hoebeke, L., Iversen, M.H., Kiørboe, T., Lalonde, J., Lana, A., Laviale, M., Lombard, F., Lorimer, T., Martini, S., Meyer, A., Möller, K.O., Niehoff, B., Ohman, M.D., Pradalier, C., Romagnan, J., Schröder, S., Sonnet, V., Sosik, H.M., Stemmann, L.S., Stock, M., Terbiyik-Kurt, T., Valcárcel-Pérez, N., Vilgrain, L., Wacquet, G., Waite, A.M., and Irisson, J. 2022. Machine learning techniques to characterize functional traits of plankton from image data. Limnol. Oceanogr.: Methods. 67(8): 1647-1669.

Owen, B.M., Hallett, C.S., Cosgrove, J.J., Tweedley, J.R., and Moheimani, N.R. 2022. Reporting of methods for automated devices: A systematic review and recommendation for studies using FlowCam for phytoplankton. Limnol. Oceanogr.: Methods. 20(7): 373-465.

Pace, M.L., Strayer, D.L., Fischer, D., and Malcom, H.M. 2010. Recovery of native zooplankton associated with increased mortality of an invasive mussel. Ecosphere. 1(1): 1-21.

R Core Team. 2022. R: A Language and Environment for Statistical Computing. R Foundation for Statistical Computing, Vienna, Austria.

Ramkissoon, C. 2021. Assessment of Convolutional Neural Networks to Classify Freshwater Zooplankton. University of Toronto (Canada).

Ratnarajah, L., Abu-Alhaija, R., Atkinson, A., Batten, S., Bax, N.J., Bernard, K.S., Canonico, G., Cornils, A., Everett, J.D., Grigoratou, M., Ishak, N.H.A., Johns, D., Lombard, F., Muxagata, E., Ostle, C., Pitois, S., Richardson, A.J., Schmidt, K., Stemmann, L.,

Swadling, K.M., Yang, G., and Yebra, L. 2023. Monitoring and modelling marine zooplankton in a changing climate. Nat. Commun. 14(1): 564.

Robertson, O.J., McAlpine, C., House, A., and Maron, M. 2013. Influence of Interspecific Competition and Landscape Structure on Spatial Homogenization of Avian Assemblages. PLoS One. 8(5): e65299.

Schartau, A.K., Mariash, H.L., Christoffersen, K.S., Bogan, D., Dubovskaya, O.P., Fefilova, E.B., Hayden, B., Ingvason, H.R., Ivanova, E.A., Kononova, O.N., Kravchuk, E.S., Lento, J., Majaneva, M., Novichkova, A.A., Rautio, M., Rühland, K.M., Shaftel, R., Smol, J.P., Vrede, T., and Kahilainen, K.K. 2022. First circumpolar assessment of Arctic freshwater phytoplankton and zooplankton diversity. Freshw. Biol. 61(1): 141-158.

Schlacher, T.A., and Wooldridge, T.H. 1995. Small-scale distribution and variability of demersal zooplankton in a shallow, temperate estuary: tidal and depth effects on species-specific heterogeneity. Cah. Biol. Mar. 36: 211-227.

Soetaert, K.E.R., and Van Rijswijk, P. 1993. Spatial and temporal patterns of the zooplankton in the Westerschelde estuary. Mar. Ecol. Prog. Ser. 97: 47-49.

Stanislawczyk, K., Johansson, M.L., and MacIsaac, H.J. 2018. Microscopy versus automated imaging flow cytometry for detecting and identifying rare zooplankton. Hydrobiologia. 807(1): 53-65.

Steeves, L.E., Filgueira, R., Guyondet, T., Chassé, J., and Comeau, L. 2018. Past, Present, and Future: Performance of Two Bivalve Species Under Changing Environmental Conditions. Front. Mar. Sci. 5(184): 1-14.

Taylor, D., Larsen, J., Buer, A.-L., Friedland, R., Holbach, A., Petersen, J.K., Nielsen, P., Ritzenhofen, L., Saurel, C., and Maar, M. 2021. Mechanisms influencing particle depletion in and around mussel farms in different environments. Ecol. Inidic. 122: 107304.

Tommasi, D.A.G., Routledge, R.D., Hunt, B.P.V., and Pakhomov, E.A. 2013. The seasonal development of the zooplankton community in a British Columbia (Canada) fjord during two years with different spring bloom timing. Mar. Biol. Res. 9(2): 129-144.

Usov, N., Khaitov, V., Smirnov, V., and Sukhotin, A. 2019. Spatial and temporal variation of hydrological characteristics and zooplankton community composition influenced by freshwater runoff in the shallow Pechora Sea. Polar Biol. 42: 1647-1665.

Varpe, O. 2012. Fitness and phenology: annual routines and zooplankton adaptations to seasonal cycles. J. Plankton Res. 34(4): 267-276.

Weitzman, J., Steeves, L., Bradford, J. and Filgueira, R., 2019. Far-field and near-field effects of marine aquaculture. *World seas: An environmental evaluation*, pp.197-220.

Wickham, H. 2016. ggplot2: Elegant Graphics for Data Analysis. Springer-Verlag New York.

Wijsman, J.W.M., Troost, K., Fang, J., and Roncarati, A. 2019. Global production of marine bivalves. Trends and challenges. Goods and services of marine bivalves: 7-26. Springer International Publishing.

Wong, W.H., and Levinton, J.S. 2006. The trophic linkage between zooplankton and benthic suspension feeders: direct evidence from analyses of bivalve faecal pellets. Mar. Biol. 148(4): 799-805.

Wooldridge, T., and Erasmus, T. 1980. Utilization of tidal currents by estuarine zooplankton. Estuar. Coast. Mar. Sci. 11(1): 107-114.

Yoccoz, N.G., Nichols, J.D., and Boulinier, T. 2003. Monitoring of biological diversity–a response to Danielsen et al. Oryx. 37(4): 410.

Yokogawa Fluid Imaging Technologies, Inc. 2020. FlowCam Macro Imaging Particle Analysis System User Guide: ViSp 4 Version B.

Yokogawa Fluid Imaging Technologies, Inc. n.d. VisualSpreadsheet 5 Version 5.6.19 User Guide.

Zeldis, J., Robinson, K., Ross, A., and Hayden, B. 2004. First observations of predation by New Zealand Greenshell mussels (*Perna canaliculus*) on zooplankton. J. Exp. Mar. Biol. Ecol. 311(2): 287-299.

APPENDIX 1

Data summary table for mesozooplankton (0.25 mm - 5.00 mm) samples obtained within study sites and regions, as part of the Aquaculture Monitoring Program. Station names refer to the sampling locations within each site as indicated in Fig 1. The station-tide count represents the number of samples obtained at each respective station and tide phase combination for each site and/or month. Samples were obtained for more than one month for Cocagne (Gulf), South Arm (Newfoundland), and Lemmens Inlet (Pacific). M-R: mid-rising, M-F: mid-falling. See Fig. 1 for station names and labels. Pac: Pacific, Mar: Maritimes, Nfld: Newfoundland.

Region	Site or month	Year	Date range	Distance between stations (km)	Station name	Tide phase	Station-tide count
Pac	Lemmens Aug 2020	2020	Aug 29-31	In-Mid: 1.8 Mid-Out: 1.4 In-Out: 3.2	Inner	High	3
					Inner	Low	3
					Mid	High	3
						Low	3
					Outer	High	3
						Low	3
							18 total
	Lemmens Mar 2021				N/A	High	1
					N/A	Low	1
							2 total
	Lemmens Jun 2021				Inner	High	3
					Inner	Low	3
					Mid	High	3
						Low	3
					Outer	High	3
						Low	3
							18 total
	Lemmens Sept 2021				Inner	High	2
					Inner	Low	2
					Mid	High	2
						Low	2
					Outer	High	2
						Low	2
							12 total
Mar	Argyle	2021	Aug 30-Sep 1	S-C: 5.2 C-N: 3.1 S-N: 8.3	Central	High	2
						Low	3
					North	High	2
						Low	2
						M-R	1
					South	High	2
						Low	2
						M-R	1

Region	Site or month	Year	Date range	Distance between stations (km)	Station name	Tide phase	Station-tide count
							15 total
	Country Harbour	2021	Aug 24	In-Mid: 3.2 Mid-Out: 3.0 In-Out: 6.2	Inner	High	1
						Low	1
					Mid	High	1
						Low	1
					Outer	High	1
						Low	1
							6 total
	Sober Island	2021	Aug 27	Out-IS: 0.7 Out-IN: 1.0 IN-IS: 0.5	Inner-North	M-R	3
					Inner-South	M-R	3
					Outer	High	3
						Low	3
							12 total
	Whitehead	2021	Aug 25	In-Mid: 1.1 Mid-Out: 2.1 In-Out: 3.1	Inner	High	1
						Low	1
						M-F	1
					Mid	High	1
						Low	1
						M-F	1
					Outer	High	1
						Low	1
						M-F	1
							9 total
Gulf	Malpeque	2020	Sept 29	S-C: 3.6 C-N: 3.7 S-N: 4.5	Central	Low	1
					North	Low	1
					South	Low	1
							3 total
	St. Peters	2020	Sept 1-4	In-Mid: 4.0 Mid-Out: 4.1 In-Out: 8.1	Inner	High	4
						Low	3
					Mid	High	4
						Low	3
						M-F	4
					Outer	High	5
						Low	3
							26 total
	Cocagne	2021	Jul 21	S-C: 2.4 C-N: 2.5 S-N: 4.4	Central	Low	1
					North	Low	1

Region	Site or month	Year	Date range	Distance between stations (km)	Station name	Tide phase	Station-tide count
					South	Low	1
		2021	Aug 26		Central	M-R	1
					North	M-R	1
					South	M-R	1
							6 total
Nfld.	South Arm Sep 2020	2020	Sep 15-16	In-Mid A: 2.5 In-Mid B: 2.0 In-Mid C: 1.5 In-Out: 3.8 Mid A-Mid B: 0.7 Mid A-Mid C: 1.1 Mid A-Out: 1.4 Mid-B-Mid-C: 0.7 Mid B-Out: 2.1 Mid C-Out: 2.3	Inner	Low	1
						M-F	1
						M-R	1
					Mid A	Low	1
						M-F	1
					Mid B	Low	1
						M-F	1
					Mid C	Low	1
						M-F	1
						M-R	1
	South Arm Jun 2021	2021	Jun 9		Mid B	Low	1
					Outer	M-F	1
	South Arm Jul 2021		Jul 7		Mid-B	M-R	1
					Outer	Low	1
	South Arm Aug 2021		Aug 12		Mid B	Low	1
					Outer	M-F	1
	South Arm Sep 2021		Sept 8		Mid B	Low	1
					Outer	M-F	1
	South Arm Oct 2021		Oct 5-7		Mid-B	High	2
						Low	3
						M-F	1
					Outer	High	3
						Low	3
	South Arm Nov 2021		Nov 9		Mid A	High	1
					Mid B	M-F	1

Region	Site or month	Year	Date range	Distance between stations (km)	Station name	Tide phase	Station-tide count
					Outer	High	1
	South Arm Dec 2021		Dec 14		Mid B	Low	1
					Outer	Low	1
	South Arm Feb 2022	2022	Feb 8		Mid A	Low	1
					Mid B	Low	1
					Outer	Low	1
	South Arm Mar 2022		Mar 29		Mid A	Low	1
					Mid B	Low	1
					Outer	Low	1
	South Arm Apr 2022		Apr 22		Mid A	High	1
					Mid B	High	1
					Outer	M-R	1
	South Arm May 2022		May 17		Mid A	M-F	1
					Mid-B	Low	1
					Outer	High	1
	South Arm Jun 2022		Jun 7		Mid A	M-R	1
					Mid B	High	1
					Outer	M-R	1
	South Arm Jul 2022		Jul 6		Mid A	High	1
					Mid B	High	1
					Outer	M-R	1
							53 total

APPENDIX 2

Technical specifications, sampling and setup protocols, and image sorting details used by the macro FlowCam within this report. The templates were obtained from the Supporting Information of Owen et al. (2022), which outlined the critical details to include in studies that use FlowCam technology for the identification of plankton specimens. Note that the final table provided in Owen et al. (2022) ("Measurement Outputs") is not included, as this includes the methods for obtaining properties such as particle size, which are being more extensively reviewed as part of ongoing departmental work.

FlowCam technical specifications	
FlowCam model number	FlowCam Macro
FlowCam unit serial number	10416
Camera resolution	1920 x 1200 pixels
Camera color/monochrome	8-bit monochrome
Fluidics	Peristaltic pump
Software details	*VisualSpreadsheet* version 5.6.14 was used for the samples collected in 2020 in Newfoundland (FlowCam Yokogawa Fluid Imaging Technologies, Inc. n.d.). *VisualSpreadsheet* version 4.18.5 used for all other samples (FlowCam Yokogawa Fluid Imaging Technologies 2020).
Any additional upgrades to the machine or optional accessories	Instead of using the sample container provided with the FlowCam, a glass beaker was used to hold the sample. A magnetic stirrer was added to prevent clumping of the sample.

Sample details	
Preservation methods	Samples were preserved in a 4% solution of buffered formaldehyde. These were run through the FlowCam within 1-5 months from the date of field collection.
Dilution or concentration details	Raw counts were converted to abundance in seawater following *Equation (1)* in the main text. See the process below for additional steps before running the samples through the FlowCam.
Pre-filtration details	Samples were rinsed through a series of stacked sieves; 2 mm mesh sieve stacked on a 125 µm or 212 µm mesh sieve. These size fractions determined the size of the flow cell for subsequent analysis: ● The specimens collected on the 125 µm or 212 µm mesh were run through the FlowCam using a 2 mm flow cell. ● The specimens collected on the 2 mm mesh that were <5 mm were processed using a 5 mm flow cell. The resulting specimens from the fraction sizes listed above were kept separate. The collected specimens were then rinsed into a beaker containing approximately 400 ml of 0.2% Triton-x. Using a large volume of 0.2% Triton-x and a

Sample details	
	magnetic stirrer in the sample beaker was shown to be successful in reducing the clumping of plankton.
Cell concentration range	The average abundance of zooplankton in seawater per sample was 3486 ind m^{-3}. Future work will compare counts as measured by the FlowCam to counts obtained from traditional microscopy.
Sample particle composition	The amount of debris/detritus was variable per sample, but was generally highest in samples from the Pacific region, and lowest in samples from the Newfoundland region.

FlowCam setup details	
Flow cell sizes and types used, and objectives used for each flow cell	As described above, both the 2 mm and 5 mm flow cells were used, depending on the particle size. The following parameters were then used for each of the flow calls:
Image acquisition mode	Auto-image
Sample volume analyzed	Auto-image acquisition mode was used with recirculating water. For example, if 500 ml of water was in the sample beaker, the water and particles pass through the FlowCam. Upon exiting the FlowCam, particles are collected on mesh. The water passes through the mesh, and is added back into the sample beaker and recirculated again through the FlowCam setup.
Cell density determination	Not applicable to this project.
Full context settings	The following parameters were applied for each of the FlowCam settings: Particle segmentation: Dark threshold 40.00 Distance to nearest neighbour: 4.00 µm Close holes: 1 iteration Basic size filter: area based diameter (ABD); Minimum of 150.00 µm, Maximum of 999999999999999.00 µm Advanced filter: none AutoImage frame rate: 10 frames per second Flash duration: 600.00 microseconds Exposure: 19 Camera trigger delay: 500 microseconds Flash amplitude: 50% Camera gain: 30

Parameter	2 mm flow cell	5 mm flow cell
Flow cell depth	2.0 mm	5.0 mm
Flow cell width	10.5 mm	10.5 mm
Area of flow cell imaged	11 x 17.5 mm	11 x 17.5 mm
Flow rate	215 ml/min (9 frames per second)	400 ml/min (7 frames per second)

Image sorting details	
Image sorting method	A detailed description of these processes will be described in future work. Briefly, *VisualSpreadsheet* software was used for semi-automated sorting of all particles upon being imaged. First, the software measures the length of all particles, and those <250 µm are removed, since only the macrozooplankton size fraction is considered (i.e., >250 µm). Next, the images are sorted according to various morphological characteristics, using settings provided by the software. These roughly group the images based on their shape. This then allows the taxonomists to review and confirm the groupings, in which the images are sorted into various predefined classes such as bubbles, clumped zooplankton, debris, fragments of zooplankton, and zooplankton. For this analysis, only images that are confirmed "zooplankton" are considered. Due to time and financial constraints, generally only a portion of the sample is reviewed to separate out the zooplankton from these other classes. Once the zooplankton have been separated from the other particles, the images within the "zooplankton" class can also be grouped based on similar shapes. This is used to quickly group similar taxa based on morphology. The taxonomists then identify the specimens to the taxonomic levels specified in Appendix 3. Due to time and financial constraints, generally only a portion of these zooplankton are identified by the taxonomist.
Software used, with version details	*VisualSpreadsheet* version 5.6.14 was used for the samples collected in 2020 in Newfoundland (FlowCam Yokogawa Fluid Imaging Technologies, Inc. n.d.). *VisualSpreadsheet* version 4.18.5 used for all other samples (FlowCam Yokogawa Fluid Imaging Technologies 2020; reference also includes the General User Guide for the FlowCam Macro Flow Imaging Particle Analyzer).
Image library description and sizes	A total of 1,054,779 images have been identified by the FlowCam, including 384,593 images of confirmed zooplankton specimens (see Table 2 in the main text for a breakdown by region.) The remaining 670,186 images contained particles that were removed from this analysis (e.g., bubbles, clumped zooplankton, debris, fragments of zooplankton, etc.) The taxonomic resolution of the identified specimens is provided in Appendix 3 in the main text. A complete breakdown of the number of images per taxa will be provided in future work (i.e., in the comparisons with the Quantitative Assessment data provided by traditional microscopy)
Particle property selections	For this analysis, only counts of zooplankton taxa were included in the analysis. Other properties for size structure analysis are being evaluated as part of ongoing departmental work.
Other setting choices	None
Evaluation of the accuracy of auto-classifications	Not applicable to this Technical Report.

APPENDIX 3

Guidelines specifying the taxonomic levels (e.g., Order, Genus, etc.) used for identification of the mesozooplankton. These represent the lowest taxonomic level the individuals can reliably be identified to, based on distinguishable morphological features, using images obtained with the macro-FlowCam.

Taxon	**Stages**	**Level (may be identified less precisely depending on stage/condition of specimen)**
Decapoda	Zoea, megalopa	Order, unless distinctive gross morphology (Brachyura, *Homarus*, Porcellanidae, etc.)
Euphausiacea	Nauplii, Calyptopis, Furcilia	Order
	Juvenile/adult	Genus
Mysidacea	Embryo, Juvenile/Adult	Order
Cumacea	Juvenile/adult	Order
Nebaliacea	Adult	Order
Cladocera	Adult	Genus (unless generic distinction requires minute details, then group together e.g., *Podon/Pleopis* spp.)
Cladocera (Freshwater)	Adult	Family
Amphipoda (pelagic)	Juvenile/adult	Genus (hyperiids)
		Family (gammarids)
Acarina	Adult	Family
Facetotecta	Nauplii, Cypris	Infraclass
Cirripedia	Nauplii, Cypris	Infraclass
Invertebrate	Eggs, Trochophore larvae	“Invertebrate”
Polychaeta	Larvae	Class
Polychaeta (pelagic)	Juvenile/Adult	Genus
Gastropoda	Larvae/small species of *Limacina*	“Gastropoda (larvae/*Limacina*)”
Gastropoda (pelagic)	Adults (including large species of *Limacina*)	Genus
Bivalvia	Larvae	Class
Echinodermata	Larvae	Phylum
Bryozoa	Larvae	Phylum
Fish	Eggs, larvae	Class
Larvacea	Adult	Genus
Ascidiacea	Larvae	Class
Thaliacea		Order
Chaetognatha	Juvenile/adult	Phylum
Cnidaria	Larvae	Phylum
Siphonophorae	Nectophore, Eudoxid	Suborder
Hydrozoa	Medusa	Class unless distinctive gross morphology (*Aglantha digitale*, Pandeidae, Bougainvillidae, etc.)
Scyphozoa	Ephyra larvae, Medusa	Class
Ctenophora	Larvae/adult	Phylum

APPENDIX 4

Due to damaged specimens, blurry photos, or poor orientation of the images, at times, specimens could not be identified to the appropriate level, and were instead labeled as “unidentified Calanoida” (i.e., could be identified to the order Calanoida but not further; includes specimens from stages Ci-Cvi; all copepod nauplii are instead classified as “Copepoda nauplii”), “unidentified Copepoda” (i.e., could be identified to the subclass Copepoda, but no further; includes specimens from stages Ci-Cvi), or “unidentified zooplankton” (confirmed to be zooplankton, but could not be identified further). In addition, in other instances, copepods identified to the order level were given overlapping stage names (e.g., i-iii, i-iv, v-vi), or could not be identified at the genus level, but could instead be identified at the order level (Calanoida, Cyclopoida, Monstrilloida) and were given the stage classification “Ci-Cvi”. Therefore, copepods identified to order contained specimens from a range of stages from Ci-Cvi, not just Ci-Ciii.

We then used best practices from Cuffney et al. (2007) to resolve these taxonomic ambiguities. Cuffney et al. (2007) presented 16 approaches to address how parent (i.e., higher taxonomic levels) and child (lower taxonomic levels) taxa should be redistributed when both are present. As recommended, we used the Distribute Parent Among Child (DPAC) method, as it had among the highest suitability scores as measured by 13 metrics. For copepods and unidentified zooplankton, the variant DPAC-S was applied, in which the abundances of ambiguous parent taxa redistributed among the associated children in proportion to the relative abundance of each child in the sample (-S). Therefore, the abundances of parent taxa (all stages, Ci-Cvi grouped) belonging to the orders Calanoida and Cyclopoida were redistributed among child taxa within each sample, based on their relative abundances. In only two instances, samples contained parent taxa with no lower-level child taxa. As recommended by Cuffney et al. (2007), the parent taxa in these cases (Cyclopoida) were redistributed among child taxa, based on the average relative abundance of child taxa per sample from all samples at the respective site or sampling month. Harpactoida were not redistributed among child taxa, as the Harpacticoida classification only contained epibenthic taxa and taxa identified to the genus level were pelagic specimens. Next, “unidentified Copepoda” were redistributed among any Copepoda taxa, based on the relative abundances within each sample. Lastly, “unidentified zooplankton” were redistributed among all taxa, based on their relative abundances within each sample.

Following the redistributions, a few higher-level parent taxa persisted with lower-level children. However, these were distinct stages, identified to the requested taxonomic level (Appendix 4). For example, Copepoda nauplii remained as a distinct taxonomic class, separate from the (distributed) Copepoda genera containing stages Ci-Cvi. In addition, invertebrate (eggs and trochophores) remained as a class (all the zooplankton taxa except Osteichthyes egg/larvae are invertebrates), and Cnidaria larvae had child taxa as Hydrozoa (medusa), Siphonophorae (nectophore), or Scyphozoa (medusa). For the taxa accumulation curves in Section 2.6.1, these taxa (i.e., Copepoda nauplii, invertebrate eggs and trochophores, and Cnidaria larvae) were removed from the analyses, to prevent double counting of taxa (e.g., Kosobokova et al. 2011). For all other analyses, these three taxa were retained in the datasets. These parent taxa were not redistributed among children since stage information can have a large impact on the observed biodiversity patterns in multivariate analyses (Domènech et al. 2022), the different stages may have distinct roles in the ecosystem (Allan 1976; Johnson and Allen 2012), and they may respond differently to environmental conditions (Lamb 2005; Varpe 2012). Furthermore, zooplankton may exhibit time lags between stages in their life cycles (Allan 1976; Varpe 2012); therefore, redistributing the abundances of early stages based on the existing relative abundance of adult stages of lower-level taxa may not be accurate.